2020

LEVERAGING PEER-TO-PEER ENERGY SHARING FOR RESOURCE OPTIMIZATION IN MOBILE SOCIAL NETWORKS

Aashish Dhungana
Virginia Commonwealth University

LEVERAGING PEER-TO-PEER ENERGY SHARING FOR RESOURCE OPTIMIZATION IN MOBILE SOCIAL NETWORKS

A dissertation submitted in fulfillment of the requirements for the degree of Doctor of Philosophy at Virginia Commonwealth University.

by

AASHISH DHUNGANA

Doctorate in Computer Engineering with specialization in Computer Science - 2016-2020

Director: Dr. Eyuphan Bulut,

Associate Professor, Department of Computer Science

Virginia Commonwealth University

Richmond, Virginia

October, 2020

Acknowledgements

First, I would like to acknowledge and express my sincere gratitude to my honorable advisor Dr. Eyuphan Bulut, for his direction, assistance, and invaluable guidance.

I would also like to thank Dr. Tomasz Arodz, Dr. Kostadin Damevski, Dr. Kemal Akkaya and Dr. Yanxiao Zhao for their kind approval to join my dissertation committee and for providing guidance and valuable feedback. I would also like to acknowledge and thank my family for their continuous assistance during my entire academic journey.

TABLE OF CONTENTS

LIST OF TABLES

LIST OF FIGURES

Abstract

LEVERAGING PEER-TO-PEER ENERGY SHARING FOR RESOURCE OPTIMIZATION IN MOBILE SOCIAL NETWORKS

By Aashish Dhungana

A dissertation submitted in fulfillment of the requirements for the degree of Doctor of Philosophy at Virginia Commonwealth University.

Virginia Commonwealth University, 2020.

Director: Dr. Eyuphan Bulut,

Associate Professor, Department of Computer Science

Mobile Opportunistic Networks (MSNs) enable the interaction of mobile users in the vicinity through various short-range wireless communication technologies (e.g., Bluetooth, WiFi) and let them discover and exchange information directly or in ad hoc manner. Despite their promise to enable many exciting applications, limited battery capacity of mobile devices has become the biggest impediment to these applications. The recent breakthroughs in the areas of wireless power transfer (WPT) and rechargeable lithium batteries promise the use of *peer-to-peer (P2P) energy sharing* (i.e., the transfer of energy from the battery of one member of the mobile network to the battery of the another member) for the efficient utilization of scarce energy resources in the network. However, due to uncertain mobility and communication opportunities in the network, resource optimization in these opportunistic networks is very challenging. In this dissertation, we study energy utilization in three different applications in Mobile Social Networks and target to improve the energy efficiency in the network by benefiting from P2P energy sharing among the nodes. More specifi-

cally, we look at the problems of (i) optimal energy usage and sharing between friendly nodes in order to reduce the burden of wall-based charging, (ii) optimal content and energy sharing when energy is considered as an incentive for carrying the content for other nodes, and (iii) energy balancing among nodes for prolonging the network lifetime. We have proposed various novel protocols for the corresponding applications and have shown that they outperform the state-of-the-art solutions and improve the energy efficiency in MSNs while the application requirements are satisfied.

CHAPTER 1

INTRODUCTION

About 5 billion users are carrying a mobile device with a service around the globe [1]. The various uses of these devices and increasing popularity of software applications such as email, Facebook, and maps have made people highly dependent on mobile devices. This intensive use of mobile devices has brought a huge load on battery requirements. The hardware capabilities have significantly improved since the advent of smartphones but the development of powerful batteries have not taken the necessary pace, making the batteries the main bottleneck. The charge on most smartphones lasts about one day with average usage, or less with intensive usage (e.g., social sensing [2]). As a result, users are required to charge their devices frequently. The most common practice for users is to charge their phones by connecting them to a wall outlet through charging cables. This requires users to carry a charging cable and find an outlet, which is mostly available indoors. Thus, the charging process can potentially be irritating and sometimes infeasible. With the integration of built-in wireless charging capability in recent phones (including iPhone 8 and X [3]), users are relieved from the need to carry charging cables but the current application of wireless charging is very limited as it requires not the phone but the charging mat to be connected to an outlet. Recently, this somewhat limited usage of wireless charging has further been extended with energy transfer between mobile devices [4, 5]. Through bidirectional chargers, mobile devices could exchange energy without the need of being connected to an outlet. Such a peer-to-peer (P2P) energy sharing opportunity brings flexibility to users for finding power ubiquitously and mitigates the risks of

facing an emergency situation with depleted battery [6, 7, 8]. This power sharing technique transforms power to a tradable commodity and can incentivize users for sharing. However, users may be concerned about the effects of power transfer on human health and safety [9]. The idea that power is transferring through the air or is buzzing around can worry people about possible radiation. Yet, the most common form of wireless charging, inductive charging, is indeed very safe to use. Several studies have been done to determine the safety limits (through several metrics such as Specific Absorption Rate (SAR), and current density) of human exposure to electromagnetic (EM) fields (created by inductive charging) by several agencies including WHO and ICNRP [10]. The reports from these studies show that there is no evidence showing that human exposure to radio frequency (RF) electromagnetic fields causes cancer, as long as they stay in given limits defined by these agencies. That's why one needs to follow these guidelines while developing new wireless charging products. Current commercially available Qi wireless chargers use low power (e.g., 5 watts) and operate at the frequencies between 110 and 205 kHz [11] which are already considered to be within these safety limits.

The charging of battery powered devices has gained a different perspective with recent breakthroughs in the areas of wireless power transfer (WPT) [12, 13] and rechargeable lithium batteries [14]. Thanks to both academic and industrial efforts, wireless charging has been adopted for the charging of various mobile nodes including not only the low-power devices such as RFID tags, sensors or other Internet-of-Things (IoT) devices but also other devices and vehicles that operate with moderate and high capacity batteries such as smartphones, tablets, and cars. There are many commercial products that can be charged wirelessly in the market today and it is expected that the global wireless charging market is projected to reach $71,213 million by 2025, with a compound annual growth rate (CAGR) of 38.7% from 2018 to 2025 [15].

A survey has also been done in [16] to understand the users interest in sharing their energy. The study shows that majority of people is interested in P2P energy sharing but they look for charging with better efficiency and at somewhat longer distances. While the current technology is not there yet, there are some breakthroughs in the literature which could lead to progress in these aspects of wireless charging. This work also develops a prototype for mobile app that aims to build a social network platform to let people find each other and share energy wirelessly. Thanks to the convenience and better user experience provided, wireless charging technologies have been recently adopted for the sharing of energy among peers. However, energy sharing not necessarily be achieved via wireless power transfer. Conductive (wired) way could also be possible and a better option for efficiency in some networks consisting of high-power vehicles (e.g., electric vehicle to electric vehicle [17]). Moreover, this energy sharing could be between some specific type of agents (e.g., mobile *c*harger to mobile *c*harger (*C2C*) [18]), between ordinary *n*odes (*N2N*) when they are equipped with necessary hardware (e.g., phone to phone [19]) or from specific agents to ordinary nodes (e.g., mobile charger to a sensor node [20] (*C2N*)). The scenarios considered for energy sharing in different mobile network applications are summarized in Fig. 1.

Depending on how the energy sharing is used within a specific application, it also comes with different design challenges including optimal trajectory planning, scheduling of multiple chargers as well as providing incentives for the sharing. Moreover, if wireless power transfer is used, the energy transfer efficiency should be taken into account during the development of protocols and algorithms. The consumption of the energy may also need to be optimized not just in terms of its distribution to other peers but also for the mobility of agents in some scenarios. For example, while in the case of smartphones the mobility is provided by people carrying them, in the case of mobile robots or vehicles as mobile chargers in a sensor network, the energy is also

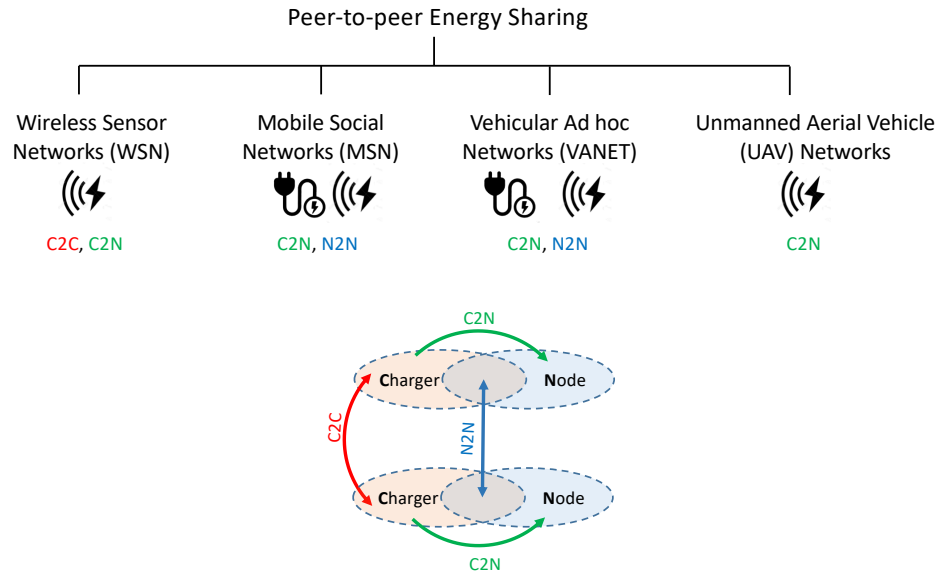

Fig. 1.: The scenarios considered for energy sharing in different mobile network applications.

consumed for their movement, thus, a joint optimization is required. In this dissertation, we only focus on resource optimization via energy sharing between mobile to mobile (N2N) devices in a mobile social network.

1.1 Motivation

Mobile Social Networks (MSN) is a type of delay tolerant networks (DTNs) where the mobility and connectivity of nodes are often non-deterministic. Mobile Social Networks (MSNs) enable the interaction of mobile users in the vicinity through various short-range wireless communication technologies (e.g., Bluetooth, WiFi) and let them discover and exchange information directly or in ad hoc manner. Despite their promise to enable many exciting applications, limited battery capacity of mobile devices has become the biggest impediment to these applications. Two recent breakthroughs in the areas of wireless power transfer (WPT) and rechargeable lithium

batteries promise the use of peer-to-peer energy sharing for the efficient utilization of scarce energy resources in the network. We refer to *energy sharing* as the transfer of energy from the battery of one member of the mobile network to the battery of the another member. Resource optimization in these opportunistic networks is challenging due to uncertainty of possible communication opportunities. Thus, efficient techniques are required to develop a strategy on optimizing the available resources in these networks for collaborative network operations. There have been many research efforts performed to provide solutions based on different methods (e.g., harvesting [21], battery replacement [22]) to this problem so that network lifetime can be prolonged.

With the recent advances in wireless power transfer (WPT) technology and increasing efforts from both the academia and industry, numerous studies considered WPT based energy replenishment of nodes in mobile networks. Most of these studies have been performed for wireless sensor networks [18, 23, 24], but it has also been considered for smartphones [25, 26, 27], electric vehicles [28, 29, 30] and Internet-of-Things (IoT) devices [31, 32]. For example, in the sensor networks domain, most of the time mobile chargers, which are special vehicles (e.g., robot, Unmanned Aerial Vehicle (UAV)) with high energy supplies are employed to periodically charge the sensors in the field.

The one-way charging of mobile devices from chargers has recently been extended to bidirectional energy sharing between the regular nodes in the network and several application specific problems have been studied benefiting from this. For example, in mobile social networks domain, thanks to the recent products (e.g., Samsung Galaxy S10, Huawei Mate 20 Pro) in the market and also some prototypes developed by research community [4, 27] bidirectional wireless charging between smartphones has been considered for crowdcharging of smartphones by other users [6, 7]. While current form of wireless charging used in these products only happen in very close distances

(i.e., almost touching), it provides a convenient process without the hassle of cables. On the other hand, peer-to-peer energy sharing has triggered a new set of research studies in different mobile network applications. For example, for an opportunistic content delivery, energy has been considered as an incentive [8, 33] to the devices to carry the message. Similarly, an interesting problem of energy balancing [34, 35, 36, 37, 38] among nodes has been studied towards prolonging the lifetime of the network, which could be vital especially when there is no access to external energy sources. In this dissertation, we study energy utilization in three different applications in Mobile Social Networks and target to improve the energy efficiency in the network by benefiting from P2P energy sharing among the nodes. More specifically, we look at the problems of (i) optimal energy usage and sharing between friendly nodes in order to reduce the burden of wall-based charging, (ii) optimal content and energy sharing when energy is considered as an incentive for carrying the content for other nodes, and (iii) energy balancing among nodes for prolonging the network lifetime. We have proposed various novel protocols for the corresponding applications and have shown that they overcome the state-of-the-art solutions and improve the energy efficiency in MSNs while the application requirements are satisfied.

1.2 Contributions

Our contributions for resource optimization in Mobile Social Networks utilizing peer-to-peer energy sharing among mobile nodes can be summarized as below:

- We investigate the utilization of peer-to-peer wireless energy sharing to relieve the users from the burden of cord-based charging. The devices of users can make use of energy available from other users' devices based on their meeting patterns so that the battery level of their devices could be maintained within an acceptable level without the need of charging it through a cable frequently.

To this end, we first use dynamic programming to find the optimal skips of existing cord-based charging sessions for each pair of users in an MSN and then use stable roommate matching to map each user to its best peer for energy exchange.

- We study the content delivery problem in mobile social networks in which nodes are motivated by energy transfers for carrying the messages. That is, each relay node carries a message forwarded by another node as long the energy provided or the corresponding time-to-live (TTL) value lasts. To this end, we utilize dynamic programming and Optimal Stopping Theory to solve this problem.

- We study the energy balancing problem that aims to minimize both the energy difference between nodes and the energy loss during this process. We propose three interaction protocols for a fully connected contact graph and discuss its performance based on the achievable balance and energy loss.

- We also present efficient and loss-aware energy balancing protocols considering the contact graph heterogeneity between nodes and a time threshold for completing the energy balancing and propose several single hop and multi hop interaction protocols to achieve the optimal energy balance.

- We also extend the idea of energy balancing to network lifetime maximization problem and also propose modifications to the energy balancing problem for lifetime maximization when a perfect energy balancing is not achievable.

1.3 Organization of the Dissertation

The rest of the dissertation is organized as follows: Next section discusses on the relevant background of the literature including various available energy sharing

techniques and problems focused by researchers in this area. Third chapter discusses on charging skip optimization algorithms that aims to reduce the burden of cord based charging utilizing P2P energy sharing between users. Similarly, fourth chapter presents the content delivery algorithm in Mobile Social Networks utilizing energy as incentives. Fifth chapter discusses on the energy balancing problem and presents several protocols to achieve optimal energy balance. Finally, in sixth chapter, we provide concluding remarks and in the last chapter we provide future research directions related to topics in this dissertation.

CHAPTER 2

LITERATURE REVIEW

The relevant backgrounds and current state-of-art technologies for peer-to-peer energy sharing in mobile networks are discussed in the sections below:

2.1 Energy Sharing Technologies

In this section, we review the various technologies and methods used to achieve energy sharing between the batteries of mobile devices in different mobile network applications. Due to its practicability and recent advances, several *wireless* charging technologies adopted recently, however, *wired* energy transfers through conductive cables or gadgets have also been considered.

Wireless power transfer (WPT) or simply wireless charging is a technology of transmitting power through the air to electrical devices for energy replenishment. There are several ways of achieving wireless charging (e.g., inductive coupling [39], magnetic resonant coupling [12] and radio frequency (RF) based charging [40]), each with advantages and disadvantages to one another. For example, RF based charging is radiative charging and uses electro-magnetic waves like RF waves and microwaves to deliver energy in the form of radiation. As it can be unsafe due to the RF exposure [9, 41], it is usually offered for low-power devices like sensor nodes and medical implants [42]. Inductive coupling based charging can provide good efficiency but has a short range. Magnetic resonance coupling based wireless charging can operate at larger distances but with less efficiency. Other forms of wireless charging (e.g., ultrasound [43], or lasers [44]) are also possible but none of those approaches yet made

it available for consumers while staying in the safety limits defined by FCC [41]. A comprehensive overview of the existing and emerging wireless charging technologies and their applications in wireless communication networks could be found in [45].

Wireless charging has also been utilized for energy sharing between mobile devices. However, due to the efficiency issues with wireless charging at larger distances, it has been mostly considered for sensor networks consisting of devices with low power requirements. A mobile robot or a vehicle usually charges itself and navigates to the sensors in the network to charge them. As sensor nodes are considered stable most of the time, peer-to-peer energy sharing among sensor nodes is not applicable. However, to increase the number of sensors that could be charged, energy sharing among charger vehicles [18] has been considered as an example of peer-to-peer energy sharing.

With the introduction of new generation mobile devices such as smartphones with built-in wireless charging capability, the adoption of wireless charging beyond sensor networks as well as its research has gained momentum. However, current common usage scenarios are very limited. For example, smartphone users need to place their devices on a charging pad and start charging their devices without the hassle of cables. While several additional convenience could be provided by embedding charging equipment in other things such as a desk [46] or a cup holder in a car [47], as the charging equipment still needs to be plugged into a power source, it does not really achieve an *energy sharing* as defined in this dissertation. Energy sharing between smartphones could indeed simply be achieved by power sharing cables [48], and power equalizer gadgets [49] in a conductive way. However, it comes with the burden of carrying such accessories. There are some recent studies [19, 50] demonstrating that current wireless power transfer technologies can easily be utilized to create an on-the-go power sharing system between mobile devices. While, due to the efficiency problems this is achieved at very close distances (i.e., almost touching), it can provide

the flexibility to users for finding energy ubiquitously from other users' devices.

Energy sharing between high-power mobile agents has also been studied recently. With the rise of electric vehicles (EV), charging of vehicles has been one of the major problems. Wireless charging has been considered as an option for electric vehicle charging by several means (e.g., convenient charging while parking [51], dynamic wireless charging on roads [52]). However, such solutions require heavy investment and high labor costs [53]. Recently, vehicle to vehicle charge sharing has been considered to address the immediate charge needs of vehicles especially in the absence of nearby charging stations. While wireless charging based energy sharing between EVs has been claimed with a recent study [54], there is actually no practical implementation due to aforementioned challenges and limitations. However, the possibility of energy exchange between two EVs has already been introduced to the market through different products by a few companies, such as Andromeda Power (AP) [55] and eMotorWerks (EMW) [56]. These products provide a direct V2V charge sharing with a DC/DC converter and a charging cable that tie the batteries of both EVs through their fast charging ports. However, these products are mainly developed for the purpose of rescuing stranded vehicles. Building on top of these solutions, there is a growing number of studies that aim to solve charging problem of EVs through V2V charge sharing. However, understanding the potential benefits of such V2V charging among a network of EVs at a large scale is a challenging question, thus several specific aspects of this problem are focused on these studies. Furthermore, recent research studies also look at the utilization of Unmanned Aerial Vehicles (UAV) to solve the charging problem. Energy sharing solutions using UAVs is more effective since UAVs can hover around a large place significantly increasing the charging coverage. However, the high speed of drones and energy constraints make energy sharing a challenging problem. Moreover, due to the longer charging distances from UAVs,

the charging efficiency will be lower. Thus, most research studies focuses on tackling these aspects of the problem.

In this dissertation, we focus on energy sharing in MSNs and its utilization for resource optimization in MSNs. Thus, in the next section, we elaborate on the state-of-art P2P energy sharing applications between mobile nodes in a Mobile Social Network.

2.2 Mobile Social Networks

With the proliferation of mobile devices used by people, a new form of networking, called mobile social networks (MSN) [57], has appeared. The unique feature of these networks is the mobility of the nodes, which is provided freely (i.e., without energy consumption from their batteries) by humans carrying them. Moreover, thanks to the growing peer-to-peer communication technologies (e.g., Bluetooth Low Energy (BLE), WiFi Direct), these devices can talk to each other when they are within the wireless ranges of each other. However, most of the time, this type of interaction is determined by the social relations of people carrying these types. Leveraging these properties of MSNs, many studies have been conducted focusing on different problems such as opportunistic routing [58, 59], friend discovery [60] and user tracking [61].

One bottleneck in the operation of these complicated mobile devices (e.g., smartphones) constituting the MSNs is their limited battery capacity. They struggle to reconcile their increasing capabilities with their battery lives. While there are ways to optimize the use of battery [62, 63] in mobile devices, the need of frequent charging of these devices by their users to keep them operational is inevitable. However, charging facilities may not be continuously accessible (e.g., when the user is outside). In response to this, for example, some crowdsourcing based apps are developed to find out the nearest available plugs (e.g., ChargeItSpot [64], Airport Power [65]). Alterna-

tively, external power banks [66], solar chargers [67] or other eco-friendly chargers like mobile hand generators [68] are also considered but they provide limited solutions in practice and come with the cost of carrying additional accessories.

To provide a more comprehensive solution, opportunistic peer-to-peer energy sharing among mobile devices is considered recently (see Fig. 2). That is, users with high energy in their devices (i.e., recently charged) can share energy with other user devices (i.e., N2N) having less energy and can consider getting it back in another time when they need. This brings flexibility to users for finding power ubiquitously and can potentially mitigate the risks of facing an emergency situation with depleted battery. Conductive energy sharing solutions could be considered but with the increasing number of mobile devices that have built-in wireless charging feature, this could be achieved in a more convenient way. While the current wireless charging application on commercial mobile devices is considered from charging pads and unidirectional only, in some recent studies [19, 50] prototype systems managing and controlling bidirectional energy exchange among mobile phones are presented.

Recently, there is a growing number of studies that utilizes the peer-to-peer energy sharing in mobile social networks. We categorize them based on the objective of the research. Below, we overview the studies in each category.

2.2.1 Optimal Energy Usage

The studies in this group aim to take the advantage of opportunistic interaction of nodes in a mobile social network for energy sharing. Their goal is to optimize the energy usage at nodes in general but different approaches are considered. Users can share energy when they travel and encounter each other such that mobile users don't run out of energy on the way or before reaching to its charging point. Thus, to maximize the benefit from opportunistic energy sharing, not only the mobility and

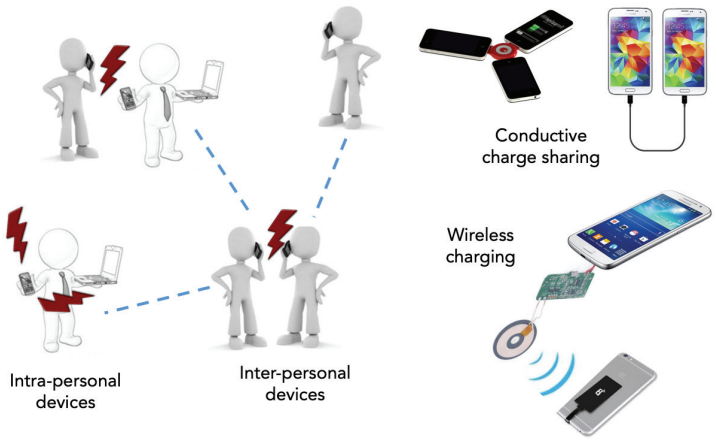

Fig. 2.: Energy sharing scenarios in a mobile social network consisting of smart mobile devices. The energy sharing can be achieved in a conductive manner via a sharing cable or a gadget or through near-field wireless power transfer.

encounter patterns of users but also energy levels of the user devices' batteries at their encounter times should be taken into account.

In[7, 8] a constrained Markov decision process is used to formulate the optimal energy sharing policy that minimizes the energy outage probability. Users are ranked based on the potential mutual benefits to each other in terms of shareable energy and the best pairs of nodes are found using stable matching. However, this concept is studied without an integrated analysis of charging habits of individual user devices and meeting patterns between the users that can exchange energy. To address this, in [6], the limits of energy sharing among mobile devices is investigated by analyzing the current charging patterns and the social interactions between these mobile users. The nodes are paired as *power buddies* and energy sharing is achieved only among them similar to [7]. Interestingly, this model is able to show that these power buddies can provide a good percentage of energy needs allowing users to delay their charging decisions and increase average charging cycle duration. In [69], a group-based charging

system is introduced and assuming two separate battery units at nodes, the burden of charging is given to only some lead nodes who are responsible for charging their second units overnight and providing energy during the day to others.

2.2.2 Energy Sharing for Content Delivery

There is a group of studies that exploit energy sharing in the context of content delivery in sparsely connected mobile networks such as Delay Tolerant Networks (DTN) [70] or Mobile Social Networks (MSN). The communication between the nodes in such networks is achieved in opportunistic manner. That is, when a source node has a message to send to a destination node, the message is forwarded or copied to other nodes in the network with some decision rationale [70, 71, 72, 73] to achieve the minimum possible delay. Then, the message is stored in the relay node, carried until another better relay node or destination node is met and forwarded again. While routing is the main problem studied in such networks, as the nodes in these networks require energy for storing, carrying and forwarding the message contents to other nodes in the network, energy management is also a major issue. Thus, there are many studies that aim to develop energy efficient routing protocols. Besides these works, recently several studies have considered the scenario in which a mobile user transfers not only the content but also energy (see Fig. 3) to intermediate users [33, 74, 75], as an incentive to them to carry this content to the destination. However, this makes the problem more challenging as the nodes need to determine not only the forwarding of the content but also the amount of energy to be given to relay nodes.

Several approaches are adopted in the literature to address this challenging problem. In [33], the problem is formulated using a Markov decision process (MDP) based on the contact state of content source to obtain the optimal energy sharing policy. The content source moves and visits a charger to receive energy and when it meets with

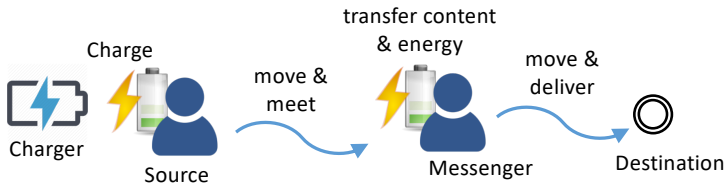

Fig. 3.: Source node charges itself at a charger and when it meets with a messenger offering better delivery option for its message to a specific destination, it transfers the message as well as the sufficient energy for the messenger to carry it to the destination.

a messenger (e.g., relay), asks for the delivery of the content to the destination node by sharing some energy to the messenger. If the energy depletes before reaching to the destination, the content is discarded by the messenger. MDP is used to carefully select a messenger node and transfer optimal energy so that the content is delivered to the destination with highest probability. Extending this study in [76] the authors show that the optimal strategy obtained by MDP is a threshold policy. In order to avoid the cumbersome of centralized solutions and achieve a decentralized decision policy, authors also formulate the problem using a decentralized partially observable Markov decision process with constraints and a decentralized learning algorithm is proposed to obtain an optimal local policy at nodes [77].

The interaction between the source and the messenger nodes has also been modeled using game theoretical models in several studies. In [74] the peer-to-peer relations between mobile nodes is exploited to form a coalition to help one another on delivering packets. They also look at the cases when these coalitions might not be beneficial and some nodes might decide to deviate away from the coalition. A different approach based on forming a non-cooperative game model is considered in [75]. The source node holds an auction for wireless energy and the nodes send their bids for it. In return of service, the nodes have to pay certain cost to the source. A stochastic

dynamic response algorithm that allows nodes to adapt their strategies to the Nash Equilibrium is presented and proved to be the optimal policy.

Different than the focus of the aforementioned works, in [78], a charging-aware mobility model is studied to integrate the charging needs of mobile nodes during their mobility. To this end, nodes are motivated to move towards energy sources when they have low energies while they are motivated to move towards the destination node when they have sufficiently high energy. Moreover, as the deadline for delivery gets close, the weight for moving towards destination increases to achieve timely delivery. It has been shown that this approach lets the nodes maintain high energy and achieve better packet delivery ratios depending on the location and the number of charger nodes in the network.

2.2.3 Energy Distribution for Balancing

One important problem studied exploiting peer-to-peer energy sharing in mobile social networks is to distribute the available energy in a desirable way. Mostly, the goal of such distribution is to achieve the energy balance in the network or to reach a certain target energy distribution. However, the distributed cooperation of the nodes towards collectively achieving global computational and communication goals can be challenging. In this effort, some studies offer peer-to-peer energy exchange between agents to achieve approximate *energy balance* [36, 79, 80, 81] in the network with minimum energy loss whereas some advocates on constructing a *network structure* [37, 38, 79], basically a star structure to reach a desired energy distribution in the network. Next, we discuss these approaches, respectively.

Energy balancing can provide efficient utilization of scarce energy in mobile social networks and can prolong the network lifetime (e.g., especially when network lifetime is defined as the duration until the first node dies). Distributing energy such

Research Objective	**Key features**
Optimal Energy Usage [6, 7, 8, 69]	• Limits the energy sharing only among assigned pairs. • Allows opportunistic energy exchange at meeting times only.
Energy Distribution for Balancing [36, 37, 79, 80, 81]	• Energy is shared in certain (e.g., half, small amount) portions between all or some (e.g., in the opposite sides of average network energy) of the interacting nodes. • Roles of nodes within a network formation problem is jointly considered for a weighted distribution.
Energy Sharing for Content Delivery [33, 74, 75, 76, 77, 78]	• Energy is provided to relay nodes to carry content to destination. • Optimal amount of energy to be transmitted is determined jointly with the decision of forwarding.

Table 1.: A summary of current research using energy sharing in mobile social networks.

that each node in the network has access to similar level of energy or energy proportional to its weight (e.g., importance in the network) can be thought of a fair way of

collaboration among mobile users in efficient utilization of energy resource. Studies focusing on energy balance mostly investigate on interactive, peer-to-peer wireless energy exchange in populations of resource limited mobile agents, without use of any special chargers with the main goal of achieving the energy balance among the mobile nodes [36, 79, 80, 81].

In these works, it is assumed that the agents are capable of achieving bi-directional wireless energy transfer acting both as energy transmitters and receivers. Both lossless and lossy cases are considered for energy sharing where the energy loss follows a fixed linear law. Under these assumptions, various interaction protocols are proposed that will achieve the energy balance. These include sharing half of the available energy or only a small amount of energy. When the average of the available energy in the network is also known, more smart sharing rules such as sharing between the agents on the opposite sides of the average, are also considered to speed up the convergence. There are also weighted versions of these protocols considered when the significance of nodes are not the same.

Energy distribution among peers has also been studied [37, 38, 79] within a network formation problem considering the roles of the nodes and their energy needs. For example, in a star topology, nodes are organized in a cluster, and a cluster head is selected to which all communications is forwarded. In view of this, the fair distribution of energy in the network could be when the energy level of the cluster head is proportional to the number of mobile nodes in its cluster. In networks, where the central agent knows the number of actual peripheral nodes, this could be easily managed by finding the proportional energy needs of nodes, however, this may not be the case always in practice. Thus, naive (e.g., transferring all or half of the energy from the peripheral nodes to the central node) solutions are simply adopted mostly favoring the heavy-duty nodes such as cluster heads.

Apart from these works, there is also an interesting work [82], which studies the fair charging of smartphones (e.g., balancing energy distribution based on their current energies) from the wireless chargers deployed at subways (i.e., C2N). This study applies a similar uni-directional charging model as considered in WSNs and aims to increase the energy gain by making the phones charged from the closest chargers during the passengers' trip times.

CHAPTER 3

MOBILE CHARGING RELIEF VIA P2P ENERGY SHARING

3.1 Introduction

In this chapter, we investigate the benefit of P2P energy sharing between mobile devices on reducing the burden of traditional cord-based charging process (simply called wall charging in the rest of the chapter). Depending on the meeting schedules with other users, a user can make use of excessive[1] energy available from other users' devices to skip some of the wall chargings while still maintaining the device's charge within an acceptable level. Our goal is to maximize the number of wall chargings that could be skipped through utilization of energy shared by other users in the vicinity. We aim to discover the potential benefit of P2P energy sharing on existing charging habits of users. Hence, we assume that the charging patterns of user devices and as well as their meeting patterns with other users (from which shareable energy amounts could be derived) are given. We exploit dynamic programming approach to find out the optimal skipping patterns for conservative and cooperative cases. In the conservative case, we assume that there is no external energy available and hence the node will utilize its own available energy to optimize its charging cycles. In the cooperative case, we allow both sharing and receiving of energy between users and study simultaneous optimization of skipping patterns from each user's perspective. Different from previous work, we define the burden of charging in terms of the number of charging sessions that the devices stay plugged to the outlet (i.e., wall charging)

[1]Current charging habits of users show that they charge their devices more often than they need [6], yielding opportunity for energy sharing with others.

and discuss the minimization of that number exploiting the energy shared by other users without changing the charging and movement patterns of any user. We also provide a satisfactory network-wide solution for all users by mapping our problem to roommate matching problem and assign partners to each user while satisfying all users with their assignments. The notations used throughout the chapter are given in Table 2.

3.2 Problem Definition

A *charging pattern* of a user device consists of alternating charging and discharging sessions. Let δ_c and δ_d denote the set of all charging and discharging sessions for a user, respectively:

$$\begin{aligned}
\delta_c &= \{\delta_c(1), \delta_c(2), \ldots, \delta_c(n)\} \\
\delta_d &= \{\delta_d(1), \delta_d(2), \ldots, \delta_d(n)\} \text{ where,} \\
&\quad \delta_d(i).l_s = \delta_c(i).l_e, \forall i \in \{1 \ldots n\} \text{ and} \\
&\quad \delta_c(i+1).l_s = \delta_d(i).l_e, \forall i \in \{1 \ldots (n-1)\}
\end{aligned}$$

We define the time from the start of one wall charging to the start of next one as a *charging cycle*. Here, each ($\delta_c(i)$, $\delta_d(i)$) represents a charging cycle with one charging and one discharging session. The attributes l_s and l_e represent the starting and ending charge levels (integers in [0-100]) for each of these periods.

We consider that when a mobile user meets another mobile user, they can exchange energy between each other wirelessly. Recent studies [4, 27] have shown that mobile devices could easily be equipped with necessary hardware and software support to realize this. We assume that the users know each other and are interested in sharing their excessive energy with their friends non-intrusively. That is, they do not

Notation	Description
$\delta_c(i)$	i^{th} charging session of user.
$\delta_d(i)$	i^{th} discharging session of user.
$\delta_c^A[t]$	Total energy gained by user A during wall charging in t^{th} decision block.
$\delta_d^A[t]$	Total energy lost by user A during discharging in t^{th} decision block.
$S_t^{A\to B}$	The energy shared from A to B during the t^{th} decision block.
l_s	Starting charging level attribute of a charging or discharging session.
l_e	Ending charging level attribute of a charging or discharging session.
l_{min}	Minimum acceptable energy level of user devices.
l_{init}	Initial charge level of the user.
X_t^A	Charging decision variable for user A in t^{th} decision block.
D	Matrix that stores the number of wall chargings required for each charge level by every decision block.
T	Matrix that stores the index of the D matrix from which the corresponding D matrix entry is derived.
$\mathcal{U}_t^A$	The total unplugged time of user A in t^{th} decision block.
$\mathcal{M}_t^{A,B}$	The meeting event between users A and B in t^{th} decision block.
$\mathcal{T}_S$	The speed of energy transfer between users.
$\mathcal{T}_E$	The efficiency of energy transfer.
n_A	Number of charging sessions of user A.
$\mathcal{R}_A(B)$	User A's charging relief from collaborative charging with user B.
$J(\mathcal{R}_A(u_i))$	Energy saving with charging skip pattern associated with $\mathcal{R}_A(u_i)$.
$\mathcal{PL}[A]$	Preference list of user A to be matched with other users for collaborative charging.

Table 2.: Notations used in Chapter 3

want to change their regular movement patterns and their own usage of the device. The amount of energy that could be exchanged depends on several factors including transfer speed, efficiency, duration of their meeting, maximum shareable energy by the sender without causing it have less than an acceptable energy level and the available capacity in the receiver.

The optimization problem is studied for two different cases; (i) conservative charging, and (ii) cooperative charging. While the former looks at the problem from only one user's perspective by trying to minimize the number of wall charging sessions while still keeping the device with sufficient power to operate, in the latter, we consider both receiving and sharing of energy between the users and aim to optimize the problem jointly from the perspective of both users. We formulate these problems using decision points that occur at the beginning of each cycle. Next, we discuss the details of the problem within each context.

3.2.1 Conservative Charging

In this case, we study the problem from the perspective of a single user who aims to skip as many wall chargings as possible. Note that in this case user is not sharing energy with others nor receiving energy from them. This case is studied in order to understand the potential charging relief users could have obtained by their own scheduling. Moreover, it also forms the base for the formulation of complicated collaborative charging case.

Fig. 4 shows example charging patterns for two different users for a certain time frame. Depending on the applications that are running on the device the discharging rate might vary at different times. Similarly, depending on the equipment used for charging or due to the active usage while charging, the charging of the device could happen at different rates. Note that in some charging sessions there could be some

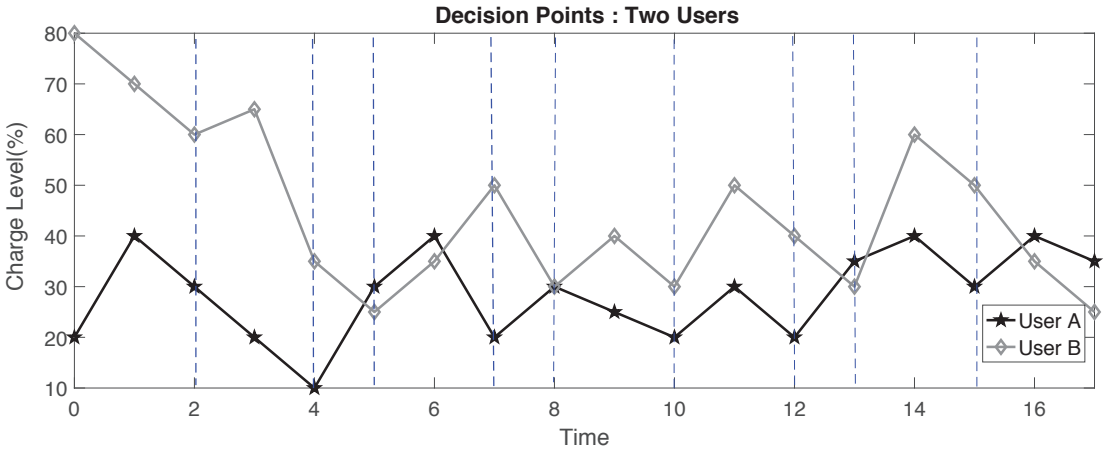

Fig. 4.: Charging patterns and decision points of two users.

idle charging duration in which the device stays plugged after being fully charged (e.g., overnight charging). While such cases could help increase the charging relief as the charging amount in the previous skipped sessions could be compensated during those idle charging times, we do not consider them in this work for the sake of brevity. However, all the formulations could be easily adapted to integrate such cases. Moreover, It has been shown by several studies conducted with smartphones that the battery voltage and state of charge (SOC) or battery level has almost a linear relation [83, 84] after the first few battery levels, thus we assume a linear but potentially with different rate charging and discharging sessions.

The conservative charging problem here is defined as follows. Given an existing charging pattern of a user, what is the minimum number of wall charging instances that would be sufficient for the user device while keeping the same device functionality and charging habits? In such scenario, the only way a user may try to skip some of its wall chargings is purely by benefiting from the unnecessarily frequent charging in its own charging schedule.

We formulate the problem using decision points that occur at the beginning of

each charging cycle. Decision points divide a given user charging pattern into blocks of time periods known as *decision blocks*. Each block starts with the start of a charging session for a user and ends with the completion of a discharging session. In this case, since there is a single user, each decision block corresponds to an individual charging cycle of the user. For user A's charging pattern shown in Fig.4, there are six decision blocks with starting times $D = \{0, 4, 7, 10, 12, 15\}$. Similarly, for user B, there are five decision blocks with starting times $D = \{2, 5, 8, 10, 13\}$.

Assume that there are n decision blocks and let $\delta_c[t]$ and $\delta_d[t]$ denote the total energy gained (i.e., $\delta_c(t).l_e$ - $\delta_c(t).l_s$) during wall charging and total energy lost (i.e., $\delta_d(t).l_e$ - $\delta_d(t).l_s$) during discharging throughout the t^{th} decision block. The objective function in conservative charging is then formally described as:

$$\min \quad \sum_{t=1}^{n} X_t \tag{3.1}$$

$$\text{subject to} \quad D_t.l_e = (D_t.l_s + \delta_c[t]X_t - \delta_d[t])\},\ \forall t \in [1, n] \tag{3.2}$$

$$D_t.l_e \geq l_{min},\ \forall t \in [1, n] \tag{3.3}$$

$$D_1.l_s = \delta_c(1).l_s \tag{3.4}$$

$$D_{t+1}.l_s = D_t.l_e\ \forall t \in [1, (n-1)] \tag{3.5}$$

where, l_{min} is the minimum acceptable level (e.g., 1%) and X_t is the charging decision variable $\in \{0,1\}$, with 0 meaning the current charging session is skipped.

3.2.2 Cooperative Charging

In this case, users are allowed to both send and receive energy between each other. Therefore, the optimal skipping pattern has to be determined considering the amount of energy that will be exchanged between users. The decision points (i.e., start of charging cycles) coming from both users will form decision blocks with

partitioned charging cycles of users. Moreover, some decision points might divide a charging session of a user into two or more parts.

The set of decision points that come from both users in Fig. 4 is $D = \{0, 2, 4, 5, 7, 8, 10, 12, 13, 15\}$, which is $D_A \cup D_B$. When a decision point causes a split in the charging session of a user, since we assume skipping of wall chargings completely (i.e., no partial skipping allowed), the skip decision made for a portion of a wall charging inside a decision block should match with the decision made for the remaining portion of the same wall charging in the next decision points. In order to reach the optimal skipping solution that maintains this, for every such decision point, both results (skipping or not) have to be stored until the split of a charging period with decision points is over and only the optimal one should be picked. The splitting of a charging session can create different types of decision blocks based on which the solution is modeled:

- **Full(u)**: The decision block contains the entire charging session of the user u.
- **First_Split(u)**: The decision block contains only the beginning portion of the split charging session of the user u.
- **Mid_Split(u)**: The decision block contains neither the start nor the end of the user u's charging session but has a middle part.
- **Last_Split(u)**: The decision block contains only the ending portion of the split charging session of the user u.

For example, in Fig. 4, the third decision block (i.e., from time 4 to 5) is First_Split(A) and the next one (i.e., from time 5 to 7) is Last_Split(A) and Full(B). It is possible that a decision block can only include discharging session for a user (e.g., user B in third decision block). Such blocks could be considered for users like a Full

split with no charging. Moreover, some of the combinations of these block types for a pair of users is not possible. For example, while there is a First_Split(A), there cannot be a Mid_Split(B). The valid combinations have to be carefully analyzed towards the solution.

Let $\delta_c^A[t]$ and $\delta_d^A[t]$ denote the total energy gained by user A during wall charging and total energy lost by user A during discharging throughout the t^{th} decision block. Moreover, let $S_t^{A\to B}$ denote the energy shared from A to B during the t^{th} decision block and $\mathcal{T}_E$ denote the efficiency of transfer. The objective function in cooperative charging is then formally described as:

$$\min \quad \sum_{t=1}^{n} (X_t^A + X_t^B) \tag{3.6}$$

$$\text{subject to} \quad D_{t+1}^A.l_e = D_t^A.l_s + \delta_c^A[t]X_t^A - \delta_d^A[t] + \mathcal{T}_E S_t^{B\to A} - S_t^{A\to B} \tag{3.7}$$

$$D_{t+1}^B.l_e = D_t^B.l_s + \delta_c^B[t]X_t^B - \delta_d^B[t] + \mathcal{T}_E S_t^{A\to B} - S_t^{B\to A} \tag{3.8}$$

$$D_t^k.l_e \geq l_{min},\ \forall t \in [1,n], \forall k \in \{A,B\} \tag{3.9}$$

$$D_1^k.l_s = \delta_c^k(1).l_s\ \forall k \in \{A,B\} \tag{3.10}$$

$$D_{t+1}^k.l_s = D_t^k.l_e\ \forall t \in [1,(n-1)],\ \forall k \in \{A,B\} \tag{3.11}$$

where, l_{min} is the minimum acceptable level (e.g., 1%) and X_t^A, and $X_t^B \in \{0,1\}$ are the charging decision variables for A and B, respectively, with 0 meaning the current charging session is skipped.

3.3 Dynamic Programming based Optimization

We use a dynamic programming based approach to find out the optimal charging pattern in both problems. At each decision point, the algorithm tries to recursively find the best charging levels that will result in the minimum number of wall chargings for each user. The solution includes two matrices: D and T. D matrix stores the

integer value that represents the number of wall chargings required for each charge level by every decision block and T matrix stores the index of the D matrix from which that value is derived. In the subsequent sections, we provide the details of the solution for each of these cases.

3.3.1 Optimization for Conservative Charging

In this case, a two dimensional D matrix is considered where the first dimension represents the decision points and the second dimension represents the charge level for the user of interest. The algorithm takes the list of wall charging amounts ($\delta_c[]$), and the list of discharging amounts ($\delta_d[]$) for the user as a parameter. l_{init} is the initial charging level for the given charging pattern. For example, for A's pattern in Fig. 4, l_{init} is 20%. Values from $D[0][l_{min}]$ to $D[0][0]$ is initialized to 0 because it is ensured that each of these charging levels could be achieved at the beginning without any wall charging. All other values in D matrix are initialized to some very high integer value.

The details of the dynamic programming based solution for the conservative charging is shown in Algorithm 6. The main principle on which the algorithm works is, for each charge level (i.e., from 0 to 100) at each decision block (D_t), it finds out what charge level could be reached by either decision (skipping (X_t=0) or not (X_t=1)) and updates the number of wall chargings at that level with the smallest ever seen as long as it is more than the minimum acceptable level and less than 100%. Note that if the smallest wall charging count is achieved with a skip from previous decision point, the number of wall chargings from previous decision point is transferred. On the other hand, if the wall charging in that decision block is used, the number of wall chargings from previous decision point is incremented by 1 and used in the update. The same logic is applied recursively for all charging cycles to find the optimal skip

Algorithm 1: Conservative Charging Decision Algorithm

```
1  Input: δ_c[]: Charging amounts; δ_d[]: discharging amounts
2  Output: Number of minimum wall charging sessions for the user
3  for each decision block D_t do
4      for each charging level 0 ≤ l ≤ 100 do
5          current = D[t][l]
6          for each X_t ∈ {0, 1} do
7              l_new = min(100, l + δ_c[t]X_t) - δ_d[t]
8              if l_new ≥ l_min then
9                  if current+X_t < D[t+1][l_new] then
10                     D[t+1][l_new]= current+X_t
11                     T[t+1][l_new] = l
12 return min{D[n][l] ∀l ≥ l_min}
```

sequence at the end. The running time of the algorithm is $O(100|D|)$, while brute force solution has $O(2^{|D|})$ complexity.

Once the algorithm finishes, we apply a general solution readout approach to find the actual wall charging sessions used. We start at the last decision block and get the index with the minimum number of charging sessions from D matrix. Each position in D matrix is associated with its previous cell using T matrix. If the value in current index of D matrix has increased compared to its previous value, then the wall charging session at that decision block is used, otherwise it is skipped.

3.3.2 Optimization for Cooperative Charging

In cooperative charging, in order to increase the overall charging relief for users, they consider exchanging energy between each other. However, for each energy exchange opportunity within the decision blocks, the amount of actual energy exchange amounts should be decided to obtain the optimal charging pattern at the end. The energy exchange between users can potentially happen when they actually meet and are not charging. Hence, the amount of energy that could be shared between these devices will be determined by their meeting and charging patterns as well as their charging decisions. In Fig. 5, an example decision block with a single meeting between two users is illustrated. If both users decide to skip their charging session in the decision block, the energy exchange opportunity duration will be equal to the total meeting duration. However, if one of the users decides to use its wall charging in that decision block, that portion of their meeting has to be excluded as we assume it is not practical to exchange energy for users while being charged.

Let $\mathcal{U}_t^A$ denote the total unplugged time of user A in decision block $t \in \{1, 2, \ldots, n\}$. The charging session in a decision block will always be earlier than the discharging session within the block by definition of blocks. $\mathcal{U}_t^A$ should be either from the start of charging till the end of discharging or from the start of discharging till its end depending on the charging decision. More formally:

$$\mathcal{U}_t^A = \begin{cases} (\delta_d^A[t].t_s, \delta_d^A[t].t_e) & \text{if } X_t^A = 1 \\ (\delta_c^A[t].t_s, \delta_d^A[t].t_e) & \text{otherwise} \end{cases} \tag{3.12}$$

Here, t_s and t_e denote the start and end times, respectively.

Let $\mathcal{M}_t^{A,B}$ denote the meeting event between users A and B, $\mathcal{T}_S$ denote the speed of wireless energy transfer. The total amount of energy that can be exchanged

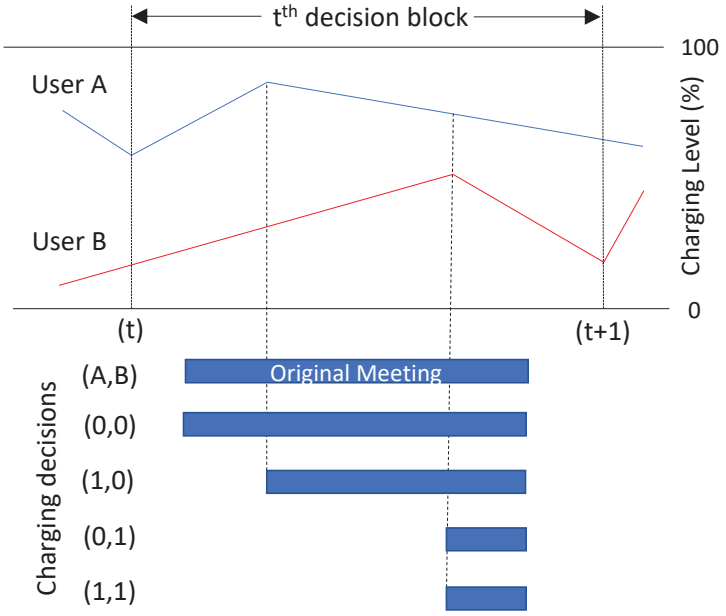

Fig. 5.: Total duration with energy exchange opportunity determined by the intersection of user meetings, charging patterns and charging decisions of users.

between A and B in decision block t, $\mathcal{E}_t^{A,B}$, can be computed by:

$$\mathcal{E}_t^{A,B} = \mathcal{I}_t^{A,B} * \mathcal{T}_S * \mathcal{T}_E \text{ where,} \tag{3.13}$$

$$\mathcal{I}_t^{A,B} = \mathcal{M}_t^{A,B} \bigcap \mathcal{U}_t^A \bigcap \mathcal{U}_t^B \tag{3.14}$$

Here, $\mathcal{I}_t^{A,B}$ is the intersection of total meeting duration between A and B and total unplugged times of A and B.

It is also important to remark that $\mathcal{E}_t^{A,B}$ should be considered as the maximum energy that could be exchanged but the actual energy exchange between users depends on the current charge level of each user device. A user device's charge level cannot exceed 100% and cannot be less than l_{min} by definition. Moreover, note that in order to reach an optimal solution at the end, the optimal energy exchange values at each individual decision block could be less than $\mathcal{E}_t^{A,B}$ even though device capacities donot

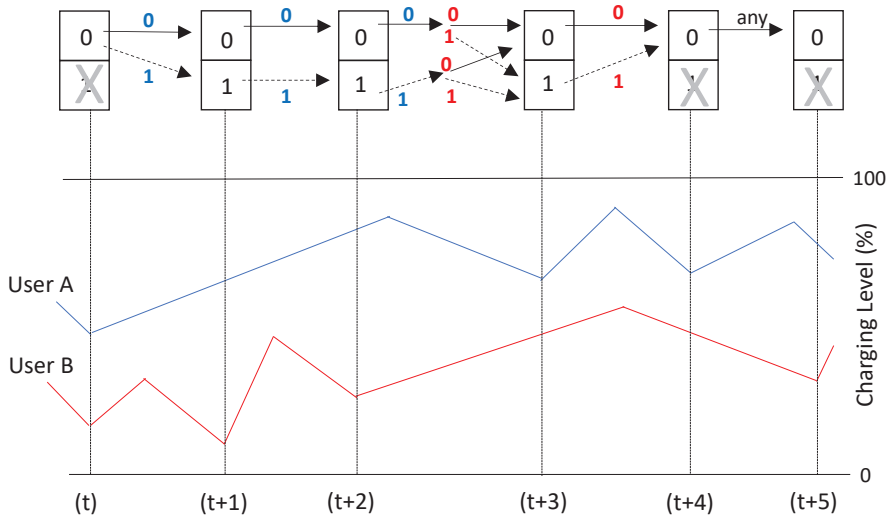

Fig. 6.: Dynamic programming table cell updates in the fourth dimension on a sample charging pattern of two users with different charging types included in decision blocks.

restrict it.

In this case, D matrix is defined as a four dimensional matrix. The first dimension represents the decision points and the second and third dimensions represent the charge level for each user. The last dimension is used to keep track of decisions made for charging sessions split into multiple decision blocks. Due to the binary decision used for skipping a charging session as a whole, the charging decision made for all portions of a charging session at different decision blocks has to match. Consider the example in Fig. 6. In the first decision block (from t to $t+1$), there is a First_Split(A) and a Full(B). Thus, updates based on different charging decisions made for user A on D matrix are written into different indexes at the fourth dimension. In the second decision block, as there is a Mid_Split(A), only the updates with consistent decisions are allowed to be made on D matrix's corresponding index at fourth dimension (e.g., there can not be skip (i.e., 0) after not skipping in previous block). In the next decision

User A/User B	Full/None	First Split	Mid-Split	Last Split
Full/None	(0,0)	(0, X_t^B)	(X_t^B, X_t^B)	(X_t^B,0)
First Split	(0, X_t^A)	N/A	N/A	(X_t^B, X_t^A)
Mid-Split	(X_t^A, X_t^A)	N/A	N/A	N/A
Last Split	(X_t^A,0)	(X_t^A, X_t^B)	N/A	N/A

Table 3.: (Source, destination) index assignments for D matrix's fourth dimension based on charging decisions of users with different types of decision blocks.

block, there is a Last_Split(A) and a First_Split(B). In this case, optimal decision for A should be selected and written on the first index (0) at fourth dimension. However, due to the split of B, the corresponding fourth dimension index for the updates is found using the B's charging decision. In the fourth decision block, as there is a Last_Split(B) with a Full(A), the final decision for user B's charging session is made and written into the first index at fourth dimension. The fifth block has a Full(A) and a Full(B), thus, only the first index at fourth dimension is used for the updates.

In Table 3, we provide (source, destination) index assignments at the fourth dimension of D matrix with different decision block type combinations. For example, for the second decision block in Fig. 6, which has a Mid_Split(A) and a Full(B), if A's decision is to skip, source index will be 0 and will be written to index 0 to keep the decision consistent. Note that some of the combinations are not possible due to the definition of decision blocks that start with the start of charging sessions.

The details of the dynamic programming based solution for cooperative charging is presented in Algorithm 2. The algorithm takes the list of all wall charging and discharging events with amounts, start and end times and finds out the minimum wall charging sessions needed to keep the both devices always more than l_{min}. The

Algorithm 2: Cooperative Charging Decision Pattern Algorithm

Input: $\delta_{\mathbf{c}}[]/\delta_{\mathbf{d}}[]$: Charging/discharging amounts; $\mathcal{M}[]$: meeting patterns

Output: Number of minimum total charging sessions for both users.

for *each decision block* D_t **do**

  $(c_A, c_B) \leftarrow$ Decide the charging types for both users

  for *each charging level* $0 \leq \mathbf{l_A} \leq 100$ **do**

    for *each charging level* $0 \leq \mathbf{l_B} \leq 100$ **do**

      for *each* (X_t^A, X_t^B) *case* **do**

        $\mathcal{I}_t^{A,B} \leftarrow$ Max duration for energy exchange with (c_A, c_B)

        $(sc, dt) \leftarrow$ Fourth dimension indexes based on current case

        for *each* $0 \leq k \leq \mathcal{I}_t^{A,B}$ **do**

          $\overrightarrow{A}$ = min(100, $l_A + \delta_c^A[\mathrm{t}]X_t$) - k*$\mathcal{T}_S$ - $\delta_d^A[\mathrm{t}]$

          $\overleftarrow{B}$ = min(100, $l_B + \delta_c^B[\mathrm{t}]X_t$) + (k*$\mathcal{T}_S$ *$\mathcal{T}_E$) - $\delta_d^B[\mathrm{t}]$

          $\overleftarrow{A}$ = min(100, $l_A + \delta_c^A[\mathrm{t}]X_t$) + (k*$\mathcal{T}_S$* $\mathcal{T}_E$) - $\delta_d^A[\mathrm{t}]$

          $\overrightarrow{B}$ = min(100, $l_B + \delta_c^B[\mathrm{t}]X_t$) - k*$\mathcal{T}_S$ - $\delta_d^B[\mathrm{t}]$

          for *each* $(l_A, l_B) \in \{(\overrightarrow{A}, \overleftarrow{B}), (\overleftarrow{A}, \overrightarrow{B})\}$ **do**

            if $l_A \geq l_{min}$ *and* $l_B \geq l_{min}$ **then**

              new = D[t][l_A][l_B][sc]+X_t^A+X_t^B

              if *new* < *D[t+1][l_A][l_B][dt]* **then**

                D[t+1][l_A][l_B][dt] = new

                T[t+1][l_A][l_B] = (l_A , l_B, sc, k)

return min$\{D[n][l_A][l_B][0]\ \forall l_A, l_B \geq l_{min}\}$

algorithm covers all four possible charging decision cases for a pair of nodes and finds out the maximum duration that could be used for energy exchanges. Then, for each possible duration less than this maximum, it finds the corresponding charge levels that will be reached by each user (lines 10-14). Considering either direction of energy exchange (i.e., when A sends and B receives ($\overrightarrow{A}$, $\overleftarrow{B}$) or when A receives and B sends ($\overleftarrow{A}$, $\overrightarrow{B}$)), it then updates the D matrix values based on previous iteration (lines 15-20). Note that the corresponding (source, destination) index values at the fourth dimension is determined using the aforementioned principle (line 9). The running time of this algorithm is $O((100)^2|D|(E))$, where E is the average shareable energy range. Brute force solution has $O(4^{|D|})$ complexity.

3.4 Network-wise Optimization

The previous section finds out the optimal collaborative charging decision patterns for a pair of nodes. In a network of smartphone users, each user can potentially consider exchanging energy with all other users. The Algorithm 2 could be extended with additional dimensions to find out an optimal solution for every size of group of users at the expense of increased complexity. On the other hand, sharing energy with multiple other users may not be practical and users may have concerns about their privacy. To this end, in this section, we focus on grouping of users into pairs and let them exchange energy with only one other user. A centralized graph based matching solution could provide the highest network-wide mobile charging relief among users. However, in reality, this may not address the individual preferences of users and may result in users not satisfied with their assignments. To address this issue, we map our problem to *stable roommate matching problem* (SRP). The goal is to find a stable matching among a group of users such that there will not exist a pair of nodes which are not assigned to each other and both prefer each other to their assigned

partners under the current matching. Note that this problem is distinct from the stable-marriage problem as the stable-roommates problem allows matches between any pair of nodes, not just between two disjoint classes such as men and women [85].

To this end, we first run the collaborative charging algorithm for every pair of nodes in the network. Then, for a given node, say A, we calculate the relieves obtained from each other user. Let n_A denote the total number of charging sessions of user A. The charging relief that user A obtains from a collaborative charging, $\mathcal{R}_{\mathcal{A}}$, is defined as the ratio of skipped charging sessions to the total number of charging sessions. That is:

$$\mathcal{R}_A = \frac{n_A - \sum_{t=1}^{n_A} X_t^A}{n_A} \tag{3.15}$$

Denoting $\mathcal{R}_A(B)$ as the user A's relief from collaborative charging with the user B, we then form a preference list for user A, $\mathcal{PL}[A]$, in the descending order of obtained relief. In some cases, however, there may be more than one user that provide the same relief to the user. To break such tie situations, we use reduction in the energy amount obtained due to the skipped charging sessions.

$$\begin{aligned} \mathcal{PL}[A] = \{u_1, u_2, \ldots u_n \mid \quad & \mathcal{R}_A(u_i) > \mathcal{R}_A(u_{i+1}) \text{ or} \\ & \mathcal{R}_A(u_i) = \mathcal{R}_A(u_{i+1}) \text{ and } J(\mathcal{R}_A(u_i)) > J(\mathcal{R}_A(u_{i+1}))\} \end{aligned} \tag{3.16}$$

Here, $J(\mathcal{R}_A(u_i))$ represents the energy saving with skipped pattern associated with $\mathcal{R}_A(u_i)$. Once each user forms its preference list as described, we then adapt Irving's algorithm [86] to find out a stable matching among users, if it exists. Note that since the matchings will be mutual, we assume that there are even number of users in the network.

Algorithm 3 shows the details of the proposed matching process. For each free

Algorithm 3: Collaborative Charging Partner Matching Algorithm

Input: a set of users $\mathcal{N}$, and their preference lists $\mathcal{PL}$

Output: Matched collaborative charging partner for all, if exists.

//step 1

for *each free user* $i \in$ *[1,* $\mathcal{N}$*] as proposer* **do**

  if $\mathcal{PL}$*[proposer] is not empty* **then**

    $u \leftarrow \mathcal{PL}[proposer]$.first()

    if *u is not proposed earlier* **then**

      Match (u, proposer)

    else

      current $\leftarrow u$.hasProposalsFrom()

      if *u prefers current over proposer* **then**

        Remove u from $\mathcal{PL}$[proposer] and *proposer* from $\mathcal{PL}[u]$

      else

        current.setFree()

        Remove u from $\mathcal{PL}$[current] and *current* from $\mathcal{PL}[u]$

        Match (u, proposer)

for *each user i matched to a user m* **do**

  Remove i from $\mathcal{PL}$[r] and r from $\mathcal{PL}[i]$, $\forall r$ with rank(r) > rank(m)

//step 2

for *each user* p_i *with* $|\mathcal{PL}[p_i]| > 1$ **do**

  Find a cycle $(p_i, q_i, p_{i+1}, q_{i+1}, \ldots q_{s-1}, p_s{=}p_i)$, where

  q_i = second preference in $\mathcal{PL}[p_i]$ and p_{i+1} = last preference in $\mathcal{PL}[q_i]$

  Remove q_i from $\mathcal{PL}[p_{i+1}]$ and p_{i+1} from $\mathcal{PL}[q_i]$ $\forall i$

return matching if $\nexists$ a user i with $|\mathcal{PL}[i]| > 1$

user not assigned a partner, the first user in the preference list is proposed. If the proposed user has not been matched with any other user yet, it immediately accepts the proposal and a pending matching is assigned. On the other hand, if the proposed user has already been matched with some other user, it checks if the new proposer has better rank in its preference list than the current matched user. If that is the case, previous proposer is set free and it is matched with this new proposer. Otherwise, both users remove each other from their preference lists mutually. Once a user is assigned a partner, it also deletes all other users in its preference list with ranking more than the assigned user. In some rare cases, this process may end up with some users having still more than 1 users in their preference lists. In that case, a further elimination is conducted with some special cycles of users described in lines 20-23. At the end, if each user has only one other user in their preference lists, the stable matching is obtained.

3.5 Evaluation

In this section, we first provide results of running conservative and cooperative charging on an example pattern of two users. Then, we conduct an empirical analysis using various mobile datasets with user meeting and charging patterns and find out the potential charging relief in realistic scenarios[2].

3.5.1 Numerical Example

We have used the charging patterns for two users shown in Fig. 4 and run the optimization algorithms for both cases. Table 4 shows the optimal charging decision

[2]The Java codes developed to generate the results in this section are available at https://github.com/aashish33128/Mobile-Charging-Relief/tree/master/EnergySharing.

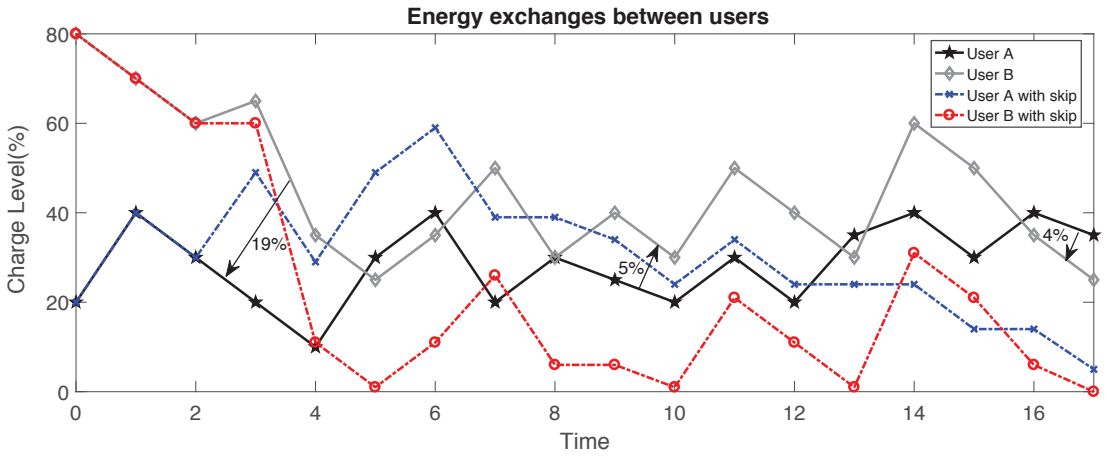

Fig. 7.: Charging patterns and skips after cooperative charging. Arrows show the direction and the amount of energy shared between the users.

results for both cases. In conservative case, decision blocks consist of charging cycles but in collaborative charging the number of decision blocks is more than the actual charging cycles. Thus, in Table 5, we show the actual decisions made for each decision block in collaborative charging.

In conservative scenario, the results show that node A could have skipped 4^{th} and 6^{th} charging blocks, while node B could have skipped its 1^{st} and 4^{th} blocks (skipping 1^{st} and 3^{rd} would also be optimal). This results in a total of 4 skips for both nodes.

Scenario	**Charging Sessions**	**1**	**2**	**3**	**4**	**5**	**6**
Conservative	**A's decisions**	1	1	1	0	1	0
	B's decisions	0	1	1	0	1	N/A
Cooperative	**A's decisions**	1	1	0	1	0	0
	B's decisions	0	1	0	1	1	N/A

Table 4.: Optimal charging decisions in each charging scenario.

Decision Blocks	**1**	**2**	**3**	**4**	**5**	**6**	**7**	**8**	**9**	**10**
Energy (B → A)	0	19	0	0	0	0	0	0	0	0
A's decisions	1	0	1	1	0	0	1	0	0	0
Energy (A → B)	0	0	0	0	0	5	0	0	0	4
B's decisions	0	0	0	1	0	0	1	0	1	0

Table 5.: Charging decisions for each decision block in cooperative case.

In cooperative charging scenario, out of 10 decision blocks, user A is able to skip 6 of them. However, not all of these are independent decisions as well as some of these decision blocks with skip decisions have only discharging. Similarly, for user B, 7 of them can be skipped. Note that there are multiple energy exchanges between users in order to get to the optimal point. As the decision blocks do not correspond to the actual individual charging cycles of users, the skipping decisions for each decision block have to be converted to the skipping pattern for charging cycles. From Fig. 7 and Table 5, we can deduce the original charging decision sequence for user A and user B shown in Table 4. This results in a total of 5 skips for both nodes, showing the advantage of cooperative P2P sharing over conservative case. To achieve that both node A and B share energy between each other and receive energy from each other. Fig. 7 shows the charging patterns after the optimal skips are done. Here, we assume that when a user skips a wall charging, a minimal/zero discharge happens during that duration in this example, however, a discharge could have been applied with an average discharging rate during a skipped charging sessions and algorithms could be updated accordingly.

3.5.2 Empirical Results

3.5.2.1 Datasets

Mobile devices should be in close proximity to be able to transfer power. In order to see the potential benefit of the proposed P2P energy sharing for charging relief of users in real settings, we have used several mobile network datasets with meeting patterns of user devices. These datasets mainly contain the logs of device-to-device (D2D) interactions of different types of wireless devices carried by people. While the D2D communication range is in the order of several meters, such interactions could be considered as an indication of users seeing each other and potentially asking for energy exchange from each other. Each of these datasets represents a different environment with a different number of users and durations [87]:

- **Haggle dataset:** [88] These are the Bluetooth sightings recorded between the iMotes carried by 41 attendants of Infocom Conference held in Miami in 2005. It spans a four day period.

- **Cambridge dataset:** [89] These are the Bluetooth recordings among 36 students with iMotes from Cambridge University for a duration of almost two months.

- **MIT Reality dataset:** [90] It consists of the mobility traces of 97 Nokia 6600 smart phones carried by MIT students and staff during an academic year. We used data from the three month period of Spring semester.

While the above datasets provide information about the meeting patterns of users, they do not include battery charge level information of the devices. Assuming that the battery energy levels of the devices are independent from the contact

patterns of their users, we use another dataset to extract that information and combine charging and meetings patterns of user devices using the time domain of these datasets.

- **DeviceAnalyzer dataset** [91]: It includes all kinds of logs of Android users who downloaded the app worldwide. For the experiment, we have extracted 9 days of battery charging status information from 40 users.

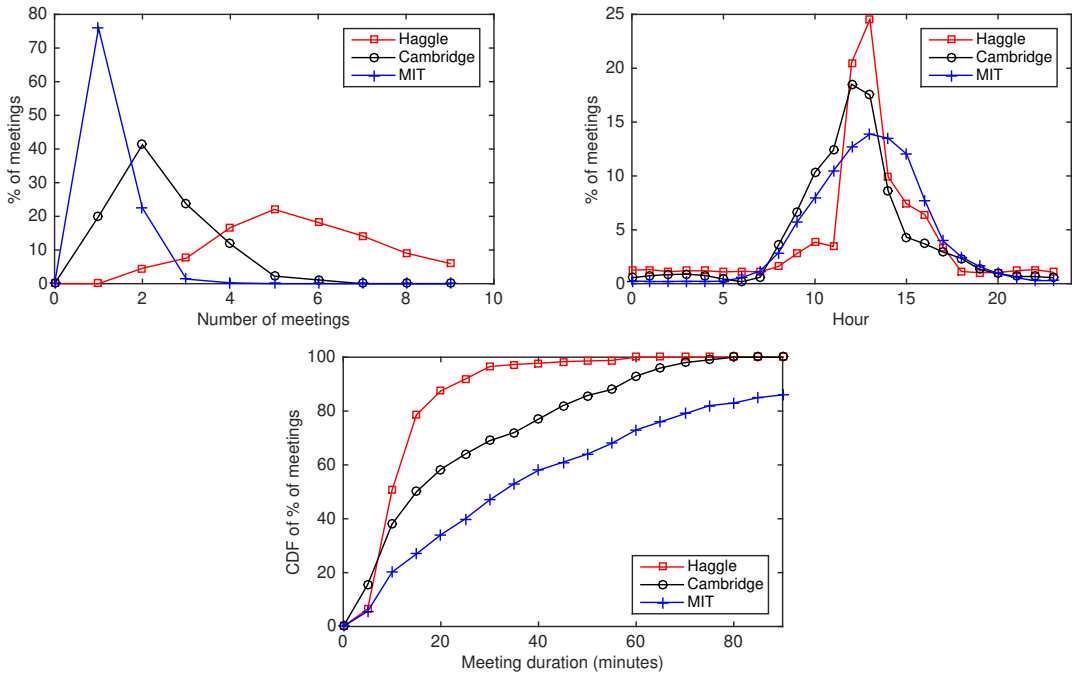

Fig. 8.: Statistics from real mobile network traces: a) distribution of number of meetings between pairs of nodes, b) hourly distribution of meeting times between nodes during a day, and c) distribution of meeting durations.

Having these datasets, we have used the following methodology to merge the charging and meeting patterns of users from different datasets. We first extract the meeting count distribution among pairs (Fig. 8-a), the hourly meeting time distribution in a day (Fig. 8-b) and the meeting duration distribution among all meetings

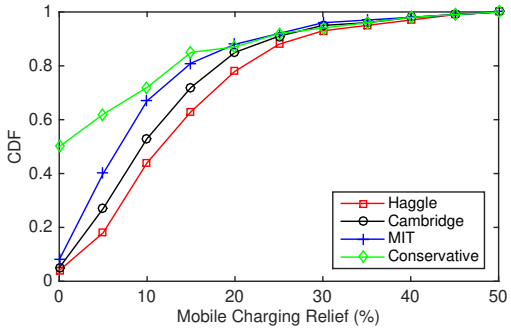

Fig. 9.: CDF of mobile charging relief obtained among all users and pairs with conservative and collaborative charging, respectively.

(Fig. 8-c). Then using the 40 users data from DeviceAnalyzer [91] with charging patterns, we assign them meetings from the aforementioned meeting count, time and duration distributions. Note that the user meeting patterns from different datasets are different from each other. In general, users in Haggle dataset have the highest number of daily meetings with the shortest durations. However, as expected naturally, the meeting time distributions are similar (e.g., with the highest frequency around lunch time).

3.5.2.2 Simulation Results

We first run the conservative charging algorithm for each of the 40 users and collaborative charging algorithm for each of the 780 pairs of nodes to obtain the mobile charging relief in each case (with $\mathcal{T}_S$=1%/min and $\mathcal{T}_E = 1$). Each of the results here is the average of 10 different runs. Fig. 9 shows the CDF of the relief among all users and pairs for conservative and collaborative charging, respectively. Note that each cooperative charging result with different dataset used for meeting pattern generation is shown with a legend of the corresponding dataset. The results show that almost half of the users can not have any charging relief with conservative charging, while there

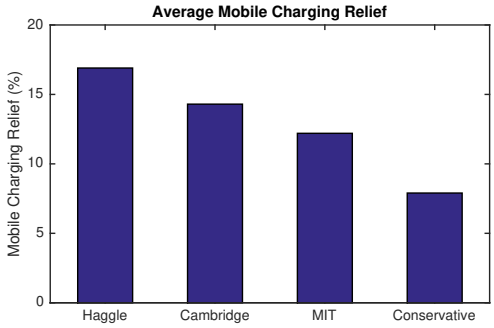

Fig. 10.: Average mobile charging relief with conservative and different collaborative charging cases.

are some users who can obtain up to 50% relief. In collaborative case, only in a few of the pairs, users cannot experience any relief. Moreover, the number of users that can experience high relief increases remarkably thanks to the power of sharing. Comparing the collaborative charging results obtained with different datasets, we observe that users obtain the highest relief with Haggle dataset while the lowest relief is obtained with MIT dataset. This is because in Haggle dataset users have more meeting than in others, which then provides more energy exchange opportunity to users yielding higher charging relief. MIT data has the smallest number of meetings. Even though the durations are longer than in other datasets, due to the fewer number of meetings, the lowest relief is obtained. However, it is still more than the relief users can achieve by conservative charging. Cambridge dataset has characteristics in between the other two datasets. Thus, a performance in between their performance is obtained.

In Fig. 10, we show the average mobile charging relief obtained for users in the network with conservative and collaborative charging. For collaborative charging, the results show the average relief obtained by users assigned after running optimal charging partner assignments in Algorithm 3. Results with Haggle dataset shows the

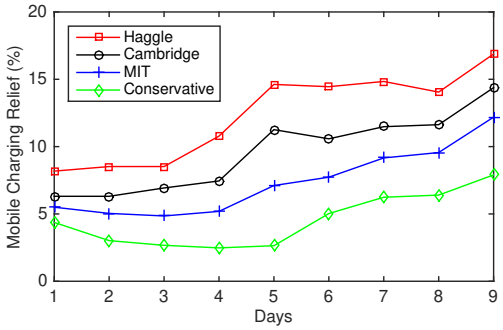

Fig. 11.: Average mobile charging relief with different number of days of data used.

highest average relief due to the aforementioned reasons. This is also the double of the relief users could experience with conservative charging only.

Next, to understand the impact of data size on the results, we obtain average charging relief with fewer than 9 days of DeviceAnalyzer dataset. Fig. 11 shows these results. Here, each data point indicates the cumulative usage of dataset. For example, results at point 5 shows the results obtained with 5 days of data from the beginning. The results show that the average user charging relief remains somewhat constant after a few days, given the same meeting patterns. The jump on the last day and the small savings in the first 3 days are due to the impact of partial charging/discharging sessions included in these end cases. We also observe that most of the users have discharging only sessions during the first day, which reduces the average charging relief for all users in the network. Similarly, for the last charging cycle, most of these cycles have only the portion of their charging session without any discharging. Thus, most of these last charging sessions are skipped easily increasing the average relief for the 9 day result.

Fig. 12 shows the impact of transfer efficiency and speed on average mobile charging relief in Haggle dataset. As expected, the results clearly show that the

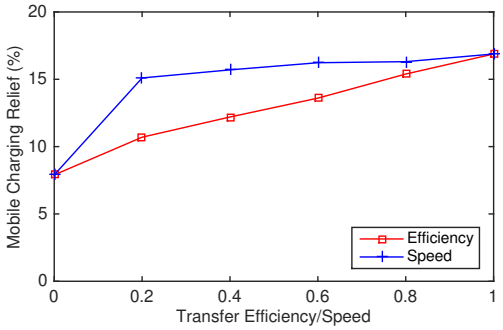

Fig. 12.: Impact of wireless power transfer efficiency and speed on the average mobile charging relief.

relief will increase if the wireless energy sharing between devices is more efficient (when $\mathcal{T}_S$=1%/min). The figure also shows that when the transfer speed is 0, it is equal to the conservative case results but when the transfer speed increases, there is a significant gain in charging relief (when $\mathcal{T}_E = 1$). However, the result is not increasing linearly because contact duration becomes dominant and optimal energy that is exchanged within the decision block does not change much. A slower but efficient transfer also performs well.

3.6 Conclusion

In this chapter, motivated by the recent technologies enabling wireless energy sharing between mobile devices, we investigate to what extent the burden of charging process on users could be released. We develop a dynamic programming based optimization model and find out the minimum number of charging sessions that would be sufficient for users to keep their devices with the energy they need through utilization of excessive energy from other users in the vicinity. We first study both conservative and collaborative charging. Then, in order to achieve a network-wide charging relief among a group of users, we map our problem to roommate matching problem and

find out the best matching among users that will achieve the highest network-wide relief while satisfying all users with their assigned partners. With the empirical results based on different datasets of user meetings and charging patterns, we observe that users can achieve up to 13-17% relief without affecting their existing usage habits of mobile devices.

CHAPTER 4

CONTENT DELIVERY WITH P2P ENERGY SHARING

4.1 Introduction

The dynamic mobility and connectivity of the nodes in opportunistic networks makes the dissemination and the delivery of content very challenging. There have been numerous works [59, 92, 93] in the literature that look at this problem under different settings and propose different routing algorithms in such networks. While the main focus has been to decide on the selection of the relay nodes to optimize the routing performance (e.g., better delivery ratio), most of the time it is assumed that there is already an incentive to carry the others' messages. Some of the works have studied the incentive oriented routing through tit-for-tat style [94] or credit-based [95] solutions. Some others have also considered the problem under social-selfishness [96] of nodes (i.e., being selfish to strangers and unselfish to friends) and provided trust management based solutions. However, such solutions compensate the actual energy consumption of relay nodes indirectly.

In some recent interesting works [33, 74, 75], this problem has been studied through energy sharing to relay nodes, providing direct compensation for the energy loss of nodes. In other words, a node with a content to be delivered to a destination transfers not only the content (e.g., copy of the message) but also sufficient energy to relay nodes, as an incentive to them to carry this content to the destination. Note that such an energy sharing between nodes can be performed in a convenient way, thanks

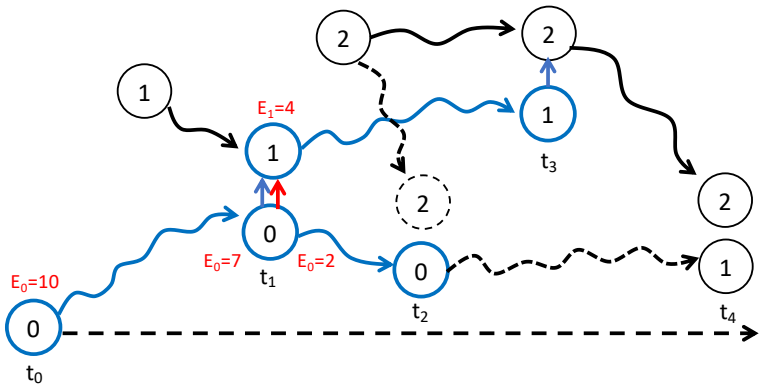

Fig. 13.: An illustration of energy sharing based content delivery in opportunistic networks, where energy is used as an incentive to carry a message copy.

to the recent advances [12] in wireless power transfer[1] and related developments to integrate them to mobile devices [4, 97, 27]. In the previous work, however, the problem is studied in a limited scenario, in which only the source node with unlimited energy resources gives the content and the energy to relay nodes with the goal of minimum energy consumption for the delivery. In a more general scenario, source node may have a limited energy budget for the delivery. Moreover, both the source node and the relay nodes can distribute the content and energy to other relay nodes met. However, this makes the problem more challenging as a more comprehensive approach has to be followed to determine not only the distribution of the content to relay nodes but also the amount of energy to be given to each of them.

4.1.1 Motivating Example

Consider the example in Fig. 13 with source node 0 having a message to deliver to destination node 2 and having an initial energy budget of 10 units to be used in the

[1]While we do not restrict the proposed solution in this work to only wireless power transfer based energy sharing, we also consider the impact of associated parameters (e.g., transfer efficiency) in the design of the proposed solution.

delivery of this message (i.e., node's actual energy may be more). Assume that each node consumes 1 unit of energy at every time unit while carrying the message. When node 0 meets node 1 at time t_1, it has a remaining energy budget of 7 units (as it spent 3 units of energy from t_0 to t_1). Node 0 predicts that its energy is more than enough to carry the message until it meets the destination with a high probability. Thus, to increase the delivery probability further, it decides to share 5 units of its energy with node 1 to have a better collaborative delivery probability than its individual delivery probability. Note that, due to the transfer efficiency, node 1 can only get 4 units of energy. After t_1, both nodes have a copy of the message and try to meet with the destination for delivery. Node 1 carries the message only 4 time units and node 0 carries the message only 2 times units after t_1. The message is delivered to node 2 at time t_3 by node 1. However, if node 2 were to follow an alternative predicted path, node 0 would deliver the message.

In a more general context, consider that node 0 and node 1 has met and node 0 has a message with some budget of energy. The options for node 0 are (i) to forward the content and available energy budget entirely (i.e., without keeping a copy and potentially with some loss during content/energy transfer), (ii) to keep the content and energy totally, or (iii) to give a copy of the content with some energy. The first two options are exactly similar to the decisions made in single-copy or forwarding based routing algorithms [98]. However, the third option is different than multi-copy based routing algorithms [99, 100, 101, 102, 103] as it divides the available energy to keep the content among nodes, thus essentially decreases time-to-live (TTL) of the messages or the deadline for delivery (on the contrary, in multi-copy based routing algorithms, the deadline is not changed). While multiple nodes carrying the content increase the likelihood for delivery, their smaller TTL values decrease the delivery chance. Such content and energy sharing can indeed provide a better cooperative

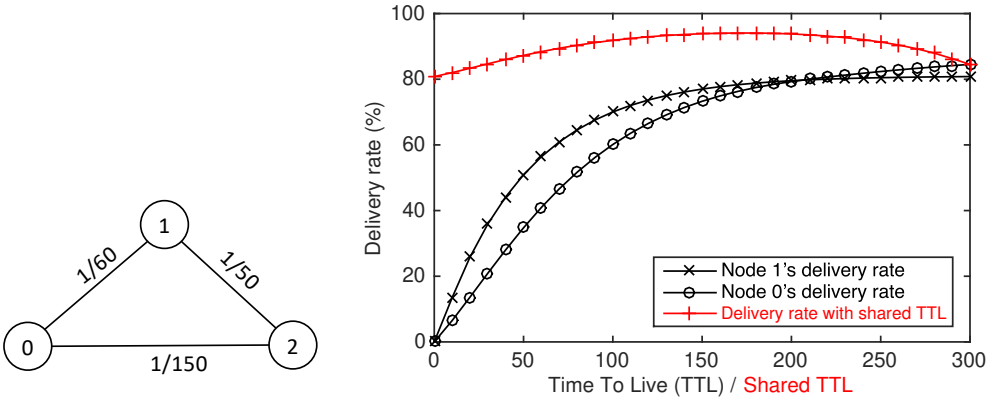

Fig. 14.: An example opportunistic network with mean intermeeting times denoted as the weights of the edges on the graph.

delivery probability with a careful and thorough decision process. In particular, in mobile social networks where messages can get lost during opportunistic content transfers between nodes, the benefit gets more pronounced.

Consider the network graph in Fig. 14 which shows the mean intermeeting times of three nodes as the link weights. The lower chart shows the delivery probability of both node 0 and node 1 for destination 2 for different TTL values. Note that for node 0, this represents a *comprehensive* [99] delivery rate including both the direct delivery and delivery through node 1, while for node 1 it is the direct delivery rate. We also assume a link loss rate of 0.1 (i.e., a message is lost with 0.1 probability during transfer from a node to another), thus the expected delivery rates will only reach 90% at most. If node 0 meets node 1 and has a remaining TTL budget of 200 time units or less (which could be obtained by dividing energy budget available by energy consumption rate), the combined delivery rate (shown in red) suggests that it should forward both the content and energy entirely as node 1 offers better delivery rate. However, if it had TTL budget of 300 time units at the meeting time, the best strategy would be sharing of around half of the energy (or the corresponding

TTL) with a copy of the content (assuming energy consumption rates of the nodes are similar and there is no loss during energy transfer).

4.1.2 Contributions

In this chapter, we study the optimal content delivery problem through sharing of both the content and the energy among the nodes in a mobile social network. The content delivery in mobile social networks happens through opportunistic non-deterministic meetings of nodes and the design of most protocols usually depends on the analysis of historical contact information [104] with the expectation that the mobility of nodes shows long-term regularities (e.g., friendship [59]). That is, for example, if some pairs of nodes meet more frequently compared to other pairs, the same is in general expected consistently over time. In this chapter, we consider a mobile social network where the long-term mean intermeeting times between nodes can be estimated from the contact history of the nodes. We assume each node has a complete information about the intermeeting times between all pairs of nodes in the network. However, in simulations, we relax this assumption and show the performance of the proposed algorithm with partial available information. Based on the available knowledge and the source's limited energy budget, our goal is to find the optimal policy for both content and energy sharing among nodes to achieve the best delivery rate. We utilize optimal stopping theory [105] and dynamic programming [106] to model and solve this problem under different settings (e.g., link loss rate, transfer efficiency rate). We also evaluate the performance of the proposed sharing based solution with simulations and show its benefit over just forwarding/keeping based strategy.

4.1.3 Optimal Stopping Theory

The theory of optimal stopping [105] deals with the problem of deciding the optimal time to take a given action based on a set of sequential observations to maximize an expected reward or to minimize an expected cost. These observations are usually assumed to be random variables with a known joint distribution. Well-known problems solved via optimal stopping theory include secretary hiring problem [107] and parking problem.

In an optimal stopping rule problem, you may observe a sequence X_1, X_2, ... for as long as you wish, where X_1, X_2, ... are random variables whose joint distribution is assumed to be known. For each stage $t = 1, 2, \ldots$ after observing X_1, X_2, ... X_t, you may stop and receive the known reward y_t, or you may continue and observe X_{t+1}. The optimal stopping rule is to stop at some stage t to maximize the expected reward.

An optimal stopping rule problem has a finite horizon if there is a known upper bound on the number of stages at which one may stop. In other words, if there are only T observations possible before making a decision, the problem has a horizon of T. Such finite horizon optimal stopping problems can be solved by using *backward induction* method. That is, as the last stage to stop is T, optimal rule for the stage $T-1$ can be found first, then based on this optimal rule for stage $T-1$, optimal rule at stage $T-2$ can be found and so on. This process can be chained until the initial stage 0. As defined in [105], let $V_t^{(T)}$ $(1 \leq t \leq T)$ represent the maximum expected reward one can obtain starting from stage t and let $V_t^T = y_T$ and then inductively for $t = T-1$, backward to $t = 0$,

$$V_t^{(T)} = \max\{y_t, E(V_{t+1}^{(T)})\}. \tag{4.1}$$

That is, we compare the reward (i.e., y_t) for stopping at stage t, with the expected reward $E(V_{t+1}^{(T)})$ to get by continuing to the next stage under the assumption that we will use the optimal rules for all stages from $t+1$ to T. If the $V_t^{(T)} = y_t$, that is $y_t \geq E(V_{t+1}^{(T)})$, it is better to stop at stage t. Otherwise, we continue making new observations.

4.2 System Model

4.2.1 Assumptions

Let $\mathcal{N}$=$\{0, 1, 2 \ldots n-1\}$ denote the set of $|\mathcal{N}| = n$ nodes in a mobile social network. Without loss of generality, we assume that 0 is the source node and $n-1$ is the destination node. The message at the source node has to be delivered to the destination node. We assume that source node has an initial energy budget, $\mathcal{E}$, to be used in the delivery of the message. Note that this energy budget can easily be converted to an estimated time-to-live (TTL) value for the message by dividing the energy by the energy consumption rate of the node, as it will be shown in next section. This also helps modeling the problem using optimal stopping theory with discrete time steps. A message is maintained until the TTL value lasts. When the source node is met with another node, it determines if it is useful to give a copy of the content and how much of its energy should be shared.

We assume that all nodes in the network have energy receiving and transferring capabilities (e.g., Samsung Galaxy S10, Huawei Mate 20 Pro) and energy sharing could be achieved via wireless energy transfer with a transfer efficiency of λ. The encountered node informs the source node or any other relay who has the content about how different its energy consumption than the source node's energy consumption rate, so that corresponding TTL at the encountered node with a specific amount of trans-

ferred energy could be found. The meetings of different pairs of nodes are assumed independent and the intermeeting times are exponentially distributed. However, the proposed algorithm can easily be updated under different distribution assumptions. We assume that the mobility of nodes exhibits long-term regularities, as it is assumed in related previous work [33, 99]. Thus, we initially assume that each node has the knowledge of mean intermeeting time information, $I_{i,j}$, for all pairs of nodes. We then relax this assumption and study the performance of the proposed solution when different levels of partial information is available to the nodes. We also assume that the links between nodes are lossy and the content will be dropped with some probability, denoted by γ, during transfers between nodes. This notion of link loss rates can be considered as a result of link failures or faulty relay nodes in the network which accept the incentive but deviates away from the delivery process. The notations used throughout the chapter are summarized in Table 6.

4.2.2 Energy and Residual Time-to-Live relation

Let $\mathcal{E}_i$ denote the energy budget of the node i to be used in the delivery of the message, and e_i denote its average energy consumption rate. The discrete remaining time-to-live (TTL) value of the message (i.e., the duration the message will be kept by node i), t_i, will then be:

$$t_i = \mathcal{E}_i / e_i \tag{4.2}$$

When this node meets with another node j, it can either keep, forward or share the content/energy with j if it estimates that the likelihood of the message delivery will increase. Let $\mathcal{E}_{i \to j}(t_i)$ denote the optimal energy that needs to be shared from node i to node j when it has a TTL of t_i. The corresponding remaining TTL values

Notation	Description
n	Total number of nodes in the network.
$\mathcal{I}_{i,j}$	Mean intermeeting time of nodes i and j.
$\mathcal{M}_{i,j}$	Meeting probability of two nodes i and j at each time slot.
U	The size of each time slot.
$\mathcal{E}$	Initial energy budget to be used in the delivery of the content.
$\mathcal{E}_i$	Energy incentive held by node i to be used in the delivery of the content.
t_i	TTL of the content carried by node i.
t_i^+	TTL of the content carried by node i in the next time slot.
$\mathcal{E}_{i\to j}(t_i)$	The optimal energy that needs to be shared from node i to node j when it has a TTL of t_i.
e_i	Energy consumption rate of node i at each time slot.
$\mathcal{P}_{i,d,k,t}$	Probability that the content is delivered from source i to destination d with remaining TTL value of t in up to k hops.
K	The maximum number of hops that a content can be forwarded before it reaches destination.
γ	Link loss rate (i.e., content drop rate) between two nodes.
λ	Energy transfer efficiency rate.

Table 6.: Notations used in Chapter 4

of each node after this exchange (i.e., in the next time unit) will be:

$$t_i^+ = \frac{\mathcal{E}_i - \mathcal{E}_{i\to j}(t_i)}{e_i} - 1 \tag{4.3}$$

$$t_j^+ = \begin{cases} \frac{\lambda \mathcal{E}_{i\to j}(t_i)}{e_j}, & \text{if } r[0,1] \leq \gamma \\ 0, & \text{otherwise} \end{cases} \tag{4.4}$$

Here, $r[0,1]$ is a random number between 0 and 1. Note that the TTL value of node j should be estimated by taking into account the energy consumption rate of node j as well as the energy transfer efficiency, λ. For node i, it also needs to consider the energy consumption at the current time (hence the -1 in (4.3)). If the content transfer is not successful due to the link loss rate, the TTL value of node j, will be assigned to 0, as having energy incentive for a message not received will be nonsense.

4.2.3 Optimal Content and Energy Sharing

We divide the time into equal size slots and assume that in each time slot, a node can either meet or not meet with another node. The intermeeting times of two nodes i and j are assumed to follow an exponential distribution with a mean of $\mathcal{I}_{i,j}$. Then, the meeting probability of two nodes i and j in each time slot of size U, denoted as $\mathcal{M}_{i,j}$, can be computed by

$$\mathcal{M}_{i,j} = 1 - e^{-U/\mathcal{I}_{i,j}}. \tag{4.5}$$

We adopt exponential distribution for intermeeting time distributions between nodes since it is a relatively general model [99, 100, 101, 102], however, the proposed solution can be adapted to other distributions.

In our model, we follow a similar terminology introduced in [99] and adopt a hop count limited opportunistic forwarding protocol. That is, there is a hop count limit of K indicating the maximum number of hops a message can be forwarded before it reaches destination. Such a forwarding scheme also helps achieve scalability as it can limit the forwarding cost per message delivery which is usually assumed to be the major cost for routing in mobile social networks. When a message with a hop limit of k is forwarded to another node, its remaining hop count limit becomes $k-1$. When a node has a message with $k = 0$, it can no longer forward the message to another

TTL	**Decision with forwarding**	
t	$P_{i,d,k,t}$	
$t-1$	Not Forward $P_{i,d,k,t-1}$	Forward $P_{j,d,k-1,t-1} \times (1-\gamma)$

TTL	**Decision with sharing**	
t	$P_{i,d,k,t}$	
$t-1$	Not Share $P_{i,d,k,t-1}$	Share (1-γ) $\times$ [1-(1-P_{i,d,k_i^*,t_i^*})$\times$ (1-P_{j,d,k_j^*,t_j^*})] + (γ) $\times$ P_{i,d,k_i^*,t_i^*}

Table 7.: Decisions with forwarding and sharing.

node but still can deliver it to the destination.

Let $\mathcal{P}_{i,d,k,t}$ denote the delivery probability of a message at node i for destination d with a remaining hop count of k and a remaining time-to-live (TTL) value of t. The direct delivery probability of the message, with $k = 0$, can be estimated by,

$$\mathcal{P}_{i,d,0,t} = \left(1 - e^{-tU/\mathcal{I}_{i,d}}\right) \times (1-\gamma) \tag{4.6}$$

The first part defines the meeting probability of node i with node d during t time slots and the second part considers the likelihood that the content will be lost during transfer, hence it will not be delivered.

When node i meets with another node j, the optimal forwarding decision can be made by simply comparing $\mathcal{P}_{i,d,k,t-1}$ with $\mathcal{P}_{j,d,k-1,t-1} \times (1-\gamma)$ (as shown in Table 7). That is, within the same remaining time of $t-1$, if node i has a higher expected delivery rate with k hops than the delivery rate node j can achieve with $k-1$ hops given that the content is successfully transferred to node j with probability $(1-\gamma)$, the optimal decision becomes not to forward the content to node j. Otherwise, forwarding

Algorithm 4: $P_{i,d,k,t}$ calculation with optimal forwarding

1 $P_{i,d,k,t} \leftarrow M_{i,d} \times (1-\gamma)$

2 $R_p \leftarrow 1 - M_{i,d}$

3 **for** $\forall j \in \mathcal{N}$ *s.t.* $j \neq i$ *and* $j \neq d$ *and* $M_{i,j} > 0$ **do**

4 $\quad P_j \leftarrow P_{j,d,k-1,t-1} \times (1-\gamma)$

5 $\quad$ **if** $P_j > P_{i,d,k,t-1}$ **then**

6 $\quad\quad P_{i,d,k,t} = P_{i,d,k,t} + R_p \times M_{i,j} \times P_j \times (1-\gamma)$

7 $\quad\quad R_p = R_p - R_p \times M_{i,j}$

8 $P_{i,d,k,t} = P_{i,d,k,t} + R_p \times P_{i,d,k,t-1}$

the content to node j will be better on average. Note that this is different than the optimal forwarding strategy presented in [99, 104] as it considers keeping a copy of the content at node i even it will be forwarded to node j, thus, it determines the optimal strategy through cumulative delivery probability of both copies and determines the optimal strategy accordingly. The likelihood of unsuccessful transfer of the content due to link failures is also not considered in [99, 104] .

In order to calculate the expected delivery probability, $\mathcal{P}_{i,d,k,t}$, for each node pair (i, d) and different k and t values, the problem can be modeled as a finite horizon optimal stopping problem and can be estimated using backward induction method. That is, we first calculate $\mathcal{P}_{i,d,k,2}$ based on $\mathcal{P}_{i,j,k-1,1}$, $\forall j \neq i, d$ and $\mathcal{P}_{i,d,k,1}$, which can be calculated using (4.6). Then, we continue calculating $\mathcal{P}_{i,d,k,3}$, $\mathcal{P}_{i,d,k,4}$, and so on.

The calculation of delivery probability $\mathcal{P}_{i,d,k,t}$ under optimal forwarding strategy is shown in Algorithm 4. It is first initialized to direct meeting probability with a potential loss (line 1) and for each node, j, that is different than destination, if forwarding to j is considered better in terms of delivery probability (line 5), the

expected increase in delivery probability through node j is added to $\mathcal{P}_{i,d,k,t}$. Note that due to the sparse nature of mobile social networks similar to delay tolerant networks, it is assumed that each node meets one another node at each time slot. Thus, the remaining probability, denoted by R_p, is calculated for each node j, by excluding the meeting probabilities with other nodes considered. Once the estimated probability increase is added from all other nodes, finally, with remaining probability, the probability of delivery from current node with one less remaining TTL value is added (line 8).

In optimal forwarding strategy, as the message is either forwarded or kept entirely, the associated strategy for energy sharing becomes either transfer or keep the entire energy, respectively. However, as sharing can potentially increase the delivery probability, as shown in Fig. 14, the calculation of delivery probability $\mathcal{P}_{i,d,k,t}$ under optimal sharing strategy should consider the split of energy and hop counts with each met node j that can achieve the best delivery probability increase. Algorithm 5 shows this calculation. Lines 7-18 show the process of finding the best TTL split (t_i^*, t_j^*) and hop split (k_i^*, k_j^*) between node i and a met node j that achieves the highest delivery probability, P_j^*. Note that each P_j calculation needs to consider potential loss during transfer thus, with probability γ, P_j is equal to node i's own delivery probability with t_i, k_i pair, while with probability $(1-\gamma)$ it is equal to the cumulative delivery probability with the corresponding optimally split TTL and hop counts, which is defined as

$$1 - (1 - P_{i,d,k_i^*,t_i^*}) \times (1 - P_{j,d,k_j^*,t_j^*}). \tag{4.7}$$

Once the maximum delivery probability with each neighbor j is found through optimal TTL and hop split, it is compared with individual delivery ratio of node i and if splitting is considered better, it is added to the comprehensive delivery probability of

Algorithm 5: $P_{i,d,k,t}$ calculation with optimal sharing

$P_{i,d,k,t} \leftarrow M_{i,d} \times (1-\gamma)$

$R_p \leftarrow 1 - M_{i,d}$

for $\forall j \in \mathcal{M}$ *s.t.* $j \neq i$ *and* $j \neq d$ *and* $M_{i,j} > 0$ **do**

  $P_j^* = 0$

  $(t_i^*, t_j^*) = (t-1, 0)$

  $(k_i^*, k_j^*) = (k, 0)$

  for $\forall t_i \in [0, t-1)$ **do**

    $t_j = (t_i - 1) \times e_i/e_j \times \lambda$

    for $\forall k_i \in [0, k-1]$ **do**

      $k_j = k - 1 - k_i$

      $P_j = (1-\gamma) \times [1 - (1 - P_{i,d,k_i,t_i}) \times (1 - P_{j,d,k_j,t_j})] + (\gamma) \times P_{i,d,k_i,t_i}$

      if $P_j^* < P_j$ **then**

        $P_j^* = P_j$

        $(t_i^*, t_j^*) = (t_i, t_j)$

        $(k_i^*, k_j^*) = (k_i, k_j)$

  if $P_j^* > P_{i,d,k,t-1}$ **then**

    $P_{i,d,k,t} = P_{i,d,k,t} + R_p \times M_{i,j} \times P_j^* \times (1-\gamma)$

    $R_p = R_p - R_p \times M_{i,j}$

$P_{i,d,k,t} = P_{i,d,k,t} + R_p \times P_{i,d,k,t-1}$

node i, as in the optimal forwarding strategy case. Finally, with remaining probability, R_p, the probability of delivery by current node i with one less remaining TTL value is added.

Table 7 shows the summary of comparisons that need to be made for a decision

Parameter	Value
n	36, 41, 50.
$\mathcal{I}_{i,j}$	Obtained from datasets.
$\mathcal{E}$	16, 8, 8 hours of energy
γ	0.1
λ	0.98
e_i	[0.95, 1.05] units of energy per time slot
L	6 relay nodes
K	4 hops

Table 8.: Simulation settings for Chapter 4

under forwarding and sharing cases. Algorithms 4 and 5 show the calculation of $P_{i,d,k,t}$ for these scenarios for a specific (i, d, k, t) tuple. Once it is calculated for every possible tuple following the backward induction order, the actual forwarding or sharing decision can be made by checking these values from the corresponding tables.

4.3 Evaluation

In this section, we evaluate the performance of the proposed energy sharing based content delivery process. Next, we first list the algorithms compared, performance metrics used, and describe how the simulations are set. Then, we provide the simulation results and analyze the impact of several parameters on results. The list of the parameters and their values used in simulations are shown in Table 8.

4.3.1 Algorithms in Comparison

Since energy is used as an incentive to relay nodes to carry the content received from other nodes and defines the time-to-live (TTL) value of the message, we define the algorithms to compare in terms of their impact on the TTL of the message:

- *TTL sharing:* This corresponds to the proposed optimal sharing based strategy obtained with Algorithm 5. TTL is shared with the met node in the amount that will provide the most significant expected benefit in delivery ratio.

- *TTL forwarding:* This corresponds to the optimal forwarding strategy obtained with Algorithm 4. TTL is either fully forwarded (with loss) to the met node or kept fully depending on whichever provides higher expected delivery ratio.

- *TTL spraying:* This is a modified version of well-known Spray-and-Wait [102] algorithm within the context of energy and TTL sharing based delivery. Source node distributes the message to L different relay nodes (who can directly meet with destination[2]) together with its $1/L$ of initial TTL budget. If the remaining TTL budget is less than that, the entire remaining TTL is forwarded.

4.3.2 Performance Metrics

We use the following metrics in the performance comparison of the aforementioned algorithms:

- *Average delivery rate:* This is the ratio of the number of messages delivered to the destination node within all messages generated before the TTL budget expires.

[2]This is considered in order to increase the likelihood of delivery. However, if there is no such node, it is not considered.

- *Average delivery delay:* This is the average of elapsed time between the delivery of the messages and their generation at the source nodes. It is the average of delivery delays of only delivered messages before the TTL budget expires.

- *Number of forwardings:* This is the number of times a message is exchanged between two nodes before the delivery of the message.

4.3.3 Datasets

We use two of the commonly used real DTN traces [89] for routing performance evaluation. Moreover, we also generate our own synthetic dataset to have a more dense connectivity graph with sufficient meeting history. Each of these datasets represents a different environment with a different number of users and duration:

- **Cambridge dataset:** These are the Bluetooth recordings among 36 students with iMotes from Cambridge University for a duration of almost two months.

- **Haggle dataset:** These are the Bluetooth sightings recorded between the iMotes carried by 41 attendants of Infocom Conference held in Miami in 2005. It spans a four day period.

- **Synthetic dataset:** This is a dataset generated randomly among 50 nodes with a mean intermeeting time of a random value between [200, 400] minutes. The nodes have a meeting history on average with 10 different nodes.

In today's technology, mobile nodes should be in close proximity (i.e., almost touching) to be able to transfer power. While the Bluetooth (which is considered in above real traces) communication range is in the order of several meters, such interactions can be considered as an indication of users being in the close proximity of each other so that they can communicate and get further close to each other for a

potential energy transfer. We assume that when nodes meet, they stay close enough to each other until they can achieve the required energy transfer under optimal *TTL sharing* scenario. We look at the impact of transfer efficiency in our results, which can be considered as the relaxation of this assumption to some extent. However, in our future work, we will enhance our algorithm considering the partial energy transfers between nodes during meetings with limited duration.

4.3.4 Performance Results

In Fig. 15, we first compare the performance of the three algorithms in the Cambridge dataset. In order to see the benefit of the sharing based delivery, source and destination pairs are selected such that they do not directly meet. *TTL sharing* offers the best delivery rate among all algorithms. Moreover, it can achieve this with a similar average delivery delay and a similar number of forwardings with *TTL forwarding*. There is a slight increase in the number of forwardings with larger TTL budgets. This is due to the increased delivery ratio achieved at those TTL budgets.

The results for Haggle traces are illustrated in Fig. 16. We observe similar performance graphs, but the gap in the number of forwardings of *TTL sharing* and *TTL forwarding* is more and starts in earlier TTL budgets. On the other hand, it is still less than the *TTL spraying* algorithm and achieves the best delivery ratio. Note that such a performance improvement in the delivery ratio can be preferred as the forwarding cost per message delivery is a small value.

In Fig. 17, we look at the performance results with synthetic dataset. The results are also similar to other dataset results but the delivery ratios of *TTL sharing* and *TTL forwarding* is closer to each other. This is because the benefit of sharing policy could be dominated with other optimal forwarding based paths which could appear more often in dense graphs.

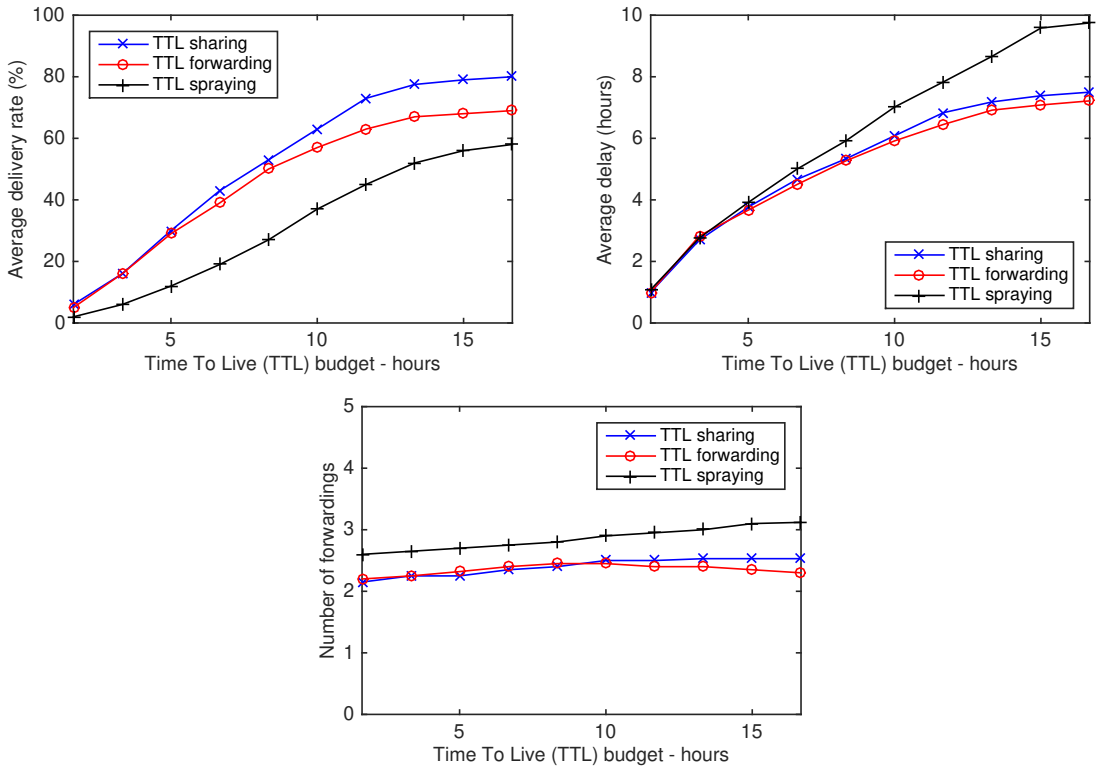

Fig. 15.: Delivery rate, delay and number of forwardings versus time-to-live in Cambridge dataset.

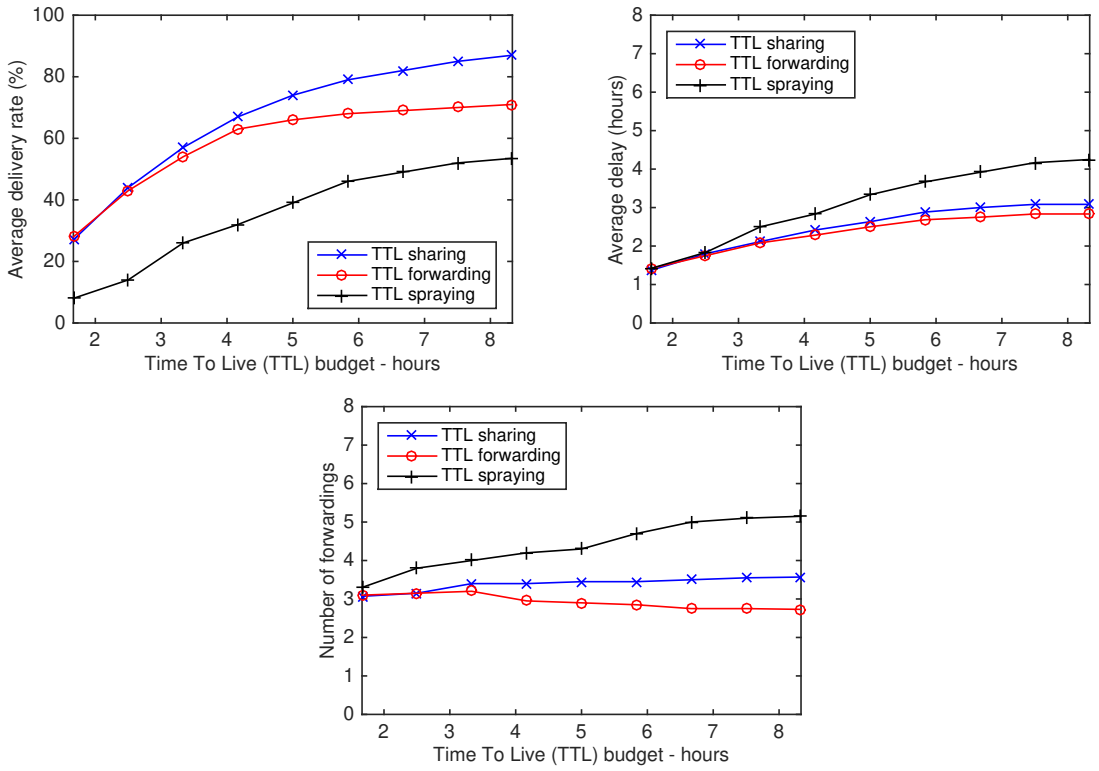

Fig. 16.: Delivery rate, delay and number of forwardings versus time-to-live in Haggle dataset.

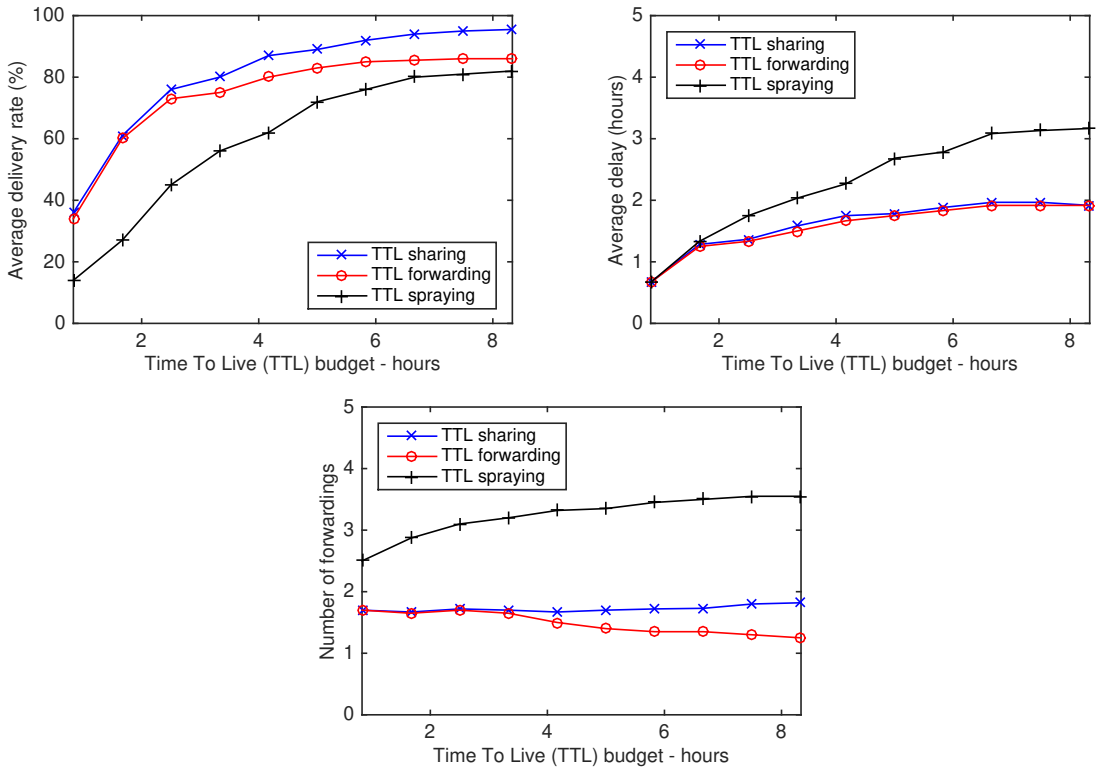

Fig. 17.: Delivery rate, delay and number of forwardings versus time-to-live in synthetic dataset.

Finally, we look at the impact of some parameters in the performance results. In Fig. 18, we plot the impact of loss rate, transfer efficiency and partially available link weight information on the performance ratio of the *TTL sharing* compared to *TTL forwarding*. As the results show, with increasing loss rates, the benefit of sharing is more pronounced as it can provide better delivery probability over multiple paths (despite the shorter TTL in each due to the split). However, this also increases the forwarding ratio which can be an issue if there is not enough buffer at nodes. On the other hand, as loss rate gets smaller, the performance ratio gets close to 1. Transfer efficiency also affects the performance ratio of the *TTL sharing* remarkably. As the efficiency gets lower, *TTL sharing* behaves like *TTL forwarding*, meaning sharing is

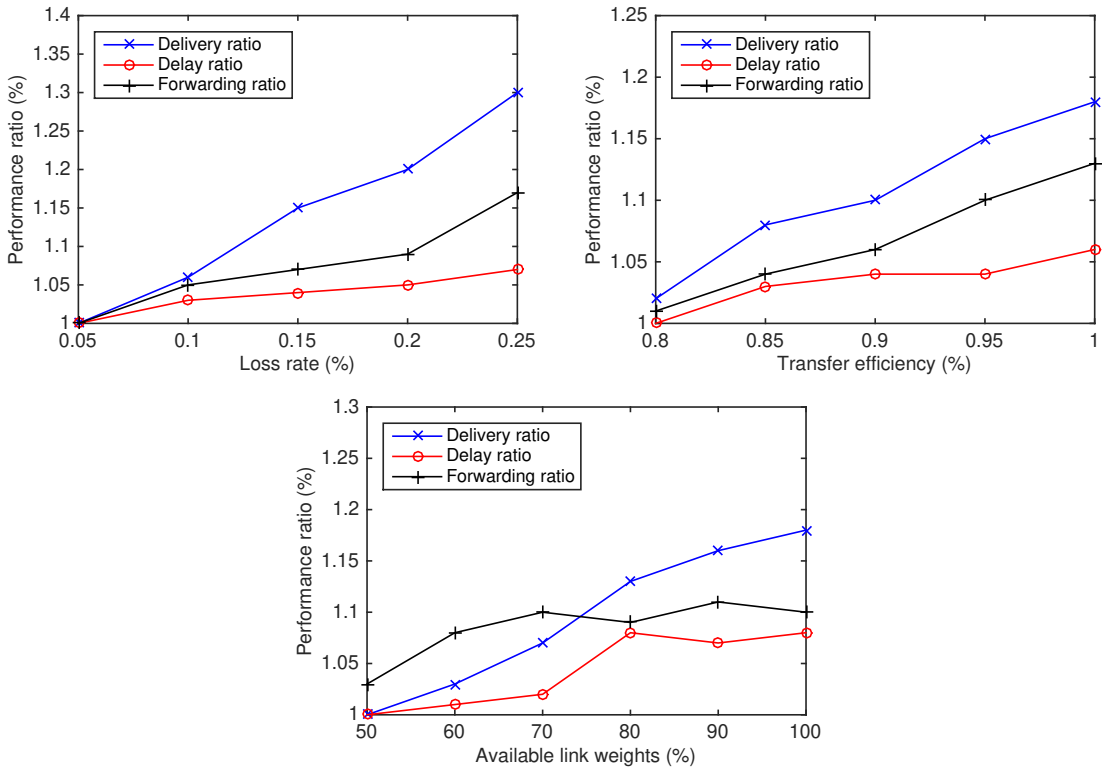

Fig. 18.: Impact of loss rate, transfer efficiency and available partial link weight on the performance ratio of sharing over forwarding.

not considered beneficial due to the loss during energy transfers. Finally, in the last graph, the impact of partially available intermeeting time information on the results is shown. For these results, we set the $\mathcal{I}_{i,j}$ values for some pairs to 0 (i.e., unknown) and calculate the $P_{i,d,k,t}$ values accordingly. The results show that when 50% of the link weights or mean intermeeting times are unknown, the benefits over *TTL forwarding* are lost. Thus, this suggests that the proposed optimal sharing policy will be more effective in networks with long-term stable relations among nodes with predictable meeting patterns.

4.4 Conclusion

In this chapter, we study the content delivery problem in mobile social networks in which nodes are motivated by energy transfers for carrying the messages. That is, each relay node carries a message forwarded by another node as long the energy provided or the corresponding time-to-live (TTL) value lasts. In order to find the optimal content and energy forwarding or sharing policy, we model and solve the problem using optimal stopping theory and dynamic programming. We evaluate the performance of the proposed solution in both real and synthetic mobile social network traces and show that sharing can offer better delivery rate, while it can also cause an increase in the cost of delivery (i.e., number of forwardings) to some extent. We also look at the impact of several parameters on the performance of the proposed sharing based content delivery process and discover the settings that provide performance enhancements.

CHAPTER 5

ENERGY BALANCING WITH P2P ENERGY SHARING

5.1 Introduction

In Mobile Social Networks, energy balancing [34, 35, 36, 37, 38] among nodes has been studied towards prolonging the lifetime of the network, which could be vital especially when there is no access to external energy sources. Energy balancing is the process of equalizing the energy at each node or minimizing the sum of the differences of their energy from the average energy (i.e., variation distance) in the network as much as possible. The main goal is to minimize the difference in the energy levels of all nodes and this can be targeted through the opportunistic energy exchanges between the nodes. However, as nodes interact and transfer energy between each other, there occurs an energy loss. Thus, both balancing the energy among nodes and keeping the loss of total network energy as low as possible is equally important.

5.1.1 Motivation

The state-of-the-art solutions [34, 35, 36] suggest that the variation distance among the target energy levels of nodes and current energy levels will decrease only if the nodes in the opposite sides of the average energy in the network interact and exchange energy. While this is correct and help reach an energy balance among the devices as fast as possible, it wastes energy due to the unnecessarily frequent interactions between nodes. For example, consider the example in Fig. 19. When node 1 and node 2 meets at time t_1, node 2 gives energy to node 1 in the amount of the half of the difference of their energies. Note that due to the loss, node 1 can only receive

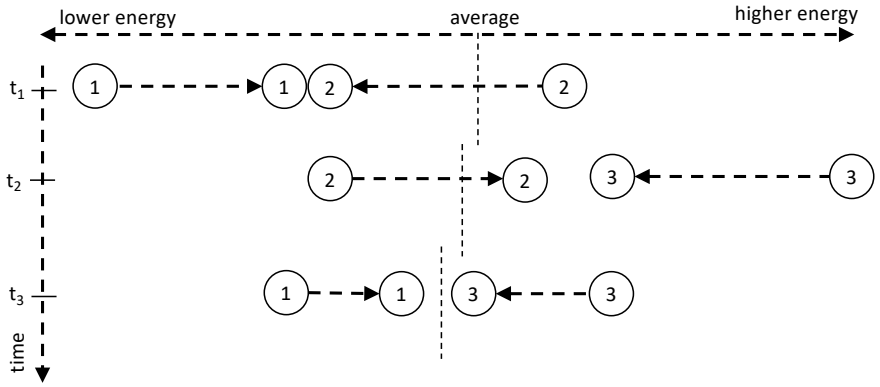

Fig. 19.: Energy balancing through interactions between nodes at opposite sides of the average energy in the network.

a portion of the shared energy, hence it has a smaller energy than node 2 after this interaction. Similarly, node 3 provides energy to node 2 at time t_2 and node 3 again provides energy to node 1 at time t_3. While such an interaction protocol can help reach an energy balance among nodes quickly, this can cause unnecessary wastage of energy as some nodes keep switching between the opposite sides of the average energy (which will decrease as the interactions with energy exchanges increase). In this specific example, after three interactions, node 2 has almost the same energy as in the beginning. A similar energy distribution could have been obtained if the first two interactions were not performed and only in the third one node 3 provided energy to node 1. It is also assumed that each pair of nodes interact with equal probability, however, this is not always true in mobile opportunistic networks. In a realistic scenario, some pairs of nodes might not have any interaction opportunity with other nodes and some pairs of nodes might have large intermeeting times incurring huge waiting times for some possible interactions to occur. Another major problem with the current approach is that they do not consider the final optimal target that can

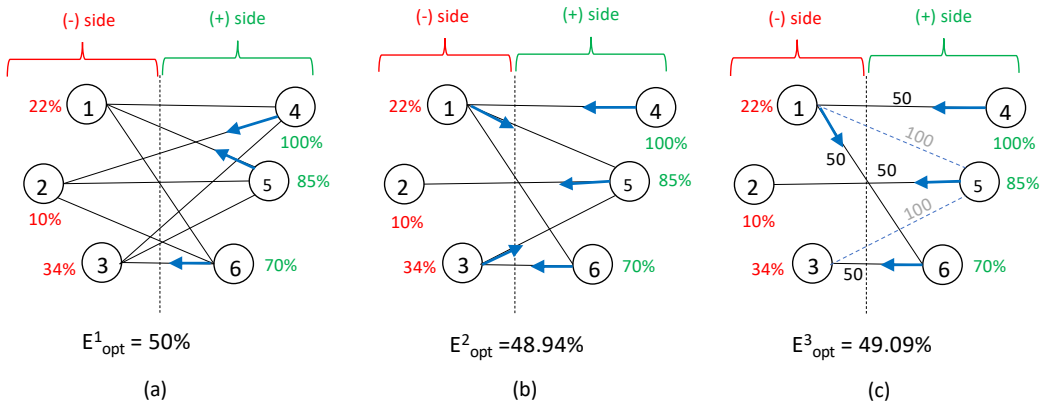

Fig. 20.: (a) Energy balancing in a fully connected contact graph. (b) Energy balancing in a partially connected contact graph. (c) Energy Balancing with time limit of 50. Edges represent that the nodes meet each other opportunistically with an average intermeeting time shown as link weight.

be reached after possible interactions and thus energy loss. Instead, they rely on the initial distribution of energy and target the initial average energy in the network. Thus, a perfect energy balance (i.e., all nodes having energy equal to the average energy in the network) can not be achieved since the average energy in the network will change after some energy exchanges between nodes.

Consider the example in Fig. 20 with six nodes in the network and with corresponding energy levels. Here, we consider three different scenarios in which energy levels of nodes are the same but the contact graphs between nodes are different. If each node on the negative side (i.e., having energy less than the average energy in the network (53.5%)) has an opportunity to meet with each node on the positive side as in Fig. 20a, the energy sharing process will be relatively easy. For example, with an 80% transfer efficiency (or with an energy loss rate of 0.2), the optimal average energy reachable by all nodes will be 50%, which happens when node 5 transfers 35%

Scenario	Energy transfer amounts	Final energy levels of nodes					
		1	2	3	4	5	6
Fig.20a	④ $\xrightarrow{50\%}$ ②, ⑤ $\xrightarrow{35\%}$ ① ⑥ $\xrightarrow{20\%}$ ③	50% for all nodes					
Fig.20b	⑤ $\xrightarrow{48.68\%}$ ②, ⑥ $\xrightarrow{21.05\%}$ ③, ④ $\xrightarrow{51.05\%}$ ①, ① $\xrightarrow{13.89\%}$ ⑤, ③ $\xrightarrow{1.89\%}$ ⑤	48.94% for all nodes					
Fig.20c	⑤ $\xrightarrow{35.90\%}$ ②, ⑥ $\xrightarrow{31.81\%}$ ③, ④ $\xrightarrow{50.90\%}$ ①, ① $\xrightarrow{13.63\%}$ ⑥	49.09%	38.72%	59.45%	49.09%		

Table 9.: Energy transfer amounts between nodes and final energy levels of nodes for scenarios in Fig.20 with 80% transfer efficiency.

to node 1 (which only gets 28% due to loss), node 4 transfers 50% to node 2 (which only gets 40%) and node 6 transfers 20% to node 3 (which only gets 16%).

On the other hand, when there is no energy exchange opportunity between some negative and positive side node pairs, as in the case of Fig. 20b, the optimal energy achievable can be less than this due to the more number of interactions required between nodes and multi-hop travel of energy, causing additional loss. In this case, nodes still reach a perfect energy balance (i.e., all nodes having the same energy level) at 48.94% through transfer amounts shown in Table 9, however, the final balanced energy level is less than it is in Fig. 20a (which has a complete contact graph between all positive and negative side nodes). Finally, there can be a time threshold for reaching an energy balance. In that case, we can simply ignore the edges (i.e., contact relations) with an average intermeeting time higher than this threshold and recalculate the average optimal energy balance. Fig. 20c shows the situation where the deadline for energy balance is set to 50 time units. The dotted edges shown in the figure are ignored; hence, nodes cannot use these edges for energy exchanges. In this case, the optimal average energy balance is 49.09%, however, as it is shown in Table 9,

not all nodes can reach this energy level. This example shows that with sparse contact graphs, the optimal energy balance can change and not all nodes may reach that.

5.1.2 Contributions

In this chapter, based on the above findings, we discuss several protocols to achieve a goal of a better variation distance with minimum energy loss. To this end, we discuss several single hop energy balancing protocols when each node can transfer energy only to its immediate neighbors in contact graph. It is not always possible to make an effective decision especially in sparse networks when the node relations are restricted to its immediate neighborhood. Hence, we would also like to relax this constraint and allow the nodes to exchange energy using multiple hops. This will allow nodes with higher energy to give energy to nodes with low energy even though they are not meeting directly (i.e., distant in contact graph). Furthermore, we also exploit the underlying social relations between nodes to develop social aware energy balancing protocols aimed for faster energy balancing between various social groups. Finally, we extend the problem of energy balancing to understand the relation of network lifetime and energy distribution. We see that when a perfect energy balancing cannot be achieved in a network, balancing energy between nodes does not guarantee the optimal network lifetime and thus requires a slight modification in the original balancing problem to address this issue. To this end, our contribution in this chapter can be summarized as below:

- We find out the optimal energy balance possible for fully connected contact graphs and propose three single hop interaction protocols to achieve the minimum variation distance.

- We also find out the optimal energy balance possible for partially connected graphs using Mixed Integer Linear Programming (MILP) only by utilizing the direct relationship between nodes and propose interaction protocols for the same.

- For networks with sparse contact graphs, we enhance the MILP model to allow multi-hop energy exchanges to achieve a better energy balance and develop the corresponding energy balancing protocol among nodes considering both the direct and relayed energy exchanges.

- We discuss the relation of the energy balancing problem to the problem of network lifetime maximization and provide the updates needed in the MILP model in disconnected contact graphs.

- We perform extensive simulations using meeting patterns from synthetic and real user traces and show that the proposed energy sharing protocols perform better than state-of-the-art.

5.2 System Model

5.2.1 Assumptions

We assume a set of m nodes denoted by $\mathcal{M} = \{u_1, u_2, ..., u_m\}$ in a mobile network. Each node is assumed to have equal battery capacity and necessary hardware for sending and receiving energy. As in previous work [34, 35, 36, 108, 109], for simplicity, we also do not consider energy loss due to mobility or other activities of the nodes.

When two nodes meet, they exchange energy according to an interaction protocol $\mathcal{P}$. The energy level of a node u at time t is denoted by $E_t(u)$, which is assumed to be between 0 and 1 (i.e., 100%). We assume each pair of nodes, (u_i, u_j), meets in an

Notation	Description
m	Number of nodes in the network.
$\mathcal{P}$	Interaction protocol between nodes for energy exchange.
β	Energy loss rate.
τ	Time threshold to complete energy balancing process.
p	Minimum expected meeting probability by time threshold.
$E_t(u)$	Energy of user u's device at time t.
$E_t(\mathcal{M})$	Total energy of a set $\mathcal{M}$ of nodes at time t.
$\lambda_{i,j}$	Meeting rate between nodes i and j.
$\overline{E_t}$	Average energy in the network at time t.
E_{opt}	Optimal average energy achievable in the network with minimum variation distance possible.
$\delta(P, Q)$	Total variation distance between two distributions, P, Q.
$\mathcal{E}_t(u)$	Ratio of node u's energy to the total energy in the network at time t.
$\mathcal{E}_t$	Energy distribution at time t on a sample space $\mathcal{M}$.
$\epsilon_{u,u'}$	The amount of energy exchanged from u to u'.
$\mathcal{L}$	The total energy loss in the network due to the energy exchanges.
$E_f(u)$	The final energy level of node u at the end of energy balancing process.
$\epsilon^s_{u,u'}$	The amount of u's *s*elf energy that is shared to u'.
$\epsilon^o_{u,u'}$	The amount of relayed energy from u to u' for *o*ther sources.
h_s	Total number of single hop energy exchanges used.
h_m	Total number of multi-hop energy exchanges used.
$\boldsymbol{L}_{u,u'}$	Minimum hop distance from node u to node u'.

Table 10.: Notations used in Chapter 5

exponentially distributed manner with a rate of $\lambda_{u_i u_j}$ (i.e., average intermeeting time is $1/\lambda_{u_i u_j}$) similar to many studies (e.g., [110, 111, 112, 101]) in mobile opportunistic networks. We also assume an energy loss rate, $\beta \in [0, 1)$, which is assumed to be a constant and depends on the technology and the equipment used. When two nodes u and u' interact at time t and node u transfers ϵ energy to node u', node u' will receive $(1 - \beta)\epsilon$ energy and their new energy levels will be:

$$\begin{aligned}(E_t(u), E_t(u')) &= \mathcal{P}(E_{t-1}(u), E_{t-1}(u')) \\ &= (E_{t-1}(u) - \epsilon, E_{t-1}(u') + (1 - \beta)\epsilon)\end{aligned}$$

As the interaction between u, and u' doesn't affect the energy levels of any other nodes, the energy levels of all other nodes remain unchanged. The notations used throughout the chapter are summarized in Table 10.

5.2.2 Problem Description

The goal is to achieve an energy balance among a population of nodes with a minimum possible variation within a given time threshold τ while minimizing the energy loss due to the energy transfers among nodes. We define the energy difference among nodes using the total variation distance from probability theory as in [34, 35, 36, 109].

Let P, Q be two probability distributions defined on a sample space $\mathcal{M}$. The total variation distance is calculated as:

$$\delta(P, Q) = \sum_{x \in \mathcal{M}} |P(x) - Q(x)| \tag{5.1}$$

Here, we do not divide the sum by two for the sake of keeping the actual differences. In our context, the total variation distance between the current energy distribution of nodes and the target energy distribution, where all nodes have the

same energy, needs to be calculated. Note that the target energy level will not be equal to the current average energy in the network, as during the energy exchanges to balance energy among nodes, there will be some energy loss. This will make the average energy level decrease over time after each interaction. At any time, we define the energy distribution $\mathcal{E}_t$ on a sample space $\mathcal{M}$ by

$$\mathcal{E}_t(u) = \frac{E_t(u)}{E_t(\mathcal{M})}, \text{where, } E_t(\mathcal{M}) = \sum_{x \in \mathcal{M}} E_t(x)$$

for any $u \in \mathcal{M}$. We also define the average energy in the network at time t

$$\overline{E_t} = \frac{E_t(\mathcal{M})}{m} \tag{5.2}$$

Note that in a network with a contact graph that connects all nodes (i.e., Fully Connected Graphs), the perfect balance with zero variation distance can always be achieved. However, depending on the hop distances between nodes in the contact graph, and energy level distribution of nodes, the optimal energy level may be different. For example, for a network with a complete contact graph between nodes, as each negative side node has the opportunity to exchange energy with any positive side node as shown in Fig. 20a, it is relatively easy to compute the optimal balanced energy for all nodes as discussed in the next section. Moreover, when $m \to \infty$, for a uniformly distributed energy levels of nodes, the final optimal balanced energy can be computed as :

$$E_{opt} = \frac{-(1-\beta) + \sqrt{(1-\beta)}}{\beta}$$

However, in networks with incomplete contact graphs (i.e., heterogeneous relations), this will be harder to compute, thus we model it as an MILP problem and solve accordingly.

5.3 Energy Balancing for Fully Connected Graphs

In this section, we give the details of the three proposed energy balancing protocols for fully connected graphs. In this, we assume the interactions are possible among all pairs of nodes. Each new protocol represents a solution attempt towards our goal to achieve an energy balance with minimal possible loss. Each solution depends on a rationale towards decreasing the loss, with the third one achieving the optimal loss.

5.3.1 Greedy Positive First Energy Balancing ($\mathcal{P}_{GP}$)

Let $\Delta_t = \delta(\mathcal{E}_t,\mathcal{U}) - \delta(\mathcal{E}_{t-1},\mathcal{U})$ be the decrease in variation distance from time $t-1$ to t, where at time t two nodes u and u' interact and $\mathcal{U}$ denotes the uniform distribution on $\mathcal{M}$ (i.e., $E_t(u) = \overline{E_t}\ \forall u$). Let also $z_t(x) = \mathcal{E}_t(x) - \frac{1}{m}$ denote the difference of node x's energy from the uniform distribution. It has been shown in [34, 35, 36] that if $z_{t-1}(u)z_{t-1}(u') < 0$, $\Delta_t < 0$. That is, if a node u with $E_t(u) < \overline{E_t}$ and a node u' with $E_t(u') > \overline{E_t}$ interact at time t and split their energy equally, the energy variation distance in the network decreases. Otherwise, with $z_{t-1}(u)z_{t-1}(u') \geq 0$, $\Delta_t = 0$.

While energy sharing in the opposite sides of the average energy will decrease the variation distance, it may cause nodes move between the negative and positive side of the average energy level in the network (as shown in Fig. 19), and causes unnecessary energy loss in the network. In order to solve this problem and minimize the energy loss in the network as much as possible while achieving low variation distance among peers, we propose to make one of the nodes greedily reach the current average energy level in the network (i.e., target) immediately. Moreover, we give priority to the positive node. That is, if two nodes u and u' at different sides of the average energy level in the network interacts, the one in the positive side gives its excessive energy

Algorithm 6: GreedyPositive (u, u', t)

Input: (u, u'): Interacting nodes

t: Time of interaction

if *(*$E_{t-1}(u) > \overline{E}_{t-1}$ ***and*** $E_{t-1}(u') < \overline{E}_{t-1}$*)* ***OR*** *(*$E_{t-1}(u) < \overline{E}_{t-1}$ ***and*** $E_{t-1}(u') > \overline{E}_{t-1}$*)* **then**

  if $E_{t-1}(u) > \overline{E}_{t-1}$ **then**

    $\mathcal{P}_{GP}(E_{t-1}(u), E_{t-1}(u')) = (\overline{E}_{t-1},\ E_{t-1}(u') + (1-\beta)(E_{t-1}(u) - \overline{E}_{t-1}))$

  else

    $\mathcal{P}_{GP}(E_{t-1}(u), E_{t-1}(u')) = (E_{t-1}(u) + (1-\beta)(E_{t-1}(u') - \overline{E}_{t-1}),\ \overline{E}_{t-1})$

else

  do nothing

above the target to the one in the negative side. Note that, as the interactions in the network continue, the target energy level will decrease thus, this node may need to interact and decrease its energy again. However, this will not waste energy as the node will still stay in the positive side. If the node in the negative side was given the priority to reach the target first, then this would make the node switch to the positive side as the new interactions happen and the average energy in the network decreases. Algorithm 6 shows the interaction process of this *G*reedy *P*ositive first protocol, or $\mathcal{P}_{GP}$ in short.

5.3.2 Greedy Closer First Energy Balancing ($\mathcal{P}_{GC}$)

In the greedy positive first protocol, it is still possible that some of the nodes in the negative side can switch to the positive side. For example, if the positive node has a very high excessive energy and can provide the node in the negative side with more energy than it actually needs to reach the target, this will make the node in the

negative side switch to the positive side. To address this, we propose a new protocol which gives priority to the node that is closest to the target energy level and let it reach the target. Note that this has to be handled separately depending on different cases.

Algorithm 7 shows the details of the *G*reedy *C*loser first protocol, or $\mathcal{P}_{GC}$ in short. If the node in the negative side, u^-, needs less than the energy that the node in the positive side, u^+, can give after loss, u^- is given priority to reach the target. The amount of energy that u^+ has to transfer should consider the loss, thus should be more than what u^- will actually need (lines 10-11). Otherwise, u^+ is given priority to reach the target and the energy of u^- is increased accordingly (line 12-13).

5.3.3 Greedy Optimal Energy Balancing ($\boldsymbol{P}_{GO}$)

The proposed protocols in previous sections aim to minimize the energy loss while achieving a small variation distance of energy level distribution of nodes with respect to the uniform distribution at the current time. However, as nodes interact, the average energy in the network, $\overline{E}_t$ will decrease and it will require the nodes that already reached the current average in the network interact again to reach this new target. For example, in $\mathcal{P}_{GC}$ protocol, there is still a possibility for negative side nodes that reach the target find themselves later in the positive side. Similarly, if priority is given to the nodes in the positive side as it is closer to the current target, even though it reaches the current average energy in the network, it can find itself again in the positive side.

To this end, we propose a third protocol called *G*reedy closer to *O*ptimal first protocol, or $\mathcal{P}_{GO}$ in short. We aim to maximize the benefit from each interaction, hence we make one of the nodes in the interacting pair reach the final optimal tar-

Algorithm 7: GreedyCloser (u, u', t)

Input: (u, u'): Interacting nodes

t: Time of interaction

$(u^+, u^-) \leftarrow (null, null)$

if $(E_{t-1}(u) > \overline{E}_{t-1}$ ***and*** $E_{t-1}(u') < \overline{E}_{t-1})$ **then**

  $(u^+, u^-) \leftarrow (u, u')$

else

  if $(E_{t-1}(u) < \overline{E}_{t-1}$ ***and*** $E_{t-1}(u') > \overline{E}_{t-1})$ **then**

    $(u^+, u^-) \leftarrow (u', u)$

if (u^+, u^-) *is not null* **then**

  $\delta_{t-1}(u^+) = E_{t-1}(u^+) - \overline{E}_{t-1}$

  $\delta_{t-1}(u^-) = \overline{E}_{t-1} - E_{t-1}(u^-)$

  if $\delta_{t-1}(u^+)(1-\beta) > \delta_{t-1}(u^-)$ **then**

    $\mathcal{P}_{GC}(E_{t-1}(u^+), E_{t-1}(u^-)) = (E_{t-1}(u^+) - \frac{\delta_{t-1}(u^-)}{(1-\beta)}, \overline{E}_{t-1})$

  else

    $\mathcal{P}_{GC}(E_{t-1}(u^+), E_{t-1}(u^-)) = (\overline{E}_{t-1}, E_{t-1}(u^-) + (1-\beta)\delta_{t-1}(u^+))$

get immediately and stop interacting with others. This achieves a larger variation distance decrease per interaction and keeps the possible maximum energy in the network. However, the key point here is to find this optimal target energy level in the final network when all interactions finish and every node's energy is balanced.

For a given population of nodes and their energies, this can be calculated in a discrete manner through iterations. Let us divide the nodes in the network into three

sets based on a reference energy level j as follows:

$$S_t^+(j) = \{x \in \mathcal{M} \mid E_t(x) > j\}$$

$$S_t^-(j) = \{x \in \mathcal{M} \mid E_t(x) < j\}$$

$$S_t^=(j) = \{x \in \mathcal{M} \mid E_t(x) = 0\}$$

Assume that E_{opt} is the optimal average target energy in the network that can be reached by all nodes with the minimum energy loss. It is clear that in the optimal way each node should reach this target directly. That is, the nodes having more energy than this target should give their excessive energy to others and the nodes having less energy than this target should receive energy from others in the amount of the difference. However, due to the loss, the nodes that will give energy to receiving nodes should transfer more than what they actually need. E_{opt} will then be obtained when the sum of receiving nodes energy can be supplied by giver nodes with minimal loss. More formally,

$$\begin{aligned} E_{opt} &= \arg\min_j \{\mathcal{B}_j^+ - \mathcal{B}_j^-\} \text{ where,} \\ \mathcal{B}_j^+ &= \sum_{\forall x \in S_0^+(j)} (E_0(x) - j) \\ \mathcal{B}_j^- &= \sum_{\forall x \in S_0^-(j)} \left(\frac{j - E_0(x)}{1 - \beta} \right) \end{aligned}$$

In a large scale network with many nodes having uniformly distributed energy levels in [0,1], the expected value of E_{opt} can also be calculated as follows:

$$\begin{aligned} \int_{y=0}^{x} (x - y)dy &= \int_{x}^{1} (y - x)(1 - \beta)dy \\ x^2 &= (x^2 - 2x + 1)(1 - \beta) \\ f(x) &= \beta x^2 + 2(1 - \beta)x - (1 - \beta) = 0 \end{aligned}$$

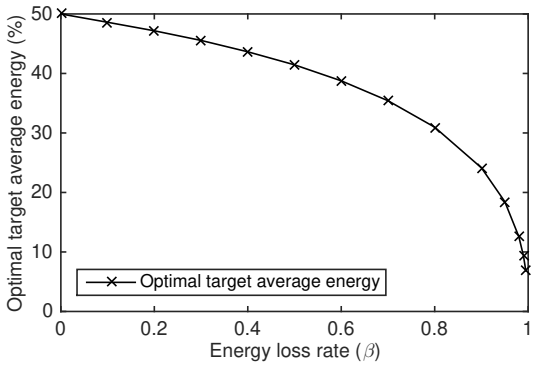

Fig. 21.: Optimal target average energy for different energy loss rates for a large-scale network with uniform energy distributions.

This function, $f(x)$ is strictly increasing function when $x \in [0,1]$ and $\beta \in [0,1]$, as $f'(x) > 0$. The solution is equal to the positive root at,

$$\begin{aligned} E_{opt} &= \frac{-2(1-\beta) + \sqrt{4(1-\beta)}}{2\beta} \\ &= \frac{-(1-\beta) + \sqrt{(1-\beta)}}{\beta} \end{aligned}$$

As $(1-\beta) \leq \sqrt{(1-\beta)}$ when $\beta \in [0,1]$, the value of E_{opt} is positive and lies in $[0,1]$.

In Fig. 21, we show the values of E_{opt} for different energy loss rates. The results are average of 1000 runs among 100 nodes where each node's energy is determined randomly between 0 and 100%. For example, when there is a 20% energy loss during transfers, the optimal energy balance with minimum loss and zero variation is 47.213%.

So, as shown in Algorithm 10, the interaction protocol between nodes will be similar to the $\mathcal{P}_{GC}$ protocol except that E_{opt} will be used instead of $\overline{E}_{t-1}$. If the nodes in the opposite sides of E_{opt} interact, the one that can reach the target first based on energy exchanges between them is given priority.

Note that in an ideal scenario, with $n/2$ interactions, a perfect energy balance

Algorithm 8: GreedyOptimal(u, u', t)

Input: (u, u'): Interacting nodes

t: Time of interaction

1 *Replace* all $\overline{E}_{t-1}$ in GreedyCloser(u, u', t) with E_{opt}

2 Run the same algorithm

among all nodes can be achieved at E_{opt}. This happens when the energy need of a node in the negative side is perfectly provided by a node in the positive side during a single interaction and they both reach the target. This requires equal number of nodes in the opposite sides of the target and perfect meeting schedule between corresponding pairs that can complement each other. In practice, usually this is not the case as due to uniform distribution, there will not be equal number of nodes in both sides of the final optimal average and the meeting patterns of nodes may be very different.

5.4 Energy Balancing for Partially Connected Graphs

In a real setting, the ideal scenario will not be the case as opportunistic interactions will be limited to only some pairs of nodes and the distribution of energy levels of nodes may not be uniform. However, in a given mobile opportunistic network contact graph[1] and the initial energy levels of nodes, we can find the optimal energy balance achievable among nodes by Mixed Integer Linear Programming (MILP).

We target an energy balance with minimum possible energy variation distance first. Then, we target minimum loss without sacrificing the variation distance. Especially, when there are multiple ways (i.e., energy exchange schedules between nodes)

[1]This can be obtained from historical meeting patterns of nodes and thanks to the long-term regularities [104, 59] in node relations, it can be used for predicting future meetings.

of reaching a zero variation distance, utilizing the one that will result in the minimum energy loss is important. By the way, depending on the application requirements, it is possible to consider other objective functions with weighted variation distance and loss combination similarly. In this section, we will discuss on two different approaches namely single hop and multi hop approaches to achieve a minimum variation distance with minimum loss given different network scenarios. We will then extend the idea of energy balancing to network lifetime and propose minor modifications to the energy balancing problem to obtain optimal network lifetime when a perfect energy balancing is not achievable.

5.4.1 Energy Balancing with Single Hop Energy Exchanges

In this section, we consider the case where only single hop energy exchanges are allowed between nodes. That is, each node is able to transfer energy only to its immediate neighbors and the total shareable energy is limited to its available energy. This makes the process easy as nodes can use every meeting opportunity with other nodes to share energy without waiting to receive any energy from some others. Below, we first provide a MILP based solution to find the optimal energy level for a given connected contact graph of any size and given characteristics of node relations (e.g., intermeeting time). Utilizing MILP results, we then propose two different energy balancing protocols.

5.4.1.1 Optimal Energy Balance

In a given mobile opportunistic network contact graph[2] and the initial energy levels of nodes, we can find the optimal energy balance achievable among nodes by MILP. In this chapter, we target an energy balance with minimum possible energy variation distance first. Then, we target minimum loss without sacrificing the variation distance. Especially, when there are multiple ways (i.e., energy exchange schedules between nodes) of reaching the same variation distance (e.g., zero), utilizing the one that will result in the minimum energy loss is important. Depending on the application requirements, it is possible to consider other objective functions with weighted combinations of variation distance and loss in a similar way.

Let $\epsilon_{u,u'}$ denote the amount of energy transferred from u to u' and $E_f(u)$ denote the final energy level of node u at the end of energy balancing process. Then,

$$E_f(u) = E_0(u) - \sum_{\forall u'} \epsilon_{u,u'} + \sum_{\forall u'} \epsilon_{u',u}(1-\beta)$$

Let also $\mathcal{L}$ denote the total energy loss in the network due to the energy exchanges between nodes during the balancing process. Then,

$$\mathcal{L} = \sum_{\forall u} \sum_{\forall u' \neq u} \epsilon_{u,u'}\beta$$

The objective is to minimize the variation distance between the final energy distribution of nodes, $\mathcal{E}_f$, and the final uniform energy distribution, $\mathcal{U}_f$, where all nodes have energy equal to the average energy in the final network (i.e., $E_f(u) = \overline{E_f}\ \forall u$) as much as possible and then minimize the total loss in the network. More

[2]This can be obtained from historical meeting patterns of nodes and thanks to the long-term regularities [104, 113, 114] in node relations, it can be used for predicting future meetings.

formally:

$$\min \quad \delta(\mathcal{E}_f, \mathcal{U}_f)m + \mathcal{L} \tag{5.3}$$

$$\text{s.t.} \quad 0 \leq \epsilon_{u,u'} \leq E_t(u) l_{uu'} \qquad \forall (u, u') \tag{5.4}$$

$$0 \leq \sum_{\forall u' \neq u} \epsilon_{u,u'} \leq E_t(u) \qquad \forall u \tag{5.5}$$

$$k_{uu'} + k_{u'u} \leq 1 \qquad \forall (u, u') \tag{5.6}$$

$$\text{where} \quad \epsilon_{u,u'} \text{ is a decimal in } [0, 1] \qquad \forall (u, u') \tag{5.7}$$

$$k_{uu'} = \begin{cases} 1, & \text{if } \epsilon_{u,u'} > 0 \\ 0, & \text{otherwise} \end{cases} \qquad \forall (u, u') \tag{5.8}$$

$$l_{uu'} = \begin{cases} 1, & \text{if } (1 - e^{-\lambda_{uu'}\tau}) \geq p \\ 0, & \text{otherwise} \end{cases} \qquad \forall (u, u') \tag{5.9}$$

In objective function (5.3), as we give priority to the minimization of variation distance over minimization of loss, we use scalarization method and multiply the former with a constant that is larger than the maximum possible value for $\mathcal{L}$. That is, we select the constant as m as each node's energy can be at most 100% or 1 and there are m nodes in the network, making the total possible loss at most $m\beta$. With a non-zero β, this guarantees that the optimization prefers a decrease in variation distance over any decrease in loss. (5.4) allows energy sharing between the nodes that are expected to meet within given time threshold τ as when $l_{uu'} = 0$ or no meeting is expected, no sharing will be allowed (i.e., $\epsilon_{u,u'}$ should be zero) and (5.5) limits the total energy sharing from each node to any other node by its available energy. This is to take into account the fact that all the energy sharing events can happen earlier than any energy receiving event potentially due to the opportunistic and non-deterministic nature of meetings between nodes. We also do not allow unnecessary

two-way energy exchanges between nodes via (5.6). In order to determine if the nodes will meet by the time threshold, in (5.9), we use a predefined probability, p, and set the link between nodes to 1 if the CDF of expected meeting by time threshold is more than p. Note that the optimal average energy level will be equal to the average energy in the final network. That is,

$$E_{opt} = \frac{\sum_{x \in \mathcal{M}} E_f(x)}{m}. \tag{5.10}$$

5.4.1.2 Energy Balancing Protocols

After the optimal energy balance and the corresponding required energy exchanges (i.e., $\epsilon_{u,u'}$) between nodes to reach that optimal balance is computed[3] via an MILP solver, we propose two different energy balancing protocols to define the actual energy exchanges during the opportunistic meetings between pairs of nodes.

In the first protocol, we require each node to follow the exact energy exchange schedule found by the MILP solution (hence, named *L*inear *E*xact or $\mathcal{P}_{LE}$ in short). Thus, each node waits for meeting with the nodes that it is supposed to perform an energy exchange with and exchanges energy only in the amount it is allowed to do so with them. This protocol will let the nodes reach the optimal variation distance in the network eventually but due to the non-deterministic nature of opportunistic meeting patterns, it may cause nodes wait longer than expected as well as cause them miss the advantage of any earlier meeting opportunity with some unexpected nodes.

In the second protocol, we aim to benefit from the non-deterministic meetings between nodes which may let the nodes reach the target energy level earlier, thus we do not require nodes to follow the energy exchange schedule found by the MILP solution.

[3]This one-time process can be computed at a central device (which can be one of the nodes in the network or a remote server) that knows all initial energy levels of nodes and can be communicated back to the nodes through cellular connection.

Optimal target average energy level, E_{opt} is still found by MILP (using (5.10)) as in the case of first protocol, however, the nodes do not need to wait specifically for the nodes that they are supposed to exchange energy with. Instead, whenever two nodes from opposite sides of E_{opt} meet, they utilize this opportunity and update their energy towards the target. Here, in order to prevent nodes from switching their sides as in the case of previous work and causing unnecessary additional energy loss, we give priority to the node whose energy is closer to the target and let it reach that target by receiving or sharing energy with the other node. We name this protocol *O*pportunistic *C*loser or $\mathcal{P}_{OC}$ in short. Note that this protocol takes the benefit of any opportunistic meeting for energy exchange besides the scheduled ones, however, it can cause nodes not reach the optimal energy levels due to the divergence from the schedule that will make them reach the optimal energy balance. This may especially adversely affect the performance when the contact graph in the network is sparse.

We show the details of these two energy balancing protocols in Algorithm 9. For $\mathcal{P}_{OC}$ protocol (lines 8-14), if the node in the negative side, u^-, needs less than the energy that the node in the positive side, u^+, can give after loss, u^- is given priority to reach the target. The amount of energy that u^+ has to transfer should consider the loss; thus, it should be more than what u^- will actually need (lines 11-12). Otherwise, u^+ is given priority to reach the target and the energy of u^- is increased accordingly (line 14). For $\mathcal{P}_{LE}$ protocol (lines 16-20), the energy of nodes are simply updated based on the scheduled energy exchanges between nodes. Note that by MILP formulation design either ϵ_{u^+,u^-} or ϵ_{u^-,u^+} will be more than zero at the same time, however, it is possible that both could be zero as the optimal schedule may not recommend an interaction between them even though they are in opposite sides of the average energy level.

Algorithm 9: Single Hop Energy Balancing ($\mathcal{P}$, u, u', t)

Input: (u, u'): Interacting nodes, t: Time of interaction

E_{opt}: Optimal average energy from MILP

$(u^+, u^-) \leftarrow (null,\ null)$

if $(E_{t-1}(u) > E_{opt}$ ***and*** $E_{t-1}(u') < E_{opt})$ **then**

  $(u^+, u^-) \leftarrow (u,\ u')$

else

  if $(E_{t-1}(u) < E_{opt}$ ***and*** $E_{t-1}(u') > E_{opt})$ **then**

    $(u^+, u^-) \leftarrow (u',\ u)$

if (u^+, u^-) *is not null* **then**

  if $\mathcal{P} = \mathcal{P}_{OC}$ **then**

    $\delta_{t-1}(u^+) = E_{t-1}(u^+) - E_{opt}$

    $\delta_{t-1}(u^-) = E_{opt} - E_{t-1}(u^-)$

    if $\delta_{t-1}(u^+)(1-\beta) > \delta_{t-1}(u^-)$ **then**

      $\mathcal{P}_{OC}(E_{t-1}(u^+), E_{t-1}(u^-)) = (E_{t-1}(u^+)$ - $\frac{\delta_{t-1}(u^-)}{(1-\beta)},\ E_{opt})$

    else

      $\mathcal{P}_{OC}(E_{t-1}(u^+), E_{t-1}(u^-)) = (E_{opt},\ E_{t-1}(u^-) + (1-\beta)\delta_{t-1}(u^+))$

  else

    if $\epsilon_{u^+,u^-} > 0$ **then**

      $\mathcal{P}_{LE}(E_{t-1}(u^+), E_{t-1}(u^-)) = (E_{t-1}(u^+)$ - $\epsilon_{u^+,u^-},\ E_{t-1}(u^-) +$
      $(1-\beta)\epsilon_{u^+,u^-})$

    else

      if $\epsilon_{u^-,u^+} > 0$ **then**

        $\mathcal{P}_{LE}(E_{t-1}(u^+), E_{t-1}(u^-)) = (E_{t-1}(u^+) + (1-\beta)\epsilon_{u^-,u^+},$
        $E_{t-1}(u^-)$ - $\epsilon_{u^-,u^+})$

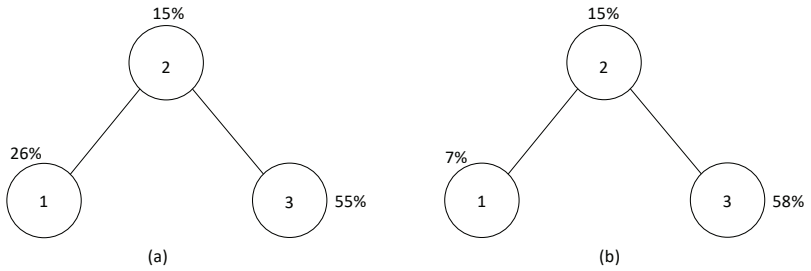

Fig. 22.: An example contact graph with 3 nodes: (a) Perfect energy balancing is possible with single hop energy exchanges. (b) Perfect energy balancing requires multi-hop energy exchanges (with $\beta = 0.2$).

5.4.2 Energy Balancing with Multi-Hop Energy Exchanges

In the previous section, we study the energy balancing problem when each node can transfer energy only to its immediate neighbors in contact graph. However, this may result in an imperfect energy balance (i.e., non-zero variation distance) especially in sparse networks. Hence, in this section, we relax this constraint and allow the nodes to exchange energy using multiple hops. This will allow nodes with higher energy to give energy to nodes with low energy even though they are not meeting directly (i.e., distant in contact graph). For example, in Fig. 22a, the optimal energy achievable is 30% by all nodes (i.e., perfect energy balance with zero variation distance) with the total energy loss of 6%. This happens when node 2 gives 5% to node 1 and gets 25% from node 3, making energy levels of all nodes equal to $E_{opt} = 30\%$. Note that all energy exchanges to reach perfect balance happen between direct neighbors and the initial energy levels of nodes is more than the energy that their neighbors need to take from them (e.g., node 2 has 15% initially and just sends 5% to node 1).

However, for the example shown in Fig. 22b, this is not the case. A perfect energy balance at 23% is possible, but node 3 should share its energy with node 1

and node 2 to make that happen. Note that node 2 cannot make node 1 reach 23% by the energy it has, as it needs to transfer 20% to node 1 but it has less than that. Thus, it has to wait for receiving energy from node 3 first. This requires a multi-hop based energy sharing process. Node 3 shares 35% of its energy with node 2, which receives 28% due to 20% loss rate. Then, node 2 keeps 8% for itself and shares the remaining 20% with node 1, which receives only 16% and reaches 23%.

While multi-hop based energy sharing can help reach a perfect energy balance when single hop exchanges cannot, there are some additional challenges that need to be addressed. That is, the average time required until an energy balance occurs as well as the loss during energy exchanges can increase as more hops result in more loss.

Thus, for the efficient modeling of this problem, we will allow the linear program to only use paths that are viable within the time constraint and has the least number of hops. To this end, we find the paths from all possible source nodes to all possible destinations and discard the paths that cannot provide an energy transfer with a probability p over the nodes on that path by the time threshold.

Then, we find the shortest hop path among the paths selected for each pair and use this path in the linear program to compute energy exchanges and energy loss. If there are multiple same hop paths, then we select the path that can achieve the energy transfer with the highest probability among them.

5.4.2.1 Optimal Energy Balance

Let G denote the (undirected connected) contact graph of nodes in the network and let $p^h_{u,u'} = \langle u_1, u_2, u_3, ..., u_h \rangle$ be a path of h hops from node u to node u' in G where $u_1 =$ u and $u_h = u'$. As we assume that the intermeeting times of nodes i and j are defined with an independent random variable $X_{ij} \sim Exp(\lambda_{ij})$, the energy transfer

time from node u to node u' on $p^h_{u,u'}$ can be modeled with a random variable $X^h_{u,u'} = \sum_{i=1}^{h-1} X_{u_i,u_{i+1}}$. Here, with a common $\lambda = \lambda_{u_i u_j},\ \forall u_i \neq u_j \in [1,h]$, this will convert to gamma distribution [115], $\Gamma(h,\lambda)$, and for different rates, one can calculate the actual CDF of $X^h_{u,u'}$, or $F_{X^h_{u,u'}}$, where the mean will be equal to $E[X] = \sum_{i=1}^{h-1} \frac{1}{\lambda_{u_i,u_{i+1}}}$ [116].

Let $\vec{\mathcal{P}}_u$ denote the set of all possible $p^h_{u,u'}$s in graph G from a source node u to any node u' for all h such that $F_{X^h_{u,u'}}(\tau) \geq p$, where p is the predefined minimum expected meeting probability as used in Section 5.4.1. Consider a new subgraph $G'_u \subset G$ such that all the edges in this new graph corresponds to the edges, $\vec{e}_{u,u'} \in \vec{\mathcal{P}}_u$.

In order to reduce the loss during multi-hop based energy sharing and balancing process, we need to use the path with the minimum hop that can achieve an energy exchange within the time threshold. Thus, we set a weight of 1 for each edge in G'_u and apply Dijkstra's shortest path algorithm to identify the minimum hop path from source u to each destination in G'_u.

Let $\boldsymbol{L}$ be an $m \times m$ matrix, where $\boldsymbol{L}_{u,u'}$ shows the minimum hop distance from node u to node u' in G'_u (we set $\boldsymbol{L}_{u,u'} = \infty$ if there is no such path). Since single hop based energy balancing, if possible, should be preferred over multi-hop based balancing as it will have lower loss, we set the objective function such that it also prioritizes using single hop over multi-hop after the priorities defined in single hop objective function. Let h_s be the total number of single hop energy exchanges used, which can be given as:

$$h_s = |\{(u,u') \mid u,u' \in \mathcal{M}, u' \neq u, \epsilon_{u,u'} > 0,\ L_{u,u'} = 1\}|$$

Similarly, let h_m be the total number of multi-hop energy exchanges used, which can be given as:

$$h_m = |\{(u,u') \mid u,u' \in \mathcal{M}, u' \neq u, \epsilon_{u,u'} > 0,\ L_{u,u'} > 1\}|$$

Total energy loss in the network can also be computed as:

$$\mathcal{L} = \sum_{\forall u} \sum_{\forall u' \neq u} (\epsilon_{u,u'} \times (1 - (1 - \beta)^{L_{u,u'}}))$$

The optimization model used in single hop case can then be extended to multi-hop energy balancing problem as:

$$\min \quad (\mathcal{M}^2 \times (\mathcal{M}^2 \times (\delta(\mathcal{E}_f, \mathcal{U}_f)m + \mathcal{L}) + h_s) + h_m) \tag{5.11}$$

$$\text{s.t.} \quad 0 \leq \epsilon_{u,u'} \leq E_t(u) l_{uu'} \qquad \forall (u, u') \tag{5.12}$$

$$0 \leq \sum_{\forall u' \neq u} \epsilon_{u,u'} \leq E_t(u) \qquad \forall u \tag{5.13}$$

$$k_{uu'} + k_{u'u} \leq 1 \qquad \forall (u, u') \tag{5.14}$$

$$\text{where} \quad \epsilon_{u,u'} \text{ is a decimal in } [0, 1] \qquad \forall (u, u') \tag{5.15}$$

$$k_{uu'} = \begin{cases} 1, & \text{if } \epsilon_{u,u'} > 0 \\ 0, & \text{otherwise} \end{cases} \qquad \forall (u, u') \tag{5.16}$$

$$l_{uu'} = \begin{cases} 1, & \text{if } L_{u,u'} \neq \infty \\ 0, & \text{otherwise} \end{cases} \qquad \forall (u, u') \tag{5.17}$$

In the objective function (5.11), in order to make sure that single hop paths are prioritized over multi-hop paths we again use scalarization method. That is, we first multiply the single hop energy balancing objective by a constant ($\mathcal{M}^2$) and add the number of single hop energy exchanges. We then multiply the overall term by the same constant and add multi-hop counts. Note that each constant is selected as it is described in single hop case such that the previous prioritized objective will be preferred over the next one. Similarly, we update the constraints for energy exchange bounds in (5.12) where $l_{uu'}$ now specifies if there is a path from node u to node u' in G'_u, i.e., $l_{uu'}$ is set to 1 if $L_{u,u'}$ is equal to some finite number of hops. Otherwise, $l_{u,u'}$

is set to 0 if there is no path from node u to node u' in G'_u (i.e., $L_{u,u'} = \infty$). With $l_{u,u'} = 0$, we again do not allow any energy exchange between nodes. Note that (5.13) still limits the total energy shared by a node (to any single and multi-hop node) by its own energy and allows the relay nodes preserve their own energy when relaying energy from other sources.

5.4.2.2 Energy Balancing Protocol

Similar to the single hop case, we adopt a *linear exact* energy balancing protocol which lets the meeting nodes exchange energy that is given by the linear program. However, using linear exact for multi-hop based energy balancing is not straightforward as it is for single hop. This is because a node acting as a relay might need to relay more energy than it can hold. Also, in order to avoid the temporary out-of-energy situations for nodes, we do not allow the relay nodes to transfer energy upon opportunistic contact with next hop nodes unless they have received energy from previous hop nodes[4]. This requires nodes to maintain information on energy amount to be transferred from its own energy as well as energy amount that is received from other sources and will be forwarded as a relay.

Let $\epsilon_{u,u'}$ be the energy amount that needs to be transferred from node u to node u', over single hop or multiple hops, to achieve the optimal solution found by the multi-hop MILP. Also, let $\epsilon^s_{u,u'}$ be the amount of u's *s*elf energy that needs to be shared to u' (for u' and all other nodes using u' as relay). Note that this also refers to the energy amount that node u can transfer to node u' without waiting for any energy reception from other nodes. Similarly, let $\epsilon^o_{u,u'}$ denote the amount of energy to be transferred from node u to u' where node u is acting as a relay for energy from

[4]Due to this restriction, we also do not develop equivalent of $\mathcal{P}_{OC}$ for multi-hop case.

other sources. In order to compute the values of $\epsilon^s_{u,u'}$ and $\epsilon^o_{u,u'}$, we also need to know the path used for energy exchanges by the linear program. In the subgraph G'_u, after applying Dijkstra's algorithm with edge weights set to 1, we can end up with multiple paths from node u to any other node u' with the same number of hops (h). In such cases, we select the path with the minimum expected time in order to increase the chance of completing the energy sharing within the time threshold. Let $p^{min}_{u,u'}$ be the minimum cost path from u to u' in G'_u, and let $\langle i, j\rangle$ denote the edge between nodes i and j. Then,

$$\epsilon^s_{u,u'} = \epsilon_{u,u'} + \sum_{k\in\mathcal{M},k\neq u,u'} (\epsilon_{u,k} \mid \langle u, u'\rangle \in p^{min}_{u,k})$$

$$\epsilon^o_{u,u'} = \sum_{\substack{k\in\mathcal{M},k\neq u,u'\\ d\in\mathcal{M},d\neq u,u',k}} (\epsilon_{k,d} \times (1-\beta)^{L_{k,u}} \mid \langle u, u'\rangle \in p^{min}_{k,d})$$

In the above equations, $\epsilon^s_{u,u'}$ is computed as the sum of energy to be transferred from u to u' and the total amount of energy to be transferred from u to every other destination in which u' is the first hop in its path. Similarly, $\epsilon^o_{u,u'}$ is calculated as the sum of total amount of energy to be transferred from all sources to all destinations in which u' is the next hop after u in its path. Note that we only take into account the energy amount that will reach node u after losses during transfers in previous hops (from the source node k to node u). After computation of necessary parameters, we can run this protocol as given in Algorithm 10.

In Algorithm 10, we divide the energy exchanges into two parts. In the first part (lines 1-9), we perform the energy exchanges originated from a node's self energy. In the second part (lines 10-19), we perform the energy exchanges due to a node's being relay between other nodes. Priority is given to the former. In the first part, we first calculate the amount of available energy that can be shared (line 4), and

Algorithm 10: P_{MLE}(u, u', $\epsilon^s_{u,u'}$, $\epsilon^o_{u,u'}$, r_u, t)

Input: (u, u'): Interacting nodes, t: Time of interaction

$\epsilon^s_{u,u'}$: Energy to be sent from u to u' directly

$\epsilon^o_{u,u'}$: Energy to be sent from u to u' as a relay

r_u: Received energy in node u as relay

for $\epsilon_{i,j} \in \{\epsilon^s_{u,u'}, \epsilon^s_{u',u}\}$ **do**
  if *(*$\epsilon_{i,j} > 0$*)* **then**
    $(u^+, u^-) \leftarrow (i, j)$
    $\epsilon \leftarrow \min(E_{t-1}(u^+), \epsilon^s_{u^+,u^-})$
    if $(E_{t-1}(u^-) + \epsilon(1-\beta) >$ *100)* **then**
      $\epsilon = 100 - \frac{E_{t-1}(u^-)}{(1-\beta)}$
    $(E_{t-1}(u^-), E_{t-1}(u^+)) = (E_{t-1}(u^-) + (1-\beta)\epsilon,\ E_{t-1}(u^+) - \epsilon)$
    $\epsilon^s_{u^+,u^-} = \epsilon^s_{u^+,u^-} - \epsilon$
    $r_{u^-} \leftarrow r_{u^-} + (1-\beta)\epsilon$

for $\epsilon_{i,j} \in \{\epsilon^o_{u,u'}, \epsilon^o_{u',u}\}$ **do**
  if *(*$\epsilon_{i,j} > 0$*)* **then**
    $(u^+, u^-) \leftarrow (i, j)$
    $\epsilon \leftarrow \min(E_{t-1}(u^+), r_{u^+}, \epsilon^o_{u+,u-})$
    if $(E_{t-1}(u^-) + \epsilon(1-\beta) >$ *100)* **then**
      $\epsilon = 100 - \frac{E_{t-1}(u^-)}{(1-\beta)}$
    $(E_{t-1}(u^-), E_{t-1}(u^+)) = (E_{t-1}(u^-) + (1-\beta)\epsilon,\ E_{t-1}(u^+) - \epsilon)$
    $\epsilon^o_{u^+,u^-} = \epsilon^o_{u^+,u^-} - \epsilon$
    $r_{u^+} \leftarrow r_{u^+} - \epsilon$
    $r_{u^-} \leftarrow r_{u^-} + (1-\beta)\ \epsilon$

depending on the available space in the receiver, we determine the actual energy transfer that will happen (lines 5-6) and update the corresponding parameters based on the transferred amount. In the second part, we again first calculate the amount of available energy that can be shared (line 13), however this time we also consider the received energy as relay so far and only let such energy transfers after receiving sufficient energy from previous hops. Then, depending on the available space in the receiver, we again determine the actual energy transfer that will happen (lines 14-15) and update the parameters once it is performed (lines 16-19). Note that, different from the first part, as both the receiver and transmitter nodes are relays in the second part, the received energy amounts as relays are updated for both.

5.5 Evaluation

In this section, we present the results of our evaluation through simulations[5]. From the beginning of the simulation, we let the devices interact following their exponentially distributed intermeeting times and exchange energy based on the characteristics of each energy balancing protocol compared. Each simulation is repeated 100 times for statistical smoothness. Error bars are not shown as the results were highly concentrated around the mean. The energy levels of nodes are uniformly distributed in (0-100]% in general. However, for the group-based synthetic contact traces generated for multi-hop protocol evaluation, we consider one group with nodes having high energy (i.e., $\geq 50\%$) and the other group with nodes having less energy (i.e., $< 50\%$). Moreover, for the partially connected graphs we use two values for expected meeting probability p within time threshold, namely, $1 - 1/e \sim 0.63$ and 0.8. Note that, for example in the single hop case, the former simply considers the edges in the contact

[5]The simulations code is available at https://github.com/aashish33128/Energy-Balancing-Journal.

graph with average intermeeting time less than or equal to τ, and the latter requires the edges to have an average intermeeting time less than or equal to $\approx \tau/1.6$.

5.5.1 Energy Balancing Protocols in Comparison

Below are the brief descriptions of all protocols compared through simulations:

- $\mathcal{P}_{GP}$: Protocol Greedy positive as discussed in 5.3.1 prioritizes the node which has energy greater than the current average network energy to reach the average first.

- $\mathcal{P}_{GC}$: Protocol Greedy Closer as discussed in 5.3.2 prioritizes the node which has energy closer to the current average network energy to reach the average energy first.

- $\mathcal{P}^*_{OA}$: This *O*nline *A*verage protocol is the updated version of the state-of-the-art protocol $\mathcal{P}_{OA}$ proposed in [34, 35, 36]. The protocol simply lets the nodes in opposite sides of the current average energy in the network interact and split their energies equally. In the original $\mathcal{P}_{OA}$, each node locally estimates the average energy level in the network using the ratio of the total energy of the encountered nodes to the number of encountered nodes, which may not be accurate. As we allow computation of MILP results at a node or a server by knowing the energy levels of all nodes, for a fair comparison we assume the same for $\mathcal{P}_{OA}$ and name it as $\mathcal{P}^*_{OA}$, which performs better than $\mathcal{P}_{OA}$. Moreover, we use E_{opt} obtained from discrete method for fully connected graphs and MILP results for partially connected graphs to decide the boundary between opposite sides in $\mathcal{P}^*_{OA}$, which helps decreasing energy loss.

- $\mathcal{P}_{LE}$: In the *L*inear *E*xact protocol, when the nodes meet, they only share the exact amount of energy that MILP solution with only single hop energy

exchanges (obtained[6] by IBM CPLEX solver [117]) finds to reach the E_{opt} with minimum possible variation and loss after that, as described in Alg. 9.

- $\mathcal{P}_{OC}$: In the *O*pportunistic *C*loser protocol, E_{opt} is obtained via the discrete method for fully connected graphs (Note: This protocol is equivalent to protocol $\mathcal{P}_{GO}$ as discussed in 5.3.3) and from MILP for partially connected graphs (with single hop energy exchanges) as in $\mathcal{P}_{LE}$, but the nodes opportunistically try to reach E_{opt}. That is, they do not wait for the other nodes that they are supposed to exchange energy with, as found by MILP, but utilize every meeting opportunity with the nodes in the opposite side. The one with closer energy level to E_{opt} is given priority to reach it first as described in Alg. 9.

- $\mathcal{P}_{MLE}$: In the *M*ulti-hop *L*inear *E*xact protocol, we first find the E_{opt} by MILP solution using multi-hop energy exchanges (obtained by IBM CPLEX solver [117]) and then depending on the actual self and relayed energy amounts calculated, we let the meeting nodes share the exact amount of energy they are supposed to exchange, as described in Alg. 10.

Note that there is no opportunistic version of $\mathcal{P}_{MLE}$ algorithm, as nodes in more than one hop distance away in the contact graph do not meet opportunistically.

5.5.2 Performance Metrics

We use the following metrics in the performance comparison of the aforementioned protocols:

- *Total variation distance:* This is calculated by $\delta(\mathcal{E}_t,\mathcal{U}_t)$. That is, we find the ratio of the energy levels of nodes to the total energy in the network at each

[6]We set the MILP gap tolerance to 0 to make sure the results obtained are optimal.

time, take the absolute difference from uniform distribution at that time and sum it for all nodes.

- *Total energy in the network:* This is the sum of energies at all nodes. As the nodes interact and exchange energy, due to the imperfect transfer efficiency the total available energy in the network decreases.

- *Number of interactions:* This is the number of interactions between nodes during which an energy exchange happens towards reaching a balance. It shows how selective the protocol is and hence it affects the efficiency of the protocol.

- *Total variation distance at a given total energy:* As the performance of the protocols may vary based on total variation distance and total energy in the network, we use this combined metric as an indicator of true performance.

- *Total variation distance at a given number of interactions:* Similarly, we use this metric to understand the impact of necessary interactions towards reaching the minimum possible total variation distance.

Note that all protocol that depends on E_{opt} calculated from MILP model at a central server, the initial computation and communication cost for all protocols will be the same. The additional computation and communication costs will come from the node interactions they result in. Thus, the performance results showing the number of interactions can also be used to compare their computation and communication cost differences.

5.5.3 Contact Traces

We use both real and synthetic user traces to define the meeting relations between the nodes in the network. Real traces are obtained from one of the commonly

used datasets in DTN literature [89] that is used for performance analysis of routing algorithms. With synthetic traces, we aim to generate different contact graphs with various sparsity levels.

- **Cambridge traces:** These are the Bluetooth recordings between the iMotes carried by 36 students from Cambridge University for a duration of almost two months. While Bluetooth has a range in the order of several meters, we use these interactions as an indication of nodes in close proximity of each other and assume that they can communicate and agree to come closer to perform energy exchange operation if needed.

- **Regular synthetic traces:** These traces are generated for 30 nodes that meet with an exponentially distributed intermeeting time with a mean selected randomly between [1000, 7000] time units for fully connected graph results and [1000, 15000] time units[7] for partially connected graph results. Through simulations, different time thresholds are also used to generate contact graphs with different average neighbor counts.

- **Group-based synthetic traces:** In order to show the benefits of multi-hop based energy exchanges during energy balancing process in particular, we use 30 nodes divided into two equal groups and allow nodes within each group meet up to 40% of other nodes in their own group and meet with a node in the other group with probability γ, which is set to 3% by default. However, we look at the impact of different γ on results. Intermeeting times are generated with an exponential distribution with a mean selected randomly between [100, 300] time

[7]Note that while generating results, we scale the time units down by 10 for proper presentation of results.

units. We selected a smaller upper bound to allow multi-hop paths within time threshold.

Note that depending on the energy sharing technology used between nodes, the proximity requirements and corresponding energy transfer efficiency might be different. While we assume a default energy loss rate, $\beta = 0.2$ (i.e., 80% transfer efficiency) for main simulations, we look at the impact of this parameter in our results. Moreover, we assume that when nodes meet, they stay close enough to each other until they can achieve the required energy transfer under the energy balancing protocol in use, as in previous work [34, 35, 36, 108, 109]. The results with different transfer efficiency however can be considered as the relaxation of this assumption to some extent.

5.5.4 Fully Connected Graphs

In Fig. 23-a, we show the total variation distance comparison for all algorithms. P^*_{OA} can provide smaller variation distance than the proposed algorithms. However, this is achieved with a very high energy loss, as shown in Fig. 23-b. Moreover, the number of interactions between nodes is also the highest among all compared algorithms, as shown in Fig. 23-c. Thus, when we compare the variation distance at the same total energy in the network in Fig. 23-d, we see that it achieves the worst performance. On the other hand, P_{GO} achieves the best performance and decreases the variation distance towards the optimal energy, E_{opt}, gradually. It also achieves this with minimum number of interactions. Thus, as it is shown in Fig. 23-e, it gives the best performance in terms of the total variation distance at a given interaction time.

The other proposed algorithms, P_{GP} and P_{GC}, perform better than P^*_{OA}, and worse than the P_{GO}. P_{GC} indeed can achieve similar total variation distance (Fig. 23-b) at a given total energy in the network as P_{GO} and very close total energy in the

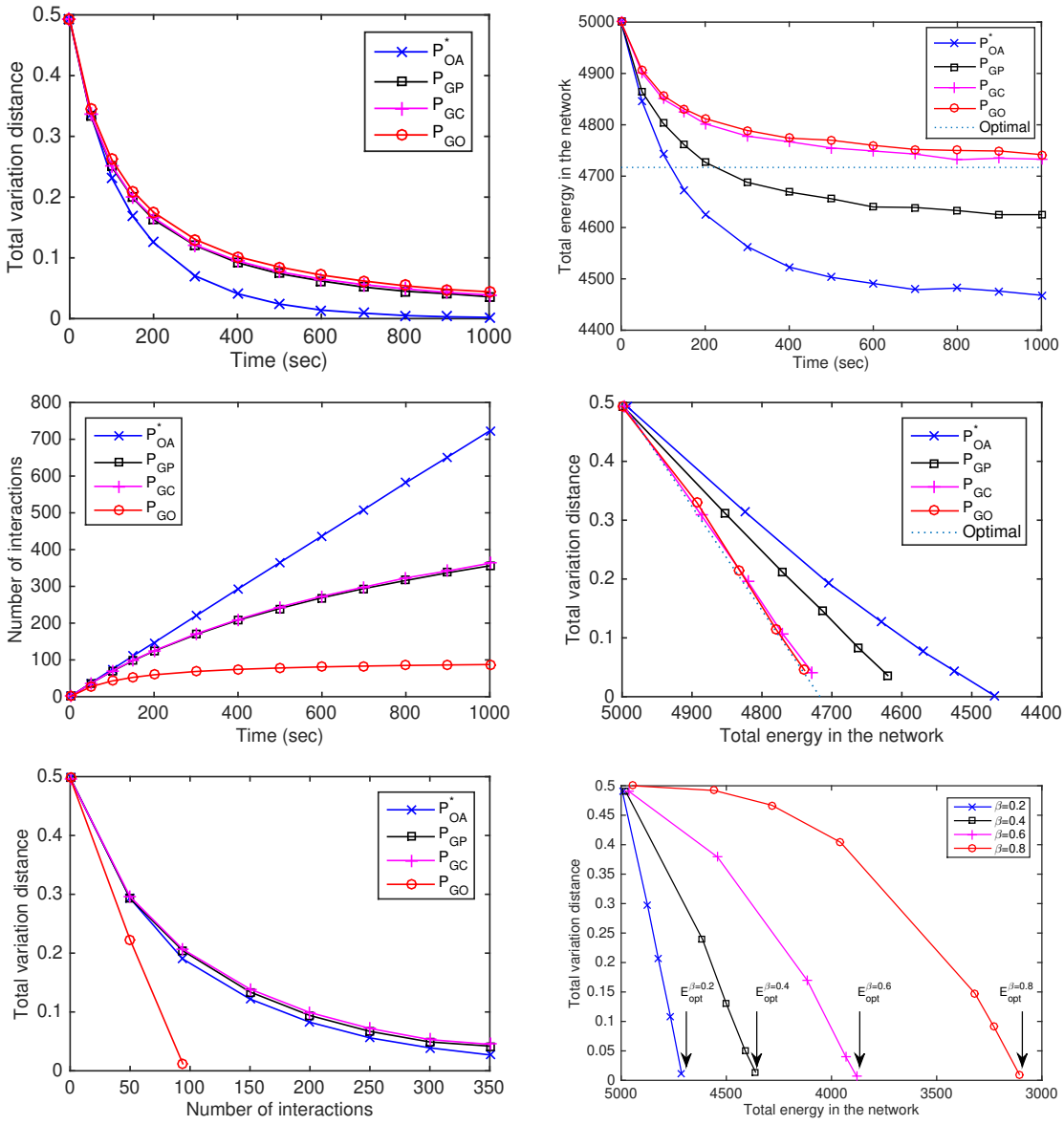

Fig. 23.: Comparison of proposed algorithms with the state-of-the-art algorithm in terms of (a) variation distance, (b) total energy remaining in the network, (c) total number of interactions, (d) variation distance at each total energy level and (e) variation distance at each total number of interactions (when β=0.2). (f) shows the impact of different loss rates on $\mathcal{P}_{GO}$ performance.

network around the same simulation time (Fig. 23-d). However, as the nodes target to reach the current average energy in the network their interaction does not stop as in P_{GO}, thus total variation distance at a given total interaction (with energy exchanges) count is worse than the case in P_{GO} (Fig. 23-e).

The impact of energy loss rate on the performance of P_{GO} is also shown in Fig. 23-f. P_{GO} always reaches the target if it is run sufficiently long. However, we notice that with higher β, the linear decrease converts to non-linear decrease. This is because, with higher β, E_{opt} gets lower, hence the difference in the number of nodes in the opposite sides of E_{opt} increases. This then results in less meeting likelihood between opposite side nodes in earlier times. Moreover, due to the high energy loss, the nodes in negative side receive small energy and cannot reach the target quickly. Thus, the variation distance decreases slowly. However, P_{GO} eventually reaches the optimal target with minimal loss.

5.5.5 Partially Connected Graphs

In Fig. 24, we first show the optimal energy balance (E_{opt}) achievable in contact graphs with different sparsity. To this end, we use regular synthetic traces and for different time thresholds (τ) and loss rates (β) we calculate the optimal average energy reachable with single hop exchanges[8] and corresponding variation distance and total loss at E_{opt} for two different p values. Note that as τ decreases the contact graph gets sparser as the edges between some pairs cannot achieve the expected meeting probability p by τ anymore, thus are removed from the graph. As the results show, optimal variation distance gets lower as τ increases and hits zero around $\tau = 400$ time units when $p = 0.63$. The loss associated with this optimal variation distance on

[8]We discuss the impact of using multi-hops on E_{opt} in Fig. 28.

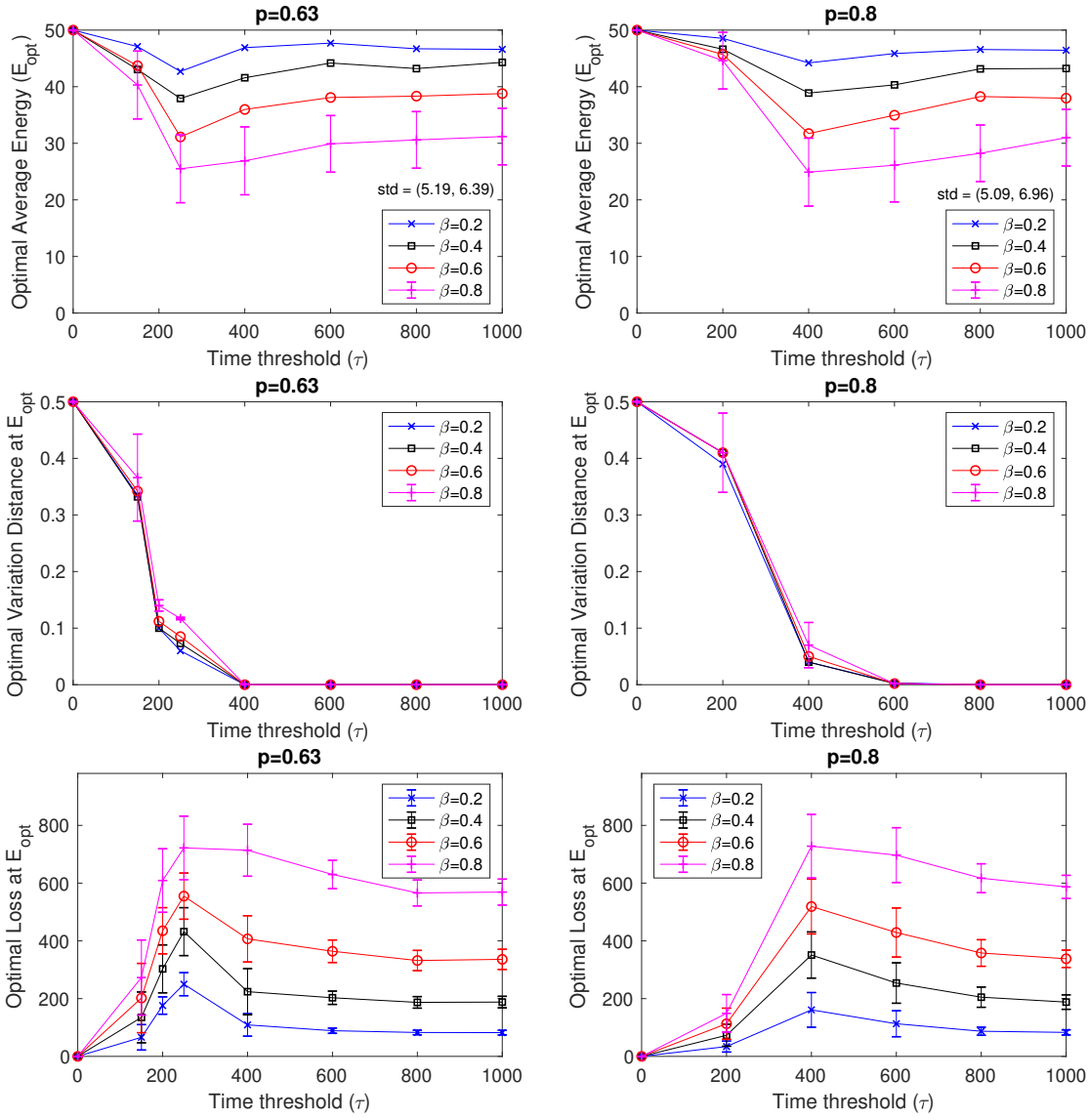

Fig. 24.: Impact of time threshold (τ) and loss rate (β) on optimal average energy achievable (E_{opt}) and corresponding variation distance and total loss at E_{opt} with expected meeting probability threshold $p = 1 - 1/e = 0.63$ and $p = 0.8$ (For visual clarity, error bars are only shown for one line in top four figures as they are similar in others).

the other hand increases initially and gets smaller later. This is because with smaller τ values, some nodes either have very small contacts or are totally isolated from others. Thus, perfect energy balance with zero variation distance was not possible. However, once this threshold is exceeded, the loss could be lowered by finding better energy exchange schedules. Note that E_{opt} results are also inline with this reasoning. Moreover, we see that as β increases, the optimal average energy achievable with different time thresholds decreases but it follows a similar pattern at different loss rates. Similarly, with $p = 0.8$, we obtain an expanded but similar pattern in all graphs compared to $p = 0.63$. This is because a time threshold $\tau = \tau_1$ with $p = 0.63$ will yield the same contact graph with a time threshold $\tau = 8\tau_1/5$ with $p = 0.8$.

In Fig. 25, we compare all protocols[9] in terms of aforementioned performance metrics using regular synthetic traces. In Fig. 25a, we see that P_{LE} can achieve the lowest variation distance among others. P^*_{OA} and P_{OC} have a similar variation distance which is slightly higher than the variation distance of P_{LE}. However, when we look at the total energy levels in the network shown in Fig. 25b, we observe that P^*_{OA} sacrifices a lot of energy during the energy balancing process. On the other hand, P_{OC} keeps more energy in the network even more than P_{LE}. This is because as it uses some unscheduled energy exchange opportunities towards the optimal average energy level, it diverges from optimal variation distance but this does not cause losing energy in the network unnecessarily. Moreover, the number of interactions between nodes in P^*_{OA} is the highest among all compared protocols, as shown in Fig. 25c, while proposed protocols limit the interactions. When we compare the variation distance at the same total energy in the network in Fig. 25d, we observe that P^*_{OA} indeed has the worst

[9]As the results for P_{MLE} are similar to P_{LE} results in regular synthetic and Cambridge traces, we do not show them in corresponding figures. We show P_{MLE} results explicitly only when group-based synthetic traces are used.

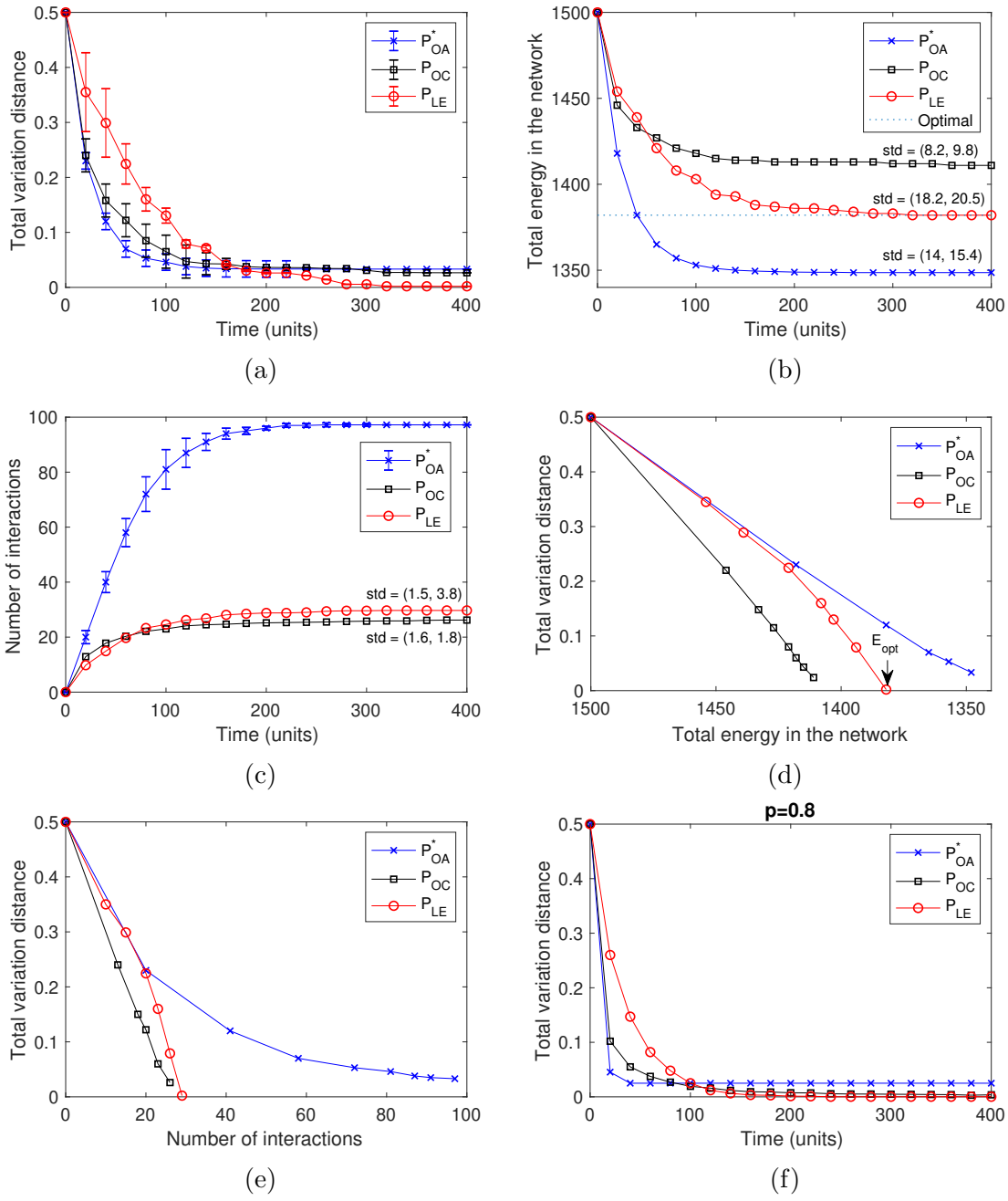

Fig. 25.: Comparison of protocols in terms of (a) variation distance, (b) total energy remaining in the network, (c) total number of interactions, (d) variation distance at each total energy level and (e) variation distance at each total number of interactions (when β=0.2, τ=400 time units, $p = 0.63$) using regular synthetic traces. (f) shows variation distance with p=0.8

performance. On the other hand, P_{LE} reaches the optimal energy level and decreases the total variation distance gradually. Here, P_{OC} shows an interesting behavior as it achieves a better variation distance at a given total energy in the network but it cannot reach the smallest possible variation distance as P_{LE} does. Thus, if some variation distance is tolerable, P_{OC} can be considered performing better than P_{LE}. Moreover, P_{OC} achieves this with smaller variation distance at a given interaction count than other protocols, as it is shown in Fig. 25e. P^*_{OA} again performs the worst due to its design. In order to show the impact of p, we provide the variation distance results as a representative in Fig. Fig. 25f. As expected, all protocols achieve a smaller variation distance in earlier times. One interesting observation here is, P_{OC} can achieve zero variation distance which was not possible when $p = 0.63$. This is because larger p allows energy exchanges only between nodes that are more likely to meet. Note that, while using larger p is desirable, it can cause the contact graph be partitioned and make the zero variation distance impossible. We discuss the situation in disconnected graphs in the next section.

In the results shown in Fig. 26, we relax the time threshold and set it to $\tau = 1000$ time units in order to increase the contact graph density and the energy exchange opportunities. Here, only results with three metrics are shown for the sake of brevity. We observe that with this increased time threshold, the total energy kept in the network increases (i.e., loss decreases). P_{OC} also causes more loss initially which is not the case in earlier results. Another significant change is that the performances of P_{OC} and P_{LE} get closer in terms of total variation distance at a given total energy and number of interactions. These can be explained by the increased energy exchange opportunities. With $p = 0.8$, as shown in Fig. 26d, total energy in the network decreases quickly due to earlier happening link selections, but eventually this also causes slightly more energy loss due to the decreased energy exchange opportunities.

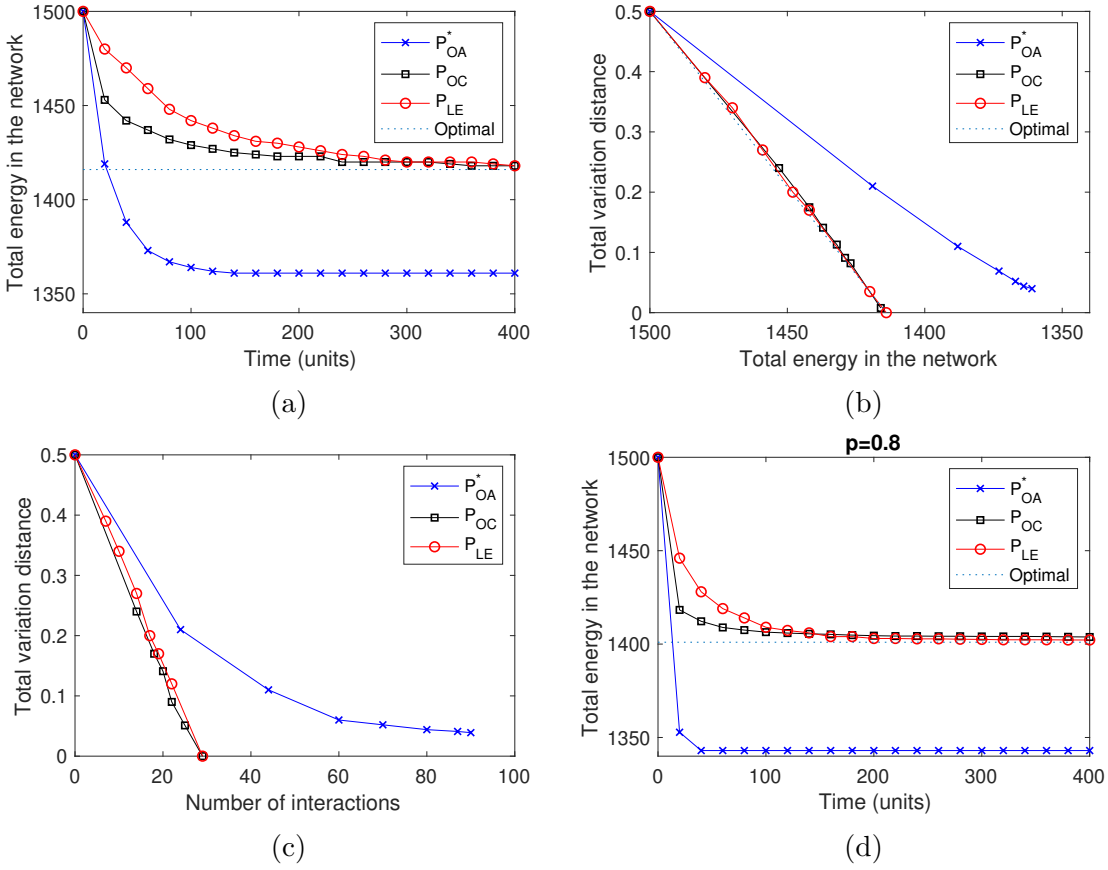

Fig. 26.: Comparison of protocols in terms of (a) total energy remaining in the network, (b) variation distance at each total energy level and (c) variation distance at each total number of interactions (when β=0.2, τ=1000 time units, $p = 0.63$) using regular synthetic traces. (d) shows total energy remaining in the network with p=0.8.

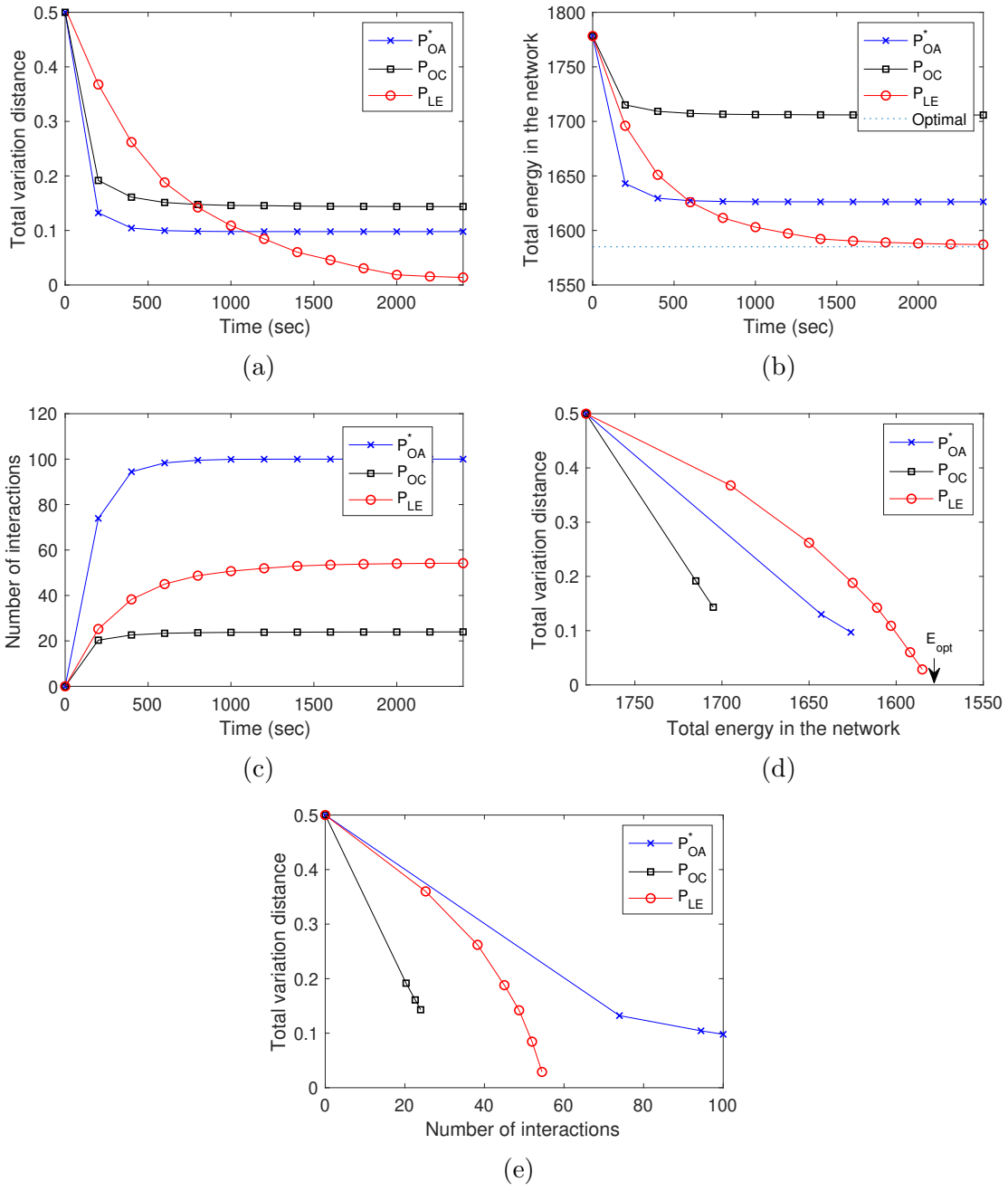

Fig. 27.: Comparison of protocols in terms of (a) variation distance, (b) total energy remaining in the network, (c) total number of interactions, (d) variation distance at each total energy level and (e) variation distance at each total number of interactions (when β=0.2, τ=5000 sec, $p = 0.63$) using Cambridge traces.

Next, we compare the performance of all protocols using Cambridge traces. In Fig. 27a, we see that P_{LE} provides close to zero variation distance and performs the best compared to others. Interestingly, P^*_{OA} achieves better variation distance than P_{OC}, which was not the case in regular synthetic traces. However, as it is shown in Fig. 27b, P^*_{OA} causes more loss in the network compared to P_{OC}. P_{LE} reaches the optimal energy in the network with the smallest possible variation distance. In terms of total variation distance at a given total energy level, P_{OC} performs better than others for earlier energy levels, but it cannot reach the variation distance others can do, as shown in Fig. 27d. The interactions for P^*_{OA} is the highest again among all protocols while P_{OC} has the smallest interactions that is also considerably less than the interactions of P_{LE} which was not the case in regular synthetic traces. This is because in Cambridge traces, the contact graph density is smaller than it is in regular synthetic traces and P_{OC} stops interacting further when nodes greedily reach the target.

In Fig. 28, we show the results with group-based synthetic traces which are particularly generated in order to show the benefit of P_{MLE} over P_{LE} clearly. From Fig. 28, we observe that P_{MLE} achieves the smallest variation distance and keeps more energy in the network, while it increases the number of interactions slightly. This is because, as the hop distance between high energy nodes and low energy nodes increases, which is the case in these group-based synthetic traces, protocols considering only single hop based energy exchanges will offer limited energy transfer opportunities. Note that a node cannot share more than what it has in both single hop and multi-hop cases. However, multi-hop case allows energy transfers between nodes that are more than one hop away in contact graph through the help of intermediate nodes. Thus, a node with more energy can transfer its excessive energy to a node with low energy even it is multi-hop away. The multi-hop energy transfers indeed

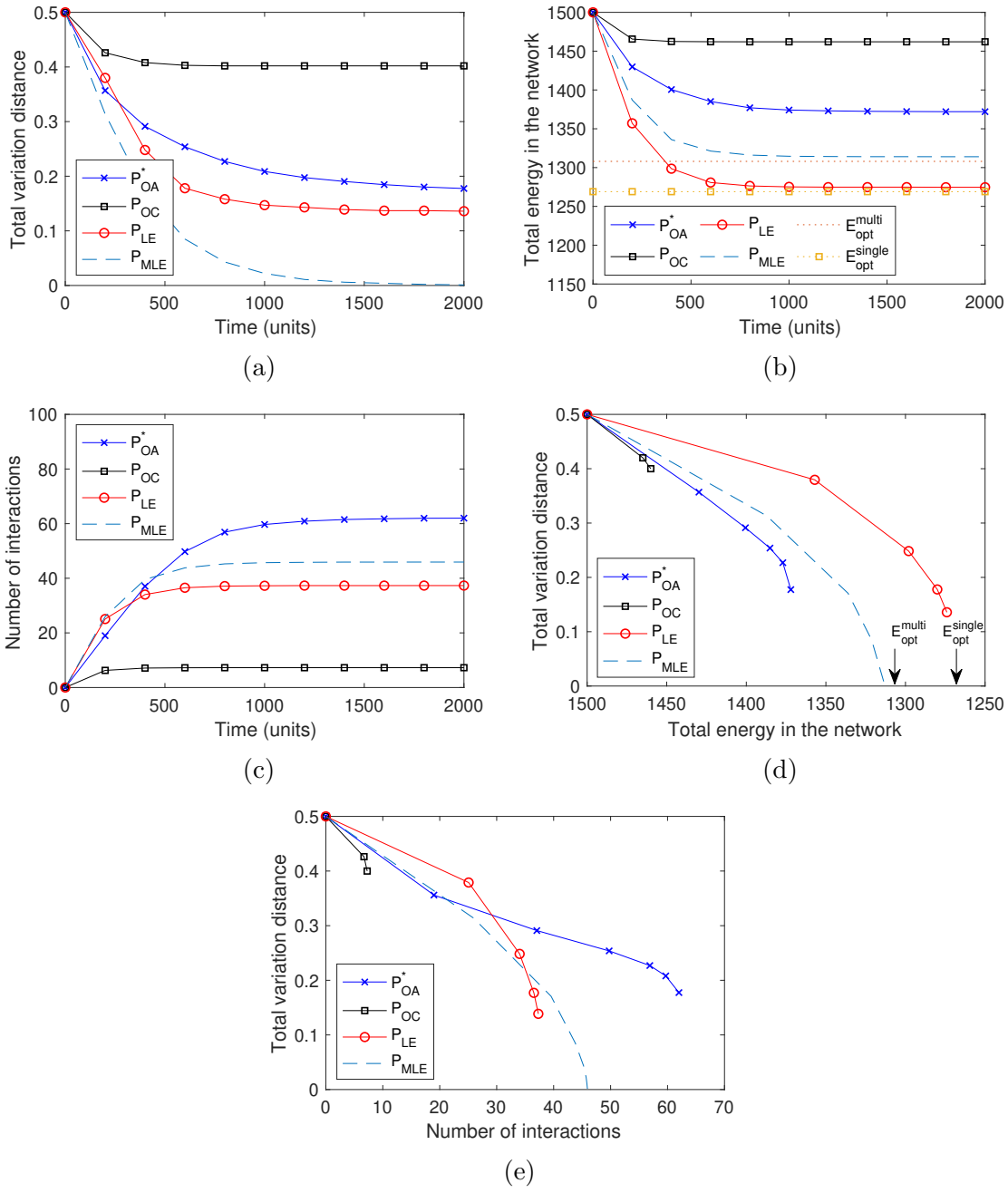

Fig. 28.: Comparison of all algorithms in terms of (a) variation distance, (b) total energy remaining in the network, (c) total number of interactions, (d) variation distance at each total energy level and (e) variation distance at each total number of interactions (when β=0.2, τ=2000, $p = 0.8$) using group-based synthetic traces.

eventually allow achieving a zero variation distance if the contact graph is connected. One interesting observation in Fig. 28b is that optimal energy balance (E_{opt}) in multi-hop case is more than it is in single hop case. This is because even though single hop exchanges may not allow reaching perfect energy balance, they leverage all possible single hop interactions and try to reduce the variation distance as much as possible. This then causes some unnecessary interactions and associated loss. Note that P_{OC} has the least amount of energy loss since the protocol cannot find useful interactions to reduce the variation distance. Moreover, P_{MLE} has more interactions than P_{LE} but it is still smaller than the number of interactions in P_{OA}.

In order to show the impact of inter-group sparsity γ on the benefit offered by multi-hop based energy exchanges, we obtain the results in Fig. 29 with different γ values in group-based synthetic traces. As the results show, with increasing γ, the performances of P_{MLE} and P_{LE} get closer. This is because larger γ connects more nodes between two groups thus decreases the hop distance between low energy nodes and high energy nodes. This makes zero optimal variation distance possible with single hop energy exchanges, thus even P_{MLE} starts using single hop interactions rather than multi-hop interactions to prevent unnecessary energy loss. Note that with $\gamma = 0$, the contact graph will be disconnected and no interactions will be helpful to reduce variation distance further as they will be all between same side nodes.

5.6 Discussion on Network Lifetime Maximization

In this section, we discuss the relation between the energy balancing problem and network lifetime maximization problem. As it is also highlighted in previous studies [34, 35, 36, 108], one of the goals of energy balancing process is to prolong the network lifetime. However, the relation of energy balancing and network lifetime has not been elaborated in these studies. Network lifetime is usually defined as the

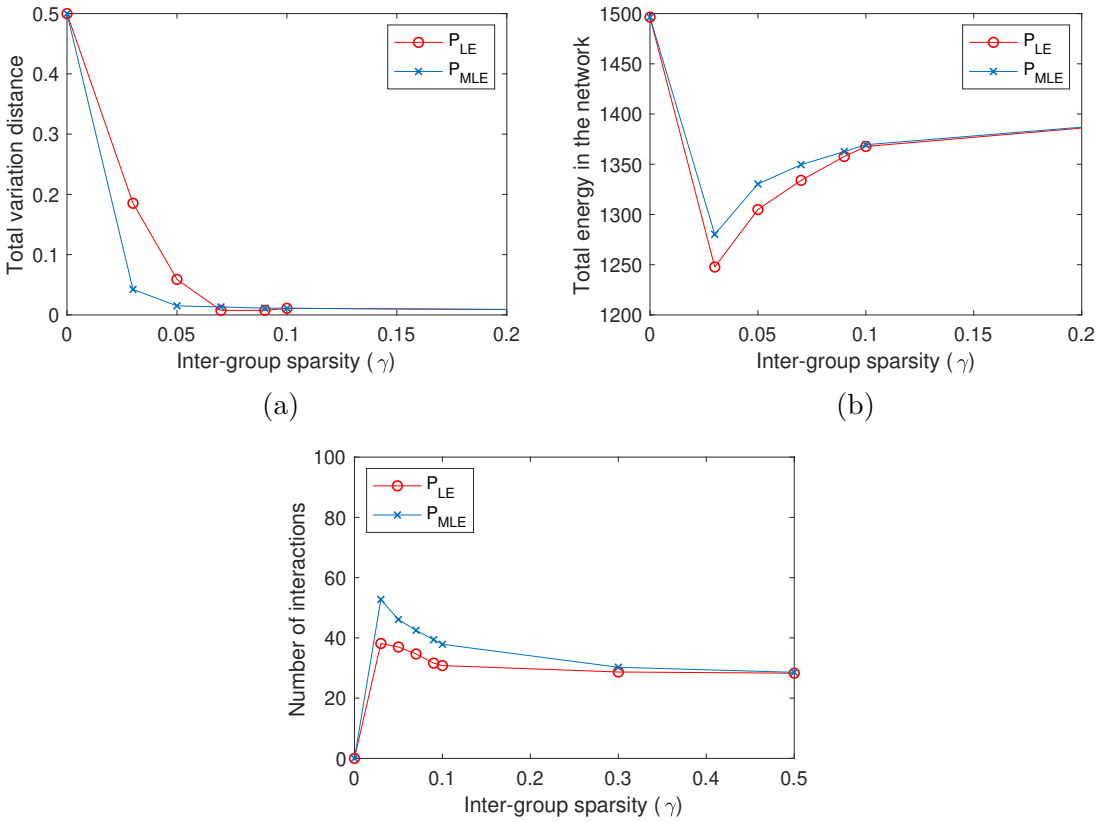

Fig. 29.: Comparison of P_{LE} and P_{MLE} in terms of (a) variation distance, (b) total energy remaining in the network, and (c) total number of interactions under different inter-group contact sparsity (γ) in group-based synthetic traces ($p = 0.8$).

time until one of the nodes in the network dies due to energy depletion. Thus, network lifetime maximization problem can simply be defined as maximizing the minimum energy level of the nodes (assuming that energy consumption rates after energy exchanges completed are the same for each node) in the network through energy exchanges in opportunistic meetings. The objective for this problem can then be defined as:

$$\max(\min\{E_f(u)\ \forall u\}) \tag{5.18}$$

where $E_f(u)$ is the final energy level of node u. Here, as opposed to the objective function in energy balancing problem, the objective function in lifetime maximization problem is not concerned about the variation distance and the total loss in the network as the main priority is increasing the energy of the node with the minimum energy level. However, the constraints of energy balancing problem are still valid with lifetime maximization objective since the interactions of nodes still depend on the node relations and the amount of energy available.

If a perfect energy balance is possible in a network (i.e., zero variation distance) such that all nodes have the same energy level, the maximum network lifetime will also be achieved. That is, these two problems converge to each other. Moreover, we know that P_{MLE} will always achieve the perfect balance if the contact graph among nodes is connected. Thus, in such networks, energy balancing and network lifetime maximization result in the same outcome. However, if the contact graph is not connected (e.g., due to the removal of links due to time threshold τ), or the protocol cannot achieve the zero variation distance (e.g., P_{LE} may not achieve a perfect balance even if the contact graph is connected), the final energy distribution of nodes after energy balancing process may not result in the maximum network lifetime achievable. Thus, the objective should be updated as (5.18).

In order to show the difference in the outcomes of energy balancing and network lifetime maximization problems, we obtain results in group-based synthetic traces. Fig. 30 shows the network lifetime obtained with balancing and maximum lifetime objectives when $\gamma = 0.03$ and $\gamma = 0$ (i.e., network is disconnected). Comparing Fig. 30a and Fig. 30b, we observe that P_{MLE} can achieve the same network lifetime with both objective functions. This is because P_{MLE} can reach zero variation distance by $\tau = 2000$ as shown in Fig.28a. On the other hand, we see that with maximum lifetime objective, network lifetime increases earlier than it does with balancing function.

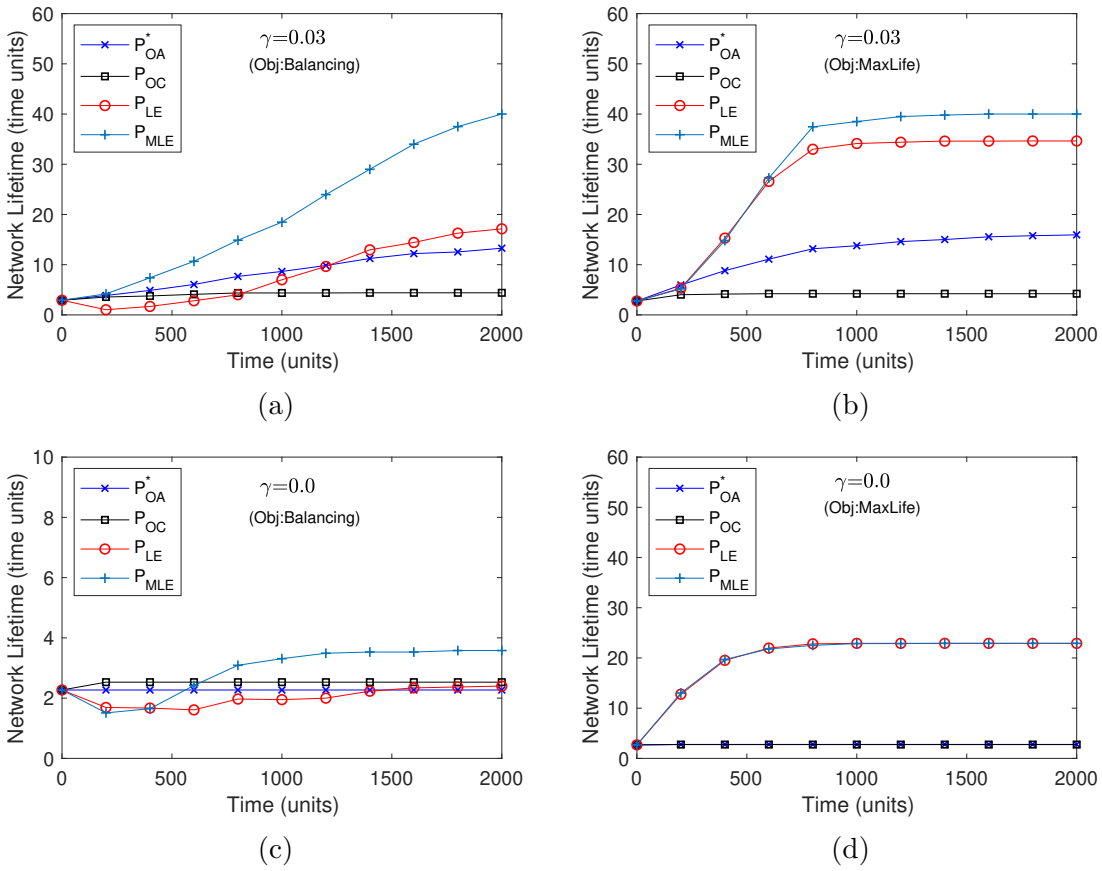

Fig. 30.: Comparison of protocols in terms of achievable network lifetime with *balancing* and *lifetime maximization* objective functions and different γ values (when β=0.2, τ=2000 time units, $p = 0.8$) using group-based synthetic traces.

This is because the outcomes of the two objectives overlap only at the end (i.e., when perfect balance is obtained) and maximum lifetime objective always considers network lifetime maximization target even before the time threshold is reached. Regarding the performance of P_{LE}, we see that it cannot achieve the same network lifetime with balancing objective as it obtains with maximum lifetime objective. This is because it cannot reach perfect balance by the time threshold thus both problems cannot converge to one another. P_{OC} and P^*_{OA} provide similar network lifetime with both

objectives as the objective function change slightly affects their performance (i.e., average energy in the final network changes slightly so do the positive and negative node sets).

When $\gamma = 0$, the network is partitioned into two groups thus no energy transfer is possible between the nodes in different groups. Thus, the balancing (Fig. 30c) and lifetime maximization objectives (Fig. 30d) yield remarkably different energy exchanges among nodes towards their goals. The balancing objective tries to decrease the variation distance in the network as much as possible through energy exchanges between positive and negative side nodes which only exist in the low energy group. However, this yields a very small network lifetime for all protocols (with P_{MLE} offering slightly more lifetime than others). On the other hand, lifetime maximization objective can help P_{MLE} and P_{LE} achieve much higher lifetime with a focus on increasing the minimum energy level among the nodes in the low energy group. Note that as the nodes within each group have high contact density (i.e., 40%), P_{MLE} and P_{LE} perform similarly, however with a smaller intra-group contact density P_{MLE} will provide better lifetime than P_{LE} as in the case of Fig. 30b.

5.7 Conclusion

In this chapter, we study the energy balancing problem among the nodes in a mobile opportunistic network. We aim to both balance the energy levels of nodes and minimize the energy loss during this process considering both the homogeneous and heterogeneous relations among nodes as well as a time threshold to finish the balancing. We first propose three protocols for homogeneous case and also suggest a method to compute the final achievable optimal energy in the network. For heterogeneous networks where the contact graph are partially connected, we find the optimal average energy achievable using a MILP based formulation. We initially con-

sider single hop based energy exchanges in our model. However, due to its limitations especially in sparse networks with long hop distances between low energy and high energy nodes, it cannot reach lower variation distances. Thus, we extend our model using multi-hop based energy exchanges, where nodes that are not meeting directly use relay nodes to exchange energy between them. We develop three different energy sharing protocols based on these models and through simulations using both synthetic and real user based traces we compare their performance with a state-of-the-art protocol. Results show that we can achieve better variation distance by keeping more energy in the network with the proposed protocols. Moreover, multi-hop based approach performs better than single hop based approach especially in sparse networks. Finally, through different network scenarios, we discuss on the implications of energy balancing process on network lifetime and propose modifications to the existing MILP model that aims to maximize the network lifetime directly instead of aiming to minimize variation distance and loss. With simulation results we show that especially in disconnected networks such modifications can help reach the maximum lifetime while energy balancing process cannot.

CHAPTER 6

FINAL REMARKS

In this dissertation, we look at the utilization of P2P energy sharing in mobile social networks for resource optimization by several means in three different ways. First, we look at mobile charging relief where we investigate to what extent the burden of charging process on users could be released. We develop a dynamic programming based optimization model and find out the minimum number of charging sessions that would be sufficient for users to keep their devices with the power they need through utilization of excessive energy from other users in the vicinity. With the empirical results based on different datasets of user meetings and charging patterns, we observe that users can achieve up to 13-17% relief without affecting their existing usage habits of mobile devices. Second, we also study the content delivery problem in mobile social networks in which nodes are motivated by energy transfers for carrying the messages. That is, each relay node carries a message forwarded by another node as long the energy provided or the corresponding time-to-live (TTL) value lasts. In order to find the optimal content and energy forwarding or sharing policy, we model and solve the problem using optimal stopping theory and dynamic programming. We evaluate the performance of the proposed solution in both real and synthetic mobile social network traces and show that sharing can offer better delivery rate, while it can also cause an increase in the cost of delivery (i.e., number of forwardings) to some extent. We also look at the impact of several parameters on the performance of the proposed sharing based content delivery process and discover the settings that provide performance enhancements.

Last, we study the energy balancing problem with the goal of balancing the energy levels of nodes with the minimal energy loss. Since, the optimal achievable target changes with the change in interaction patterns, we discuss energy balancing protocols in two different settings. First, when nodes are fully connected (i.e. a complete contact graph), we propose three different energy sharing protocols and show better results than the state of the art solutions. In second setting, we assume heterogeneous nodes relations (i.e. partially connected contact graph) as well as a time threshold to finish the balancing. We then find the optimal average energy achievable using a MILP based formulation then propose several single hop and multi hop protocols to achieve an efficient and a faster energy balancing process. We also provide a discussion on the relation of energy balancing and network lifetime maximization problem and propose updates to the balancing problem to achieve optimal network lifetime when an optimal energy balance is not achievable (e.g. in disconnected networks.) Simulation results in both synthetic and real traces show that the proposed algorithms perform better than the previous work and they have advantages to one another in different performance metrics and contact graph densities.

The solutions proposed in these different contexts provide important results and algorithms to improve energy efficiency in mobile social networks. However, this area of research is relatively new and a lot has yet to be done in order to realize its applications in real world. We believe that this work will provide significant contribution for opening up new insights into the existing problems and help conduct further research for energy sharing in mobile networks.

CHAPTER 7

FUTURE RESEARCH DIRECTIONS

Utilization of peer-to-peer wireless energy sharing among low power mobile nodes opens up a variety of research topic in the field of wireless networks. While many different problems including the problems discussed in this dissertation have been studied, the topic is still in its infancy and there are many directions that the research can go. Below, we discuss some of the potential new research directions in this area. While this does not cover every aspect of the research directions, it provides few research topics that is necessary to be addressed in order to implement these technologies in real world.

- Incentive and energy consumption aware energy sharing:

  The problem of energy sharing in mobile social networks have been studied in several aspects but these works assume that the nodes in the network are friendly and are willing to share their energy (e.g., due to altruism). However, some nodes may act selfishly, or may ask for incentives, thus without them they can deviate from collaboration significantly diverging the stability of the system. Thus, designing energy sharing protocols by considering differences in user interests as well as through incentives could be an interesting problem to investigate. Moreover, all of the studies including our works on energy balancing in this dissertation do not take into account the energy consumption due to mobility or other operations of devices during energy balancing process. Thus, new approaches are needed as current solutions cannot be used directly.

- Reactive charging with controlled mobility:

  The notion of energy sharing in MSNs has been considered mostly in uncontrolled mode as the mobility of devices is maintained by the humans carrying the devices. While this is an advantage compared to other networking scenarios in which the mobility also causes energy consumption on the mobile nodes, it makes the energy sharing possible only opportunistically, i.e., when nodes encounter. A more interesting scenario could be when the mobility of the agents are controllable at least partially through incentives. Thus, we can develop effectual strategies of energy sharing as contingency measures to energy depletion problem.

- Long-distance charging:

  In the current form, wireless energy sharing has been mostly considered between the devices that are within close-proximity of each other (<1cm). While it is possible to charge sensor networks at higher distances, due to the higher power requirements of smartphone like devices (e.g., 5-10 watt hours [118]), it cannot be applied directly. In some recent studies [119, 120] it has been shown that long distance charging for such devices is possible through beamforming the magnetic field. Moreover, when it is applied to multiple devices simultaneously, an increasing efficiency could be achieved (e.g., 6 devices at distances of up to 50 cm). However, such concept has not been considered for peer-to-peer energy sharing which could be challenging but can provide more flexibility.

REFERENCES

[1] GSMA. *Number of Mobile Subscribers of Worldwide hits 5 billion*. 2017. URL: https://www.gsma.com/newsroom/press-release/number-mobile-subscribers-worldwide-hits-5-billion/.

[2] Dong Wang et al. "The Rise of Social Sensing". In: *arXiv preprint arXiv:1801.09116* (2018).

[3] Apple. *Iphone X*. 2017. URL: https://www.apple.com/iphone-x/.

[4] Paul Worgan et al. "Powershake: Power transfer interactions for mobile devices". In: *Proc. of the 2016 CHI Conference*. ACM. 2016, pp. 4734–4745.

[5] Tekla Perry. *CES 2013: Share Battery Power Between Mobile Devices*. Online. Jan. 2013. URL: http://spectrum.ieee.org/tech-talk/consumer-electronics/portable-devices/mobile-devices-share-everything.

[6] Eyuphan Bulut and Boleslaw Szymanski. "Mobile Energy Sharing through Power Buddies". In: *Wireless Communications and Networking Conference (WCNC)*. IEEE. 2017, pp. 1–6.

[7] Dusit Niyato et al. "Finding the best friend in mobile social energy networks". In: *Proceedings of IEEE International Conference on Communications (ICC)*. IEEE. 2015, pp. 3240–3245.

[8] Dusit Niyato et al. "Mobile energy sharing networks: Performance analysis and optimization". In: *IEEE Transactions on Vehicular Technology* 65.5 (2016), pp. 3519–3535.

[9] WiTricity Corp. *Highly resonant wireless power transfer: Safe, efficient, and over distance*. Technical report. 2012.

[10] ICNIRP Guidelines. "Guidelines for limiting exposure to time-varying electric, magnetic, and electromagnetic fields (up to 300 GHz)". In: *Health Phys* 74.4 (1998), pp. 494–522.

[11] Ian Poole. *Qi Wireless Charging Standard*. URL: http://www.radio-electronics.com/info/power-management/wireless-inductive-battery-charging/qi-wireless-charging-standard.php.

[12] Andre Kurs et al. "Wireless power transfer via strongly coupled magnetic resonances". In: *science* 317.5834 (2007), pp. 83–86.

[13] Benjamin L Cannon et al. "Magnetic resonant coupling as a potential means for wireless power transfer to multiple small receivers". In: *IEEE Transactions on Power Electronics* 24.7 (2009), pp. 1819–1825.

[14] Kisuk Kang et al. "Electrodes with high power and high capacity for rechargeable lithium batteries". In: *Science* 311.5763 (2006), pp. 977–980.

[15] Allied Market Research. *Wireless Charging Market by Technology and Industry Vertical - Global Opportunity Analysis and Industry Forecast, 2018-2025*. 2018. URL: https://www.alliedmarketresearch.com/wireless-charging-market.

[16] Eyuphan Bulut et al. "Is crowdcharging possible?" In: *2018 27th International Conference on Computer Communication and Networks (ICCCN)*. IEEE. 2018, pp. 1–9.

[17] Rongqing Zhang, Xiang Cheng, and Liuqing Yang. "Flexible energy management protocol for cooperative EV-to-EV charging". In: *IEEE Transactions on Intelligent Transportation Systems* (2018).

[18] Sheng Zhang, Jie Wu, and Sanglu Lu. "Collaborative mobile charging". In: *IEEE Transactions on Computers* 64.3 (2015), pp. 654–667.

[19] Paul Worgan et al. "Powershake: Power transfer interactions for mobile devices". In: *Proceedings of the 2016 CHI Conference on Human Factors in Computing Systems*. ACM. 2016, pp. 4734–4745.

[20] Liguang Xie et al. "Making sensor networks immortal: An energy-renewal approach with wireless power transfer". In: *IEEE/ACM Transactions on networking* 20.6 (2012), pp. 1748–1761.

[21] Teodora Sanislav et al. "Wireless energy harvesting: Empirical results and practical considerations for Internet of Things". In: *Journal of Network and Computer Applications* 121 (2018), pp. 149–158.

[22] Bin Tong et al. "Node reclamation and replacement for long-lived sensor networks". In: *IEEE Transactions on Parallel & Distributed Systems* 9 (2011), pp. 1550–1563.

[23] Chi Lin et al. "MPF: Prolonging Network Lifetime of Wireless Rechargeable Sensor Networks by Mixing Partial Charge and Full Charge". In: *2018 15th Annual IEEE International Conference on Sensing, Communication, and Networking (SECON)*. IEEE. 2018, pp. 1–9.

[24] Chien-Fu Cheng and Chen-Chuan Wang. "The Energy Replenishment Problem in Mobile WRSNs". In: *2018 IEEE 15th International Conference on Mobile Ad Hoc and Sensor Systems (MASS)*. IEEE. 2018, pp. 143–144.

[25] Wenzheng Xu et al. "Maximizing charging satisfaction of smartphone users via wireless energy transfer". In: *IEEE Transactions on Mobile Computing* 16.4 (2016), pp. 990–1004.

[26] Vikram Iyer et al. “Charging a smartphone across a room using lasers”. In: *Proceedings of the ACM on Interactive, Mobile, Wearable and Ubiquitous Technologies* 1.4 (2018), p. 143.

[27] Eyuphan Bulut et al. “Is Crowdcharging Possible?” In: *27th International Conference on Computer Communication and Networks, ICCCN 2018, Hangzhou, China, July 30 - August 2, 2018*. 2018, pp. 1–9.

[28] Dimitrios Kosmanos et al. “Route Optimization of Electric Vehicles Based on Dynamic Wireless Charging”. In: *IEEE Access* 6 (2018), pp. 42551–42565.

[29] Giuseppe Buja, Chun-Taek Rim, and Chunting C Mi. “Dynamic charging of electric vehicles by wireless power transfer”. In: *IEEE Transactions on Industrial Electronics* 63.10 (2016), pp. 6530–6532.

[30] Rui Zhang et al. “Collaborative Interactive Wireless Charging in a Cyclic Mobispace”. In: *Proc. of the IEEE/ACM International Symposium on Quality of Service (IEEE/ACM IWQoS 2018)*. 2018.

[31] Xiaoran Fan et al. “Energy-Ball: Wireless Power Transfer for Batteryless Internet of Things through Distributed Beamforming”. In: *Proceedings of the ACM on Interactive, Mobile, Wearable and Ubiquitous Technologies* 2.2 (2018), p. 65.

[32] Wen Fang et al. “Fair scheduling in resonant beam charging for IoT devices”. In: *IEEE Internet of Things Journal* 6.1 (2019), pp. 641–653.

[33] Dusit Niyato et al. “Content messenger selection and wireless energy transfer policy in mobile social networks”. In: *Communications (ICC), 2015 IEEE International Conference on*. IEEE. 2015, pp. 3831–3836.

[34] Sotiris Nikoletseas, Theofanis P Raptis, and Christoforos Raptopoulos. "Energy balance with peer-to-peer wireless charging". In: *2016 IEEE 13th International Conference on Mobile Ad Hoc and Sensor Systems (MASS)*. IEEE. 2016, pp. 101–108.

[35] Sotiris Nikoletseas, Theofanis P Raptis, and Christoforos Raptopoulos. "Wireless charging for weighted energy balance in populations of mobile peers". In: *Ad Hoc Networks* 60 (2017), pp. 1–10.

[36] Sotiris E. Nikoletseas, Theofanis P. Raptis, and Christoforos Raptopoulos. "Interactive Wireless Charging for Energy Balance". In: *36th IEEE International Conference on Distributed Computing Systems, ICDCS 2016, Nara, Japan, June 27-30, 2016*. 2016, pp. 262–270.

[37] Adelina Madhja et al. "Energy aware network formation in peer-to-peer wireless power transfer". In: *Proceedings of the 19th ACM International Conference on Modeling, Analysis and Simulation of Wireless and Mobile Systems*. ACM. 2016, pp. 43–50.

[38] Adelina Madhja et al. "Peer-to-peer energy-aware tree network formation". In: *Proceedings of the 16th ACM International Symposium on Mobility Management and Wireless Access*. ACM. 2018, pp. 1–8.

[39] M Stoopman et al. "A self-calibrating RF energy harvester generating 1V at-26.3 dBm". In: *2013 Symposium on VLSI Circuits*. IEEE. 2013, pp. C226–C227.

[40] Triet Le, Karti Mayaram, and Terri Fiez. "Efficient far-field radio frequency energy harvesting for passively powered sensor networks". In: *IEEE Journal of Solid-State Circuits* 43.5 (2008), pp. 1287–1302.

[41] François C Delori, Robert H Webb, and David H Sliney. "Maximum permissible exposures for ocular safety (ANSI 2000), with emphasis on ophthalmic devices". In: *JOSA A* 24.5 (2007), pp. 1250–1265.

[42] Pengfei Li and Rizwan Bashirullah. "A wireless power interface for rechargeable battery operated medical implants". In: *IEEE Transactions on Circuits and Systems II: Express Briefs* 54.10 (2007), pp. 912–916.

[43] New York Times. *Wireless charging, at a distance, moves forward for ubeam.* Aug. 2014. URL: http://bits.blogs.nytimes.com/2014/08/06/ubeam-technology-will-enable-people-to-charge-devices-through-the-air/.

[44] Wi-charge. *To power with light.* URL: http://www.wi-charge.com.

[45] Xiao Lu et al. "Wireless charging technologies: Fundamentals, standards, and network applications". In: *IEEE Communications Surveys & Tutorials* 18.2 (2016), pp. 1413–1452.

[46] IKEA. *Chargers you'll actually want everywhere.* 2017. URL: http://www.ikea.com/us/en/%20catalog/categories/%20departments/wireless_charging/.

[47] Best Wireless Charger. *Zens car wireless charger review.* 2016. URL: http://bestwirelesscharger.org/zens-car-wireless-charger-review/.

[48] Samsung. *Micro USB Battery Power Sharing Cable.* July 2016. URL: http://www.samsung.com/uk/consumer/mobile-devices/accessories/battery/EP-SG900UBEGWW.

[49] *ChargeBite: A Social Charger.* URL: http://chargebite.com/.

[50] Eyuphan Bulut et al. "Is Crowdcharging Possible?" In: *27th International Conference on Computer Communication and Networks, ICCCN 2018, Hangzhou, China, July 30 - August 2, 2018*. 2018, pp. 1–9.

[51] *Wireless Electric Vehicle Charging*. 2019. URL: https://www.pluglesspower.com/.

[52] Srdjan Lukic and Zeljko Pantic. "Cutting the cord: Static and dynamic inductive wireless charging of electric vehicles". In: *IEEE Electrification Magazine* 1.1 (2013), pp. 57–64.

[53] *Global EV outlook: beyond one million electric cars*. [Online; accessed 01-Oct-2016]. 2016.

[54] Rui Zhang et al. "Collaborative Interactive Wireless Charging in a Cyclic Mobispace". In: *Proc. of the IEEE/ACM International Symposium on Quality of Service (IEEE/ACM IWQoS 2018)*. 2018.

[55] *Andromeda Power*. 2018. URL: www.andromedapower.com.

[56] *eMotorWerks*. 2018. URL: https://emotorwerks.com/.

[57] Xiping Hu et al. "A survey on mobile social networks: Applications, platforms, system architectures, and future research directions". In: *IEEE Communications Surveys & Tutorials* 17.3 (2015), pp. 1557–1581.

[58] Jianwei Niu, Danning Wang, and Mohammed Atiquzzaman. "Copy limited flooding over opportunistic networks". In: *Journal of Network and Computer Applications* 58 (2015), pp. 94–107.

[59] Eyuphan Bulut and Boleslaw K Szymanski. "Exploiting friendship relations for efficient routing in mobile social networks". In: *IEEE Transactions on Parallel and Distributed Systems* 23.12 (2012), pp. 2254–2265.

[60] Wei Dong et al. "Secure friend discovery in mobile social networks". In: *INFOCOM, 2011 Proceedings IEEE*. IEEE. 2011, pp. 1647–1655.

[61] Muyuan Li et al. "All your location are belong to us: Breaking mobile social networks for automated user location tracking". In: *Proceedings of the 15th ACM international symposium on Mobile ad hoc networking and computing*. ACM. 2014, pp. 43–52.

[62] Sara H Basson et al. *Optimizing battery usage*. US Patent 9,306,243. Apr. 2016.

[63] Anil Tiwari. *Battery consumption optimization for mobile users*. US Patent 7,359,713. Apr. 2008.

[64] ChargeItSpot. *Free and Secure Public Charging*. 2017. URL: https://chargeitspot.com/.

[65] WraithNet. *Airport Power*. 2017. URL: https://play.google.com/store/apps/details?id=com.silverwraith.airportpower&hl=en.

[66] Simon Hill. *30 of the juiciest portable battery chargers money can buy*. May 2016. URL: http://www.digitaltrends.com/mobile/best-portable-battery-chargers/.

[67] Dan Tennant. *Solar Phone Chargers Reviews*. July 2016. URL: http://solar-phone-charger-review.toptenreviews.com/.

[68] Kay Tan. *30 Smartphone Chargers You Have Not Seen Before*. July 2016. URL: http://www.hongkiat.com/blog/extraordinary-smartphone-chargers/.

[69] Eyuphan Bulut, Mehmet Eren Ahsen, and Boleslaw K Szymanski. "Opportunistic wireless charging for mobile social and sensor networks". In: *Globecom Workshops (GC Wkshps), 2014*. IEEE. 2014, pp. 207–212.

[70] Kevin Fall. "A delay-tolerant network architecture for challenged internets". In: *Proceedings of the 2003 conference on Applications, technologies, architectures, and protocols for computer communications*. ACM. 2003, pp. 27–34.

[71] Elizabeth M Daly and Mads Haahr. "Social network analysis for routing in disconnected delay-tolerant manets". In: *Proceedings of the 8th ACM international symposium on Mobile ad hoc networking and computing*. ACM. 2007, pp. 32–40.

[72] Sushant Jain, Kevin Fall, and Rabin Patra. *Routing in a delay tolerant network*. Vol. 34. 4. ACM, 2004.

[73] Aashish Dhungana and Eyuphan Bulut. "Timely information dissemination with distributed storage in delay tolerant mobile sensor networks". In: *Computer Communications Workshops (INFOCOM WKSHPS), 2017 IEEE Conference on*. IEEE. 2017, pp. 103–108.

[74] Dusit Niyato et al. "Cooperation in delay-tolerant networks with wireless energy transfer: Performance analysis and optimization". In: *IEEE Transactions on Vehicular Technology* 64.8 (2015), pp. 3740–3754.

[75] Dusit Niyato and Ping Wang. "Competitive wireless energy transfer bidding: A game theoretic approach". In: *Communications (ICC), 2014 IEEE International Conference on*. IEEE. 2014, pp. 1–6.

[76] Yang Zhang et al. "Optimal Wireless Energy Charging for Incentivized Content Transfer in Mobile Publish–Subscribe Networks". In: *IEEE Transactions on Vehicular Technology* 66.4 (2017), pp. 3420–3434.

[77] Dinh Thai Hoang, Dusit Niyato, and Dong In Kim. "Cooperative bidding of data transmission and wireless energy transfer". In: *Wireless Communications*

and Networking Conference (WCNC), 2014 IEEE. IEEE. 2014, pp. 1597–1602.

[78] Wanxin Gao and Janelle Harms. "Charging-aware mobility modeling for wirelessly chargeable intermittently connected MANETs". In: *Personal, Indoor, and Mobile Radio Communications (PIMRC), 2017 IEEE 28th Annual International Symposium on*. IEEE. 2017, pp. 1–7.

[79] Adelina Madhja et al. "Peer-to-Peer Wireless Energy Transfer in Populations of Very Weak Mobile Nodes". In: *Wireless Communications and Networking Conference Workshops (WCNCW), 2017 IEEE*. IEEE. 2017, pp. 1–6.

[80] Sotiris Nikoletseas, Theofanis P Raptis, and Christoforos Raptopoulos. "Wireless charging for weighted energy balance in populations of mobile peers". In: *Ad Hoc Networks* 60 (2017), pp. 1–10.

[81] Sotiris Nikoletseas, Theofanis P Raptis, and Christoforos Raptopoulos. "Energy balance with peer-to-peer wireless charging". In: *Mobile Ad Hoc and Sensor Systems (MASS), 2016 IEEE 13th International Conference on*. IEEE. 2016, pp. 101–108.

[82] Wenzheng Xu et al. "Maximizing charging satisfaction of smartphone users via wireless energy transfer". In: *IEEE Transactions on Mobile Computing* 16.4 (2017), pp. 990–1004.

[83] Mohammad A Hoque and Sasu Tarkoma. "Characterizing smartphone power management in the wild". In: *Proceedings of the 2016 ACM International Joint Conference on Pervasive and Ubiquitous Computing: Adjunct*. ACM. 2016, pp. 1279–1286.

[84] Mohammad Ashraful Hoque et al. "Full charge capacity and charging diagnosis of smartphone batteries". In: *IEEE Transactions on Mobile Computing* 16.11 (2017), pp. 3042–3055.

[85] URL: `https://en.wikipedia.org/wiki/Stable_roommates_problem`.

[86] Robert W Irving. "An efficient algorithm for the stable roommates problem". In: *Journal of Algorithms* 6.4 (1985), pp. 577–595.

[87] *A community resource for archiving wireless data at Dartmouth*. URL: `https://crawdad.org/`.

[88] J Leguay et al. *CRAWDAD data set upmc/content (v. 2006-11-17)*. 2006. URL: `http://crawdad.cs.dartmouth.edu`.

[89] Jeremie Leguay et al. "Opportunistic Content Distribution in an Urban Setting". In: *Proc. ACM SIGCOMM 2006 - Workshop on Challenged Networks (CHANTS)*. Pisa, Italy, Sept. 2006.

[90] A Pentland, N Eagle, and D Lazer. "Inferring social network structure using mobile phone data". In: *Proceedings of the National Academy of Sciences (PNAS)* 106.36 (2009), pp. 15274–15278.

[91] Daniel T Wagner, Andrew Rice, and Alastair R Beresford. "Device analyzer: Understanding smartphone usage". In: *International Conference on Mobile and Ubiquitous Systems: Computing, Networking, and Services*. Springer. 2013, pp. 195–208.

[92] Panagiotis Matzakos, Thrasyvoulos Spyropoulos, and Christian Bonnet. "Joint Scheduling and Buffer Management Policies for DTN Applications of Different Traffic Classes". In: *IEEE Transactions on Mobile Computing* (2018).

[93] Kazuya Sakai et al. “On Anonymous Routing in Delay Tolerant Networks”. In: *IEEE Transactions on Mobile Computing* (2018).

[94] Ting Ning et al. “Incentive-aware data dissemination in delay-tolerant mobile networks”. In: *Sensor, Mesh and Ad Hoc Communications and Networks (SECON), 2011 8th Annual IEEE Communications Society Conference on*. IEEE. 2011, pp. 539–547.

[95] Bin Bin Chen and Mun Choon Chan. “Mobicent: a credit-based incentive system for disruption tolerant network”. In: *INFOCOM, 2010 Proceedings IEEE*. IEEE. 2010, pp. 1–9.

[96] Ray Chen et al. “Dynamic trust management for delay tolerant networks and its application to secure routing”. In: *IEEE Transactions on Parallel and Distributed Systems* 25.5 (2014), pp. 1200–1210.

[97] Jouya Jadidian and Dina Katabi. “Magnetic mimo: How to charge your phone in your pocket”. In: *Proceedings of the 20th annual international conference on Mobile computing and networking*. ACM. 2014, pp. 495–506.

[98] Thrasyvoulos Spyropoulos, Konstantinos Psounis, and Cauligi S Raghavendra. “Efficient routing in intermittently connected mobile networks: The single-copy case”. In: *IEEE/ACM transactions on networking* 16.1 (2008), pp. 63–76.

[99] Cong Liu and Jie Wu. “An optimal probabilistic forwarding protocol in delay tolerant networks”. In: *Proceedings of the tenth ACM international symposium on Mobile ad hoc networking and computing*. ACM. 2009, pp. 105–114.

[100] Eyuphan Bulut, Zijian Wang, and Boleslaw K Szymanski. “Time dependent message spraying for routing in intermittently connected networks”. In:

IEEE GLOBECOM 2008-2008 IEEE Global Telecommunications Conference. IEEE. 2008, pp. 1–6.

[101] Eyuphan Bulut, Zijian Wang, and Boleslaw K Szymanski. "Cost efficient erasure coding based routing in delay tolerant networks". In: *2010 IEEE International Conference on Communications*. IEEE. 2010, pp. 1–5.

[102] Thrasyvoulos Spyropoulos, Konstantinos Psounis, and Cauligi S Raghavendra. "Efficient routing in intermittently connected mobile networks: The multiple-copy case". In: *IEEE/ACM Transactions on Networking (ToN)* 16.1 (2008), pp. 77–90.

[103] Eyuphan Bulut and Boeslaw K Szymanski. "Secure multi-copy routing in compromised delay tolerant networks". In: *Wireless personal communications* 73.1 (2013), pp. 149–168.

[104] Cong Liu and Jie Wu. "On multicopy opportunistic forwarding protocols in nondeterministic delay tolerant networks". In: *IEEE Transactions on Parallel and Distributed Systems* 23.6 (2012), pp. 1121–1128.

[105] *Optimal Stopping and Applications*. URL: `http://www.math.ucla.edu/tom/Stopping/Contents.html`.

[106] Richard Bellman. *Dynamic programming*. Courier Corporation, 2013.

[107] *Secretary Problem*. URL: `https://en.wikipedia.org/wiki/Secretary_problem`.

[108] Aashish Dhungana and Eyuphan Bulut. "Loss-aware efficient energy balancing in mobile opportunistic networks". In: *IEEE Global Telecommunications Conference (GLOBECOM) 2019*. 2019, pp. 1–6.

[109] Theofanis P Raptis. "When Wireless Crowd Charging Meets Online Social Networks: A Vision for Socially Motivated Energy Sharing". In: *Online Social Networks and Media* 16 (2020), p. 100069.

[110] En Wang, Yongjian Yang, and Jie Wu. "Energy efficient beaconing control strategy based on time-continuous markov model in DTNs". In: *IEEE Transactions on Vehicular Technology* 66.8 (2017), pp. 7411–7421.

[111] Wei Gao et al. "Supporting cooperative caching in disruption tolerant networks". In: *2011 31st International Conference on Distributed Computing Systems*. IEEE. 2011, pp. 151–161.

[112] Cong Liu and Jie Wu. "An optimal probabilistic forwarding protocolin delay tolerant networks". In: *10th ACM international symposium on Mobile ad hoc networking and computing*. 2009, pp. 105–114.

[113] E. Bulut and B. K. Szymanski. "Exploiting Friendship Relations for Efficient Routing in Mobile Social Networks". In: *IEEE Transactions on Parallel and Distributed Systems* 23.12 (2012), pp. 2254–2265.

[114] Eyuphan Bulut, Sahin Cem Geyik, and Boleslaw K Szymanski. "Utilizing correlated node mobility for efficient DTN routing". In: *Pervasive and Mobile Computing* 13 (2014), pp. 150–163.

[115] *Gamma distribution*. May 2020. URL: `https://en.wikipedia.org/wiki/Relationships_among_probability_distributions`.

[116] Markus Bibinger. "Notes on the sum and maximum of independent exponentially distributed random variables with different scale parameters". In: *arXiv preprint arXiv:1307.3945* (2013).

[117] *IBM Cplex Optimization Solver*. June 2019. URL: https://www.ibm.com/products/ilog-cplex-optimization-studio.

[118] Christopher Helman. *How Much Electricity Do Your Gadgets Really Use?* Nov. 2015. URL: http://www.forbes.com/.

[119] Lixin Shi et al. "Wireless power hotspot that charges all of your devices". In: *Proceedings of the 21st Annual International Conference on Mobile Computing and Networking*. ACM. 2015, pp. 2–13.

[120] Jouya Jadidian and Dina Katabi. "Magnetic MIMO: How to charge your phone in your pocket". In: *Proceedings of the 20th annual international conference on Mobile computing and networking*. ACM. 2014, pp. 495–506.

VITA

Aashish Dhungana (M'17) received the BS degree from Kathmandu University in Nepal in 2014. He is now doing his PhD in the Computer Science Department of Virginia Commonwealth University under the supervision of Dr. Eyuphan Bulut. Currently, he is working as a research assistant in MoWing lab. His research interests include mobile social networks, Delay-tolerant networks, and Device-to-Device (D2D) communications and energy sharing.

Publications

1. **Dhungana**, **Aashish**, Tomasz Arodz, and Eyuphan Bulut. "Exploiting peer-to-peer wireless energy sharing for mobile charging relief." Ad Hoc Networks 91 (2019): 101882.

2. **Dhungana**, **Aashish**, and Eyuphan Bulut. "Energy sharing based content delivery in mobile social networks." 20th International Symposium on" A World of Wireless, Mobile and Multimedia Networks"(WoWMoM). IEEE. 2019.

3. **Dhungana**, **Aashish**, Tomasz Arodz, and Eyuphan Bulut. "Charging skip optimization with peer-to-peer wireless energy sharing in mobile networks."International Conference on Communications (ICC). IEEE, 2018.

4. Bulut, Eyuphan, Steven Hernandez, **Aashish Dhungana**, and Boleslaw K. Szymanski. "Is crowdcharging possible?." In 27th International Conference on Computer Communication and Networks (ICCCN), pp. 1-9. IEEE, 2018.

5. **Dhungana**, **Aashish**, and Eyuphan Bulut. "Timely information dissemination with distributed storage in delay tolerant mobile sensor networks."International

Conference on Computer Communications Workshops (INFOCOM WKSHPS). IEEE, 2017.

6. **Dhungana**, **Aashish**, and Eyuphan Bulut. "Loss-Aware Efficient Energy Balancing in Mobile Opportunistic Networks", in International Global Communications (Globecom) Conference: Ad Hoc and Sensor Networks. IEEE, May, 2019.

7. **Dhungana**, **Aashish**, and Eyuphan Bulut. "Mobile Energy Balancing in Heterogeneous Opportunistic Networks", in IEEE MASS 2019: Systems and Applications Track. June, 2019.

8. **Dhungana**, **Aashish**, and Eyuphan Bulut. "Peer-to-Peer Energy Sharing in Mobile Networks: Applications, Challenges, and Open Problems", in AdHoc Networks. June, 2019.

9. **Dhungana**, **Aashish**, and Eyuphan Bulut. "Opportunistic wireless crowd charging of iot devices from smartphones", in 16th International Conference on Distributed Computing in Sensor Systems (DCOSS). IEEE, 2020.

10. Eyuphan Bulut, and **Dhungana**, **Aashish**. "Social-aware energy balancing in mobile opportunistic networks", in 16th International Conference on Distributed Computing in Sensor Systems (DCOSS). IEEE, 2020.

11. **Dhungana**, **Aashish**, and Eyuphan Bulut. "Energy Balancing in Mobile Opportunistic Networks with Wireless Charging: Single and Multi-hop Approaches", Submitted in Ad-Hoc Networks (2020) (Major Review).